Precision spectrometry of radiations of radioactive nuclides by means of semiconductor detectors

Ts. Vylov, B. P. Osipenko, and V. M. Chumin

Joint Institute for Nuclear Research, Dubna
Fiz. Elem. Chastits At. Yadra 9, 1350–1459 (November–December 1978)

Methods of detecting γ rays, internal-conversion electrons, and α particles from radioactive nuclides by means of semiconductor detectors are described. Effects distorting the shape of the uncorrected spectrum are discussed. The techniques of measurement of the energies and relative intensities of monoenergetic radiations are described. A complete set of standards is given for the energies and relative intensities of γ rays and also internal-conversion electrons.

PACS numbers: 29.30.Ep, 29.30.Kv, 29.40.Pe

INTRODUCTION

The energy distribution of the radiations emitted by radioactive nuclides is called the true energy spectrum. The distribution of signals from detectors in pulse height is called the uncorrected or instrumental spectrum. The relation between the uncorrected and true spectra is described by a Fredholm integral equation of the first kind

$$N(V)=\int \Phi(E)\,G(E,V)\,dE, \qquad (1)$$

where E is the energy of the detected radiation, $\Phi(E)$ is the true distribution function of the radiation, and $G(E,V)$ is the probability that radiation with energy E incident on the detector produces a signal V (the instrumental or response function). The problem of measurement consists in obtaining $N(V)$ by means of a spectrometer and then, knowing $G(E,V)$, finding the true spectrum.

The ideal means of analyzing the uncorrected spectrum is to solve Eq. (1) and find $\Phi(E)$. As a rule, this method is inapplicable both because of the difficulty of determining $G(E,V)$ experimentally and because of the incorrectness of the problem posed.[1] Since in nuclear spectroscopy it is very common to study discrete spectra, a model approach is used in analysis of experiment there, i.e., a mathematical model of the investigated portion of the spectrum is constructed and those model parameters for which $N(V)$ is most accurately approximated are determined. An important condition of the correctness of this approach is the necessity of satisfying all of the assumptions of a given model (for example, instrumental line shape, shape of the continuous distribution, absence of effects distorting the shape of the instrumental spectrum, and so forth). We note that in the practical case of a physical experiment these conditions are often forgotten.

The quality of a spectrometer in measurement of the radiations of radioactive nuclides is characterized by

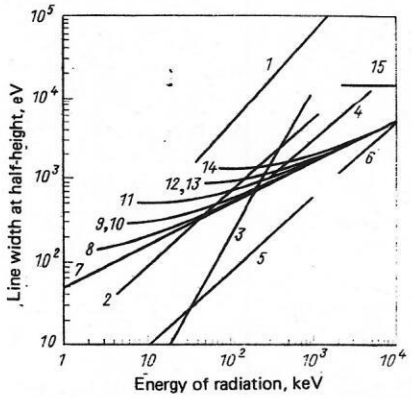

FIG. 1. Spectral line width at half-height as a function of energy for various spectrometers. The solid angle values are given below in parentheses. 1—NaI(Tl);2—iron-free toroidal, $\Delta p/p=0.4\%$ (7%);3—DuMond-type crystal diffraction; 4—magnetic steel $2\pi\sqrt{2}$, $\Delta p/p=0.2\%$ (0.015%); 5—Danish-type magnetic steel, $\Delta p/p=0.04\%$ (0.01%);6—magnetic α spectrograph $\pi\sqrt{2}$, $\Delta p/p=0.04\%$ (0.04%);7—limiting resolution for Ge with Fano factor $F=0.13$;8—25 $mm^2\times 5$ mm Ge for measurement of x rays;9—200 $mm^2\times 5$ mm Ge(Li) for measurement of x rays and γ rays;10—80 $mm^2\times 4$ mm Si(Li) for measurement of x rays (1%);11—1.3 cm^3 Ge(Li) for measurement of x rays and γ rays (1.5%);12—80 $mm^2\times 4$ mm Si(Li) for measurement of conversion electrons;13—80 $mm^2\times 4$ mm Si(Li) in uniform magnetic fields;14—37 cm^3 Ge(Li) (1.5%);15—80 $mm^2\times 0.5$ mm Si(Au) for measurement of α particles.

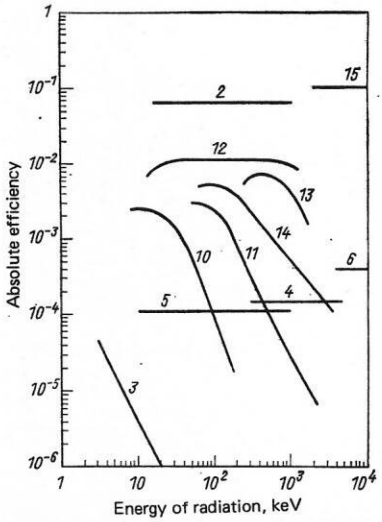

FIG. 2. Absolute efficiencies for various spectrometers as a function of the energy of the detected radiation (the designations are the same as in Fig. 1).

 0090-4759/78/060530-41$02.80

the following parameters:

a) the energy resolution ΔE, i.e., the width of the total-absorption peak at half-height (ΔE is usually expressed in eV, and sometimes the ratio $\Delta E/E$ is given in percent);

b) the absolute efficiency ε, i.e., the ratio of the number of pulses recorded in the total-absorption peak to the total number of particles or quanta of the monoenergetic radiation emitted by the source;

c) the selectivity of the spectrometer, i.e., the ratio of the probabilities of recording the radiation under study and the accompanying radiation.

The widths of spectral lines at half-height and the absolute efficiencies are given in Figs. 1 and 2 for the types of spectrometers widely used. As the result of the single-channel nature or of the use of the low-efficiency emulsion technique, a realistic comparison of the absolute efficiencies of magnetic β spectrometers cannot be made, and therefore in Fig. 2 we have indicated the aperture of the spectrometer. As can be seen, spectrometers with semiconductor detectors have comparatively high energy resolution and high absolute efficiency, which makes them the most important devices of nuclear-spectroscopy research.

Below we discuss the questions of precision spectrometry of monoenergetic radiations of radioactive nuclides by means of semiconductor detectors. The term "precision" is used in the sense that the errors obtained here are comparable with the errors of the standards against which comparative measurements are made (absolute measurements with semiconductor detectors are impossible). The use of this technique involves the necessary and complete analysis of effects which distort the shape of the uncorrected spectrum and use of a complete and consistent set of standards. As has been made clear, no such sets of standards are available, and therefore we shall discuss also the problems of constructing such sets.

1. SPECTROMETRIC APPARATUS

Work has been going on at the Laboratory of Nuclear Problems at our Institute for more than ten years on the development and production of semiconductor spectrometers. During this time detectors based on Si and Ge have essentially reached the limit of possible energy resolution. The corresponding analog electronics has undergone very rapid development. The extensive use of semiconductor detectors in the performance of physics experiments and in a number of applied studies has enabled several companies (ORTEC, Princeton Gamma Technology, SAIP, etc.) to perfect the manufacture of complete x-ray and γ-ray spectrometer units and also charged-particle detectors working at room temperature. The only instruments not manufactured industrially are high-quality β spectrometers permitting measurement of nuclear radiation with rapid replacement of the source without destroying the vacuum in the detector chamber.

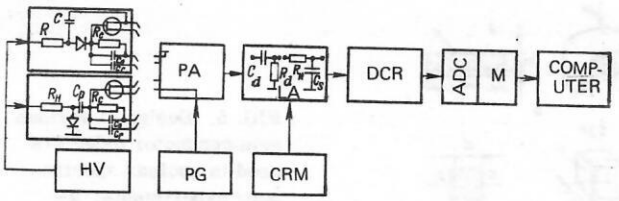

FIG. 3. Structural scheme of spectrometers with semiconductor detectors for study of radiations of radioactive nuclides: PA—preamplifier, HV—high voltage, PG—standard pulse generator, LA—linear amplifier, CRM—counting-rate meter, DCR—dc restorer; ADC—analog to digital converter; M—memory.

Structural arrangement of a semiconductor spectrometer[2]

A diagram of a spectrometer for investigation of the energy distribution of radiations of radioactive nuclides is shown in Fig. 3. Signals from a semiconductor detector are fed to the input of a charge-sensitive preamplifier (PA) and then to a spectrometric linear amplifier (LA). From the linear amplifier the signals go to a DC restorer and then to an amplitude-to-digital converter (ADC). Then the digital information is stored and processed by computer.

Taking into account all sources of noise, for a charge-sensitive preamp and a linear amplifier with single CR–RC shaping we can write[2]:

$$(\Delta E\,[\text{eV}])^2 = (2.354\sqrt{\varepsilon EF})^2 + (4.52\varepsilon/q)^2 \times \left\{\frac{0.6kT}{\tau S}(C_d + C_{\text{in}} + C_0)^2 + 0.15kTC_{sg}^2 + kT\tau\left[\left(\frac{1}{R_c} + \frac{1}{R_H}\right) + \frac{q}{2kT}(I_d + I_g)\right]\right\} + \Delta_m^2 + \Delta_{\text{res}}^2, \quad (2)$$

where F is the Fano factor, $q = 1.6\times10^{-19}$ °K, τ is the shaping constant in the linear amplifier in sec, ε is the electron-hole pair formation energy in the semiconductor detector in eV, S is the field effect transistor (FET) slope a/b, C_d and C_0 are the semiconductor capacitance and the feedback capacitance in farads, C_{sg} is the source-gate capacitance of the FET in F, C_{in} in the input capacitance of the FET excluding C_d and C_0 in F; $k = 1.38\times10^{-23}$ J/°K is the Boltzmann constant, T is the absolute temperature in °K, I_d is the inverse current of the semiconductor detector in amperes, I_g is the gate

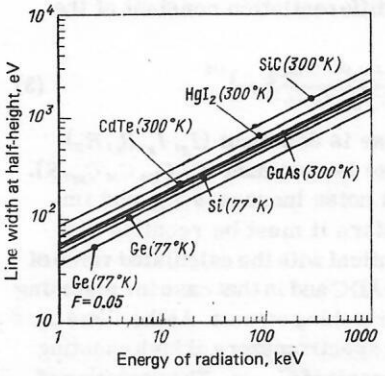

FIG. 4. Limiting energy resolution of various semiconductor detectors as a function of the energy of the detected radiation. The Fano factor is assumed arbitrarily to be $F = 0.13$.

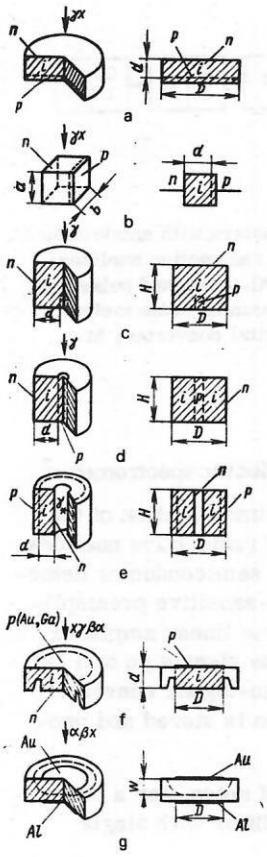

FIG. 5. Design of various semiconductor detectors used in nuclear spectroscopy experiments: a—plane parallel Ge(Li), $5 \leq d \leq 18$, $5 \leq D \leq 40$; b—plane parallel Ge(Li), $5 \leq d \leq 10$, $8 \leq a \leq 14$, $8 \leq b \leq 14$; c—coaxial with one open end, Ge(Li), $12 \leq d \leq 18$, $38 \leq D \leq 48$, $20 \leq H \leq 40$; d—coaxial with two open ends. Ge(Li), $12 \leq d \leq 18$, $38 \leq d \leq 48$, $20 \leq H \leq 40$; e—coaxial with well, Ge(Li), $12 \leq d \leq 18$, $38 \leq D \leq 50$, $30 \leq H \leq 40$; f—surface-barrier Si(Li), Ge(Li, Au), implanted Ge(Li), $2 \leq d(\mathrm{Si}) \leq 5$, $5 \leq d(\mathrm{Ge}) \leq 10$, $5 \leq D \leq 15$; g—surface-barrier Si(Au), $0.05 \leq W \leq 4$, $6 \leq D \leq 40$.

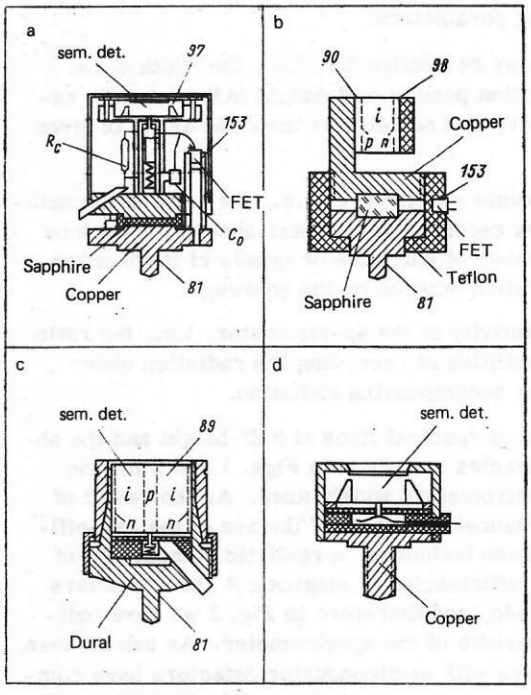

FIG. 6. Characteristic packaging arrangements of semiconductor detectors (the number shows the temperature in °K; FET is a field effect transistor).

current of the FET in amperes; Δ_m is the resolution due to microphonic noise in eV, and Δ_{res} is the resolution due to the noise of all subsequent electronic circuits. Here we have not taken into account the contribution of the effect of charge-carrier capture.

From Eq. (2) we obtain all of the requirements which are imposed on the elements of the spectrometer: the necessity of cooling the semiconductor detector (I_d is decreased), the necessity of increasing (or even removing for certain types of preamplifier; see Fig. 3) the values of R_c and R_H, the necessity of decreasing C_d (either at the expense of the area or the depth of the sensitive layer), and the need to use an FET with a large slope S.

The minimum value of noise is obtained for $\tau_{opt} = \tau_{int} = \tau_{diff}$, where τ_{int} is the integration constant of the linear amplifier and τ_{diff} is the differentiation constant of the linear amplifier. Then

$$\tau_{opt}[\mathrm{sec}] = \left\{ \frac{0.6\,(C_d + C_{in} + C_0)^2 + 0.15 C_{sg}^2}{S/R_H + S/R_c + (I_d + I_g)\,Sq/2kT} \right\}^{1/2}. \quad (3)$$

If $\tau > \tau_{opt}$, the parallel noise is dominant (I_d, I_g, R_c, R_H), and if $\tau < \tau_{opt}$, series noise is dominant (C_d, C_{in}, C_0, C_{sg}, S). Reduction of the parallel noise increases τ_{opt} and improves the resolution. Here it must be recalled that frequently τ_{opt} is not identical with the calculated value of τ of the input signal of the ADC and in that case for matching it is necessary to use a stretching circuit. At the same time the characteristics of the spectrometers at high counting rates deteriorate as the result of pileup. The variation of the signal-to-noise ratio as the result of short integration and differentiation times can be found in comparative tables, for example, in Ref. 3.

We note the inconsistency of the requirements on the values of R_c and on the circuit connecting the semiconductor detector with the preamplifier, depending on the signal-to-noise ratio and the high-counting-rate characteristics. In fact, for resistance coupling of the semiconductor detector and preamplifier the instantaneous value of the voltage drop across R_c is[3]:

$$U_{c.\,max} = (Qn + I_d)\,R_c + 3\left(\frac{Q}{C_0}\right)\sqrt{n\tau_c/2}, \quad (4)$$

where $Q = qE/\varepsilon$, $\tau_c = R_c C_0$, and n is the particle counting rate in sec^{-1}. Obviously the permissible counting rate of the spectrometer can be increased if the semiconductor detector is coupled by means of a capacitance divider (the first term is zero).

Semiconductor detectors[2]

The limiting energy resolution of various types of semiconductor detectors is shown in Fig. 4 as a function of the energy of the radiation detected. Although at the present time there have been some advances in the technology of preparing detectors of GaAs and CdTe, the requirements of experiments in nuclear spectroscopy are still satisfied only by detectors of Si and Ge.

Ge(Li) detectors. The principal purpose of these detectors is γ-ray spectrometry. The energy resolution is at the limit allowed by statistical fluctuations in the production of charge carriers in the semiconductor detector and the intrinsic noise of the electronic circuits. Ge(Li) detectors are prepared in various configurations.[4] Investigations have shown that from the point of view of the spectral line shape and the carrier collection time the uniformity of the electric field is very

TABLE I. Characteristics of detectors used.

No.	Detector	Radiation	Working temperature, °K	Geometry (see Fig. 5)	Parameters	Sensitive layer thickness, mm	Bias voltage, V	Energy resolution, keV					Region of use, keV	Manufacturer
								$E_\alpha \sim$ ~ 5 MeV	$E_e \sim$ ~ 100 keV	$E_\gamma \sim$ ~ 5 keV	$E_\gamma \sim$ ~ 100 keV	$E_\gamma \sim$ ~ 1.3 MeV		
1	Si (Au)	α	300	g	100mm² × 0.5 mm	0.5	250	15	—	—	—	—	1000—10000	LNP, JINR
2	Si (Au)	β	300	g	80mm² × 2 mm	2	1000	—	9	—	—	—	200—1000	LNP, JINR
3	Si (Li)	β x	77	f	80mm² × 4 mm	4	1500	—	0.880	0.300	0.600	—	30—3000 3—160	LNP, JINR
4	Ge (Li, Au)	β γ	77	f	80mm² × 4 mm	4	1200	—	1.3	0.400	0.600	1.65	100—4000 20—1000	LNP, JINR
5	Si (Li)	x	77	f	80mm² × 4 mm	4	1500	—	—	0.290	0.550	—	5—160	LNP, JINR
6	Ge	γ	77	(g)	25mm² × 5 mm	5	1200	—	—	0.150	0.500	—	14—279	PGT
7	Ge (Li)	γ	77	b	1.3 cm³	8	1500	—	—	—	0.600	1.65	14—600	LNP, JINR
8	Ge (Li)	γ	77	(f)	200mm² × 5 mm	5	1000	—	—	0.240	0.550	1.65	14—600	ORTEC
9	Ge	γ	77	(g)	300mm² × 7 mm	7	1500	—	—	0.250	0.550	—	14—600	PGT
10	Ge (Li)	γ	77	a	11 cm³	12	2500	—	—	—	1.3	2.2 P/C = 10/1 *	59—2750	LNP, JINR
11	Ge (Li)	γ	77	d	37 cm³	15	3000	—	—	—	1.5	2.1 P/C = 20/1	72—2750	LNP, JINR
12	Ge (Li)	γ	77	c	38 cm³	16	3000	—	—	—	0.9	1.9 P/C = 25/1	59—4000	LNP, JINR
13	Ge (Li)	γ	77	c	50 cm³	18	3000	—	—	—	1.4	2.1 P/C = 35/1	120—4000	ORTEC
14	Ge (Li)	γ	77	e	18 cm³	8	900	—	—	—	3	—	50—1500	LNP, JINR

*P/C is the peak-to-Compton ratio for a given detector.

important. Detectors are usually made in five different shapes which are used to solve the following problems (Fig. 5): a) detection of low-energy γ-ray energies with a large solid angle, b) precision measurements of γ-ray energies with exclusion of the field effect,[5] c) measurement of γ-ray spectra with high efficiency but with poorer time characteristics and in the presence of a field effect in the semiconductor detector, d) measurement of γ-ray spectra with high time resolution and in the absence of a field effect but with a lower efficiency, and e) measurement of the γ-ray spectra of weak activities.

Si(Li) detectors. The principal purpose of these detectors is spectrometry of β rays and γ rays. We can assume that the energy resolution of these detectors is close to the best possible value. Actually the best energy resolution in measurement of internal-conversion electron spectra is 880 eV for $E_e \approx 100$ keV.[6] Taking into account the features of detection of β particles with energies <100 keV (the importance of the entrance window, the conditions of charge-carrier collection, the quality of the sources, etc.), we cannot expect a substantial improvement in energy resolution. Difficulties exist also in spectrometry of low-energy γ rays (<50 keV) with high energy resolution, where preamplifiers with large values of R_c or with electron-optical (and sometimes also output-current) feedback are used. In the study of the radioactive decay of nuclides there are a number of accompanying radiations (β particles, internal-conversion electrons, α particles, γ rays) whose detection is accomplished with high efficiency in spectrometers with thin entrance windows. Difficulties with removal of charge [see Eq. (4)] from the gate of an FET lead to major restrictions on the high-counting-rate characteristics and also to deterioration of the stability of the spectrometer (see Fig. 23 of Ref. 5). Therefore a rational step to improve the quality of a spectrometer is the perfection of preamplifiers with resistive feedback.

The parameters and design of surface-barrier Si(Li) detectors are shown in Fig. 5f.

Surface-barrier Si(Au) detectors. The principal purpose of these detectors is the spectrometry of α particles, low-energy β particles, and x rays. Independently of the high energy resolution and comparatively large sensitive-layer thickness which can be achieved in Si(Au) detectors, their use in precision β and x-ray spectrometry is limited as the result of the difficulty of maintaining a constant thickness of the sensitive layer, since it depends on the bias voltage and the inverse currents in the semiconductor detector. The latter, in turn, depend greatly on the degree of vacuum achieved

in the system.

Si(Au) detectors are made of n-type silicon with a resistivity 0.5–100 kilohm-cm. The parameters and design are shown in Fig. 5g. We recall[7] that

$$W \approx 0.35\sqrt{\rho U}, \quad (5)$$

where ρ is the resistivity of n-type silicon in ohm-cm; U is the bias voltage in volts and W is the sensitive-layer thickness.

In some problems use is also made of surface-barrier detectors of p-type silicon, Si(Al). They have such advantages over Si(Au) detectors as better time characteristics for the case when the particle range is significantly less than W, radiation stability, and less difficulty in preparation of high-resistivity material. However, for the reasons mentioned above they have not found application in precision β and x-ray spectroscopy.

Surface-barrier Ge(Li, Au) detectors.[1] The principal purpose of these detectors is spectrometry of internal-conversion electrons and low-energy γ rays, the greatest interest being in simultaneous measurement of these radiations to determine the internal-conversion coefficient. Ge(Li, Au) detectors are prepared from p-type germanium. The parameters and design are shown in Fig. 5f.

We note that at an earlier stage in these same problems implanted Ge(Li) detectors were developed which had the possibility of α-particle spectrometry (see Fig. 15).[8] Unfortunately, the high rate of diffusion of lithium in Ge and the necessity of preserving the current-carrier lifetime make it impossible to anneal at optimal temperatures the radiation defects produced in implantation of gallium. This greatly hinders the further improvement of the parameters of such detectors.

Detectors of ultrapure germanium (Ge). The principal purpose is spectrometry of x rays and γ rays. The advantage over Ge(Li) detectors is that they can be stored at room temperature and cooling is necessary only during use. In our experiments we use semiconductor detectors from the firm Princeton Gamma Technology. We note that the technology developed by us for preparation of Ge(Li, Au) detectors is applicable also to initial material of ultrapure germanium.

Packaging of detectors

The packaging of detectors[2] must assure optimal operation of semiconductor detectors under working conditions [see Eq. (2)]. Depending on the type of detector and the radiation being detected, the packaging must be planned to minimize distortion of the uncorrected spectrum. The designs used are shown in Fig. 6. Special attention has been devoted to choice of the optimal temperature conditions of the crystal and of the cooled FET. For example, to obtain high energy resolution, small-volume semiconductor detectors are connected resistively to the FET and this has required testing of various insulators with good thermal conductivity to provide optimal crystal temperature; to improve the conditions of cooling of coaxial detectors and to reduce the temperature gradients, lids of thin aluminum are used; to

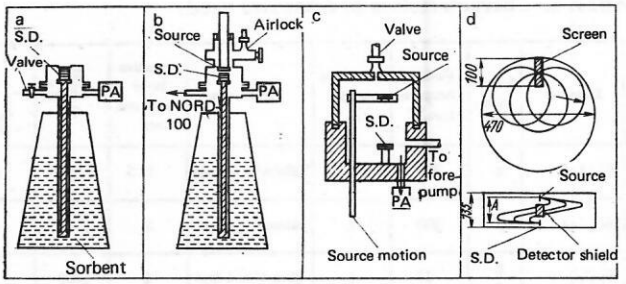

FIG. 7. Construction of spectrometers for study of the spectra of radiations from radioactive nuclides.

obtain high energy resolution the choice of the optimal temperature regime of the FET is of considerable importance; to reduce the contribution to the uncorrected spectrum from excitation of fluorescence in the materials surrounding the semiconductor detector, the mounting must be made of a material with the lowest possible Z.

The characteristics of the spectrometers used in our experiments are shown in Table I. For the commercial detectors we have indicated the manufacturer and a number of the known parameters. We note that the characteristics of charged-particle detectors are in a certain sense averaged, since they deteriorate during operation and the detectors are replaced.

Design of spectrometers

The design of the spectrometers was developed[2] with allowance for the characteristics of detection of α, β, γ, and x rays (Fig. 7). The vacuum in the chambers of the charged-particle spectrometers is produced by a system employing ion pumps of the type NORD-100. The possibility is provided of replacement of the source without destroying the vacuum in the system. All vac-

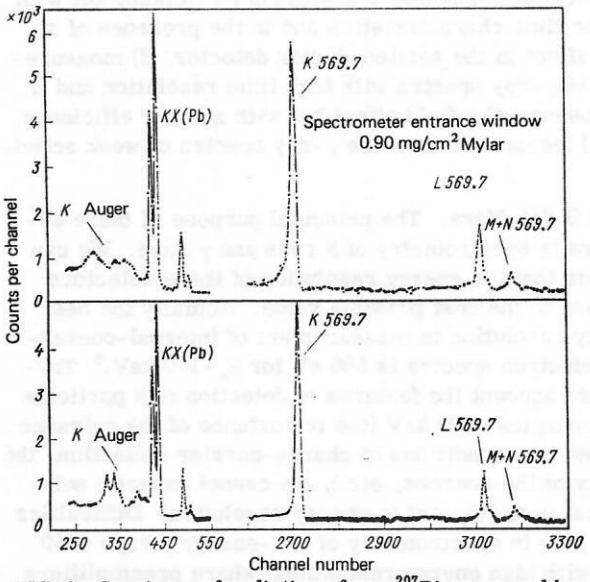

FIG. 8. Spectrum of radiations from ^{207}Bi measured by an 80 mm² × 4 mm Si(Li) detector. The entrance window was 0.90 mg/cm² Mylar.

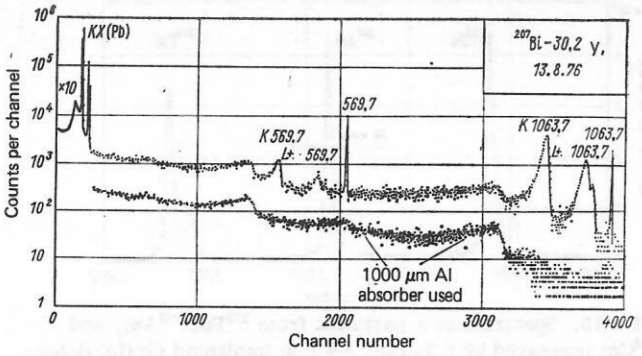

FIG. 9. Spectrum of radiations from ^{207}Bi measured by 200 mm^2 × 5 mm Ge(Li) detector. Also shown is the uncorrected ^{207}Bi spectrum with use of an absorber of 1000 μm of Al. $T_1 = 5$ years is the time elapsed since the source was obtained, $T_2 = 1$ hour is the duration of a measurement, $P = 3$ cm is the source–detector distance, B is background, SE is the single-escape peak, and DE is the double-escape peak.

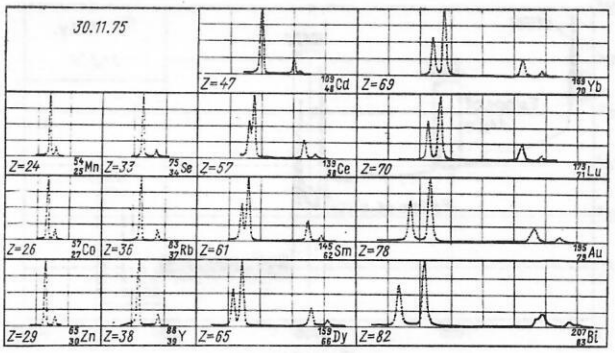

FIG. 11. Characteristic K x rays of several nuclides, measured by a 25 mm^2 × 5 mm Ge detector at constant gain.

uum seals used are greaseless.

Spectrometers for β rays, x rays, and γ rays. The mandrels with Si(Li) and Ge(Li) detectors are mounted in a cryostat with a cold finger and a sorbent, which is emersed in a standard Dewar vessel with liquid nitrogen (see Fig. 7a). Depending on the radiation being detected, various materials are used for the entrance windows: Mylar (0.90 mg/cm^2), beryllium (100–200 μm), Dural (~400 μm), and stainless steel (~200 μm). The characteristic uncorrected spectra are shown in Figs. 8–11.

Spectrometers for internal-conversion electrons. In comparison with the designs which have been described, only one change is made here: the source is replaced by means of an airlock system without destroying the vacuum (see Fig. 7b). The change requires about three minutes. The source holder permits variation of the distance from the source to the detector in the range 0.5–20 cm. Characteristic uncorrected spectra are shown in Figs. 12 and 13.

Spectrometers for α particles. Alpha spectrometers use a definite design: for simultaneous measurement of x rays, α's, γ's, and β's, an airlock chamber is used (see Fig. 7b), and for measurement of α-particle spectra without cooling the semiconductor detector use is made of a chamber which is covered during the replacement of the source [a screw permits the source-detector distance to be varied in the range 0.5–5 cm without breaking the vacuum (see Fig. 7c)]; to measure α-particle spectra without cooling the detector for purposes of precision energy measurements a special chamber is used (the standard source and the source being investigated are mounted on a rotating device with collimators before beginning the experiment). Characteristic uncorrected spectra are shown in Figs. 14 and 15.

Semiconductor beta spectrometer with a uniform magnetic field.[2] Here use is made of the motion of the electrons or positrons along a helical path in a uniform magnetic field (see Fig. 7b).[9] The energy range of the electrons collected by the detector is determined by the geometrical dimensions of the chamber and the magnetic field strength H. Use of an absorbing block in the chamber and variation of H allows discrimination against low-energy electrons and allows the weaker high-energy transitions to be studied without overloading the detector. The detector is placed under the source, the shielding from direct radiation is accomplished by a layer of W (40 mm), Cd (1 mm), Cu (0.5 mm), and Al (0.5 mm). An L-shaped cryostat connected to the spectrometer vacuum chamber is used to cool the detector. Change of the source without breaking the vacuum in the spectrometer chamber is carried out by means of an airlock system in three minutes. The operation of the spectrometer is illustrated by the internal-conversion spectrum of ^{206}Po+^{206}Bi measured at four values of H: 250, 500, 750, and 1000 G (Fig. 16).

Still other dispersion-free magnetic arrangements

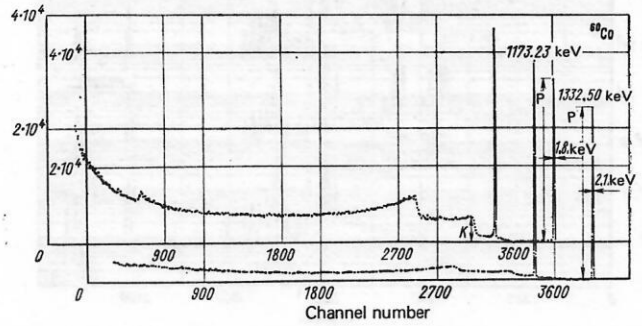

FIG. 10. Spectrum of γ rays from ^{60}Co measured by Ge(Li) detectors of volume 1 and 37 cm^3 (P is the peak height and K is the height of the Compton edge).

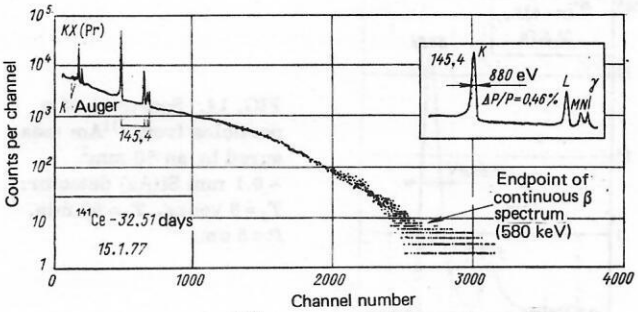

FIG. 12. Spectrum of ^{141}Ce measured by an 80 mm^2 × 4 mm Si(Li) detector: $T_1 = 22$ days, $T_2 = 6$ hours, $P = 6$ cm.

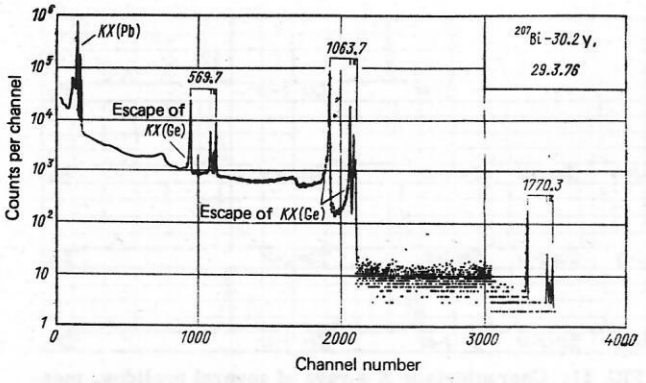

FIG. 13. Spectrum of ^{207}Bi measured by an 80 mm^2 × 5 mm Ge(Li, Au) detector: T_1 = 5 years, T_2 = 6 hours, P = 5 cm.

permitting significant reduction of the background of accompanying β particles are described in the literature. They all have disadvantages. For example, the version of Ref. 9 has comparatively low efficiency; the version of Ref. 10 assumes use of a superconducting solenoid and has a high efficiency but unfortunately does not separate electrons from positrons; the version of Ref. 11 is based on the Thibault spectrometer and has comparatively high efficiency, but the electron drift time depends greatly on the energy. In addition, the last two versions[10,11] have a common deficiency: the detected β particles hit the semiconductor detector at a small angle to the surface, which leads to enhancement of the dependence of backscattering on energy.

Spectrometric apparatus

Proceeding from the requirements of the physical problem, we used various combinations of detectors, spectrometer channels, and analyzing apparatus (Fig. 17). The electronic circuits were chosen on the basis of the following requirements: optimum signal-to-noise ratio, good characteristics at high counting rates (up to 5×10^4 counts per second), stability with change of temperature, and linearity. In the first stage all of the analog and auxilliary circuits were constructed by us.[4] Later we used some electronic circuits and γ-ray detectors from several commercial firms, namely ORTEC, Princeton Gamma Technology, and Polon. In the linear amplifier we used a discrete system of amplification switching which provides simplicity of conversion during an experiment and satisfies the requirements arising in measurements of the characteristics of the radiation (system nonlinearity, suitability for half-life measurements, and so forth). Monitoring of the spectrometer counting rate is carried on by means of an analog counting-rate meter (CRM) which is connected to the appropriate channel at the time of measurement. All of the analyzing apparatus (the analyzers TRIDAC-C and DIDAC) was made by Intertechnique. For transmission of digital information to the Minsk-2 computer we constructed a special unidirectional connection by means of an RG-23 tape recorder.[12]

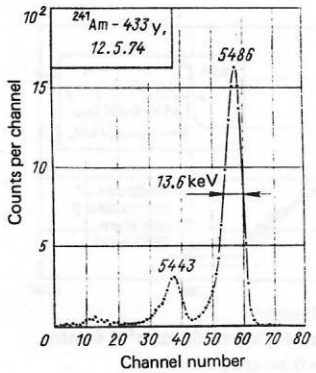

FIG. 14. Spectrum of α particles from ^{241}Am measured by an 80 mm^2 × 0.1 mm Si(Au) detector: T_1 = 3 years, T_2 = 60 min, P = 5 cm.

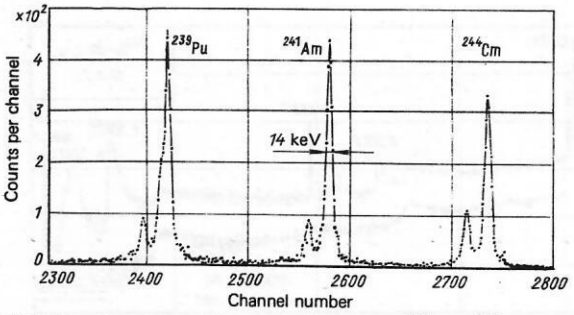

FIG. 15. Spectrum of α particles from ^{239}Pu, ^{241}Am, and ^{244}Cm measured by a 30 mm^2 × 4 mm implanted Ge(Li) detector.

We shall discuss briefly the instrumental effects leading to deterioration of the shape of a spectral line[5]:

a) The time stability is checked by means of source of ^{57}Co + ^{137}Cs + ^{60}Co and a Ge(Li) detector for a period of thirty hours; the measurement time is twenty minutes and the intervals between the measurements are ten minutes. The results of the experiment are shown in Fig. 18. The data provide a basis for discussion of the randomness of the spread after the temperature conditions have been established for five hours, and consequently this factor can be considered as an additional contribution to the energy resolution for extended ex-

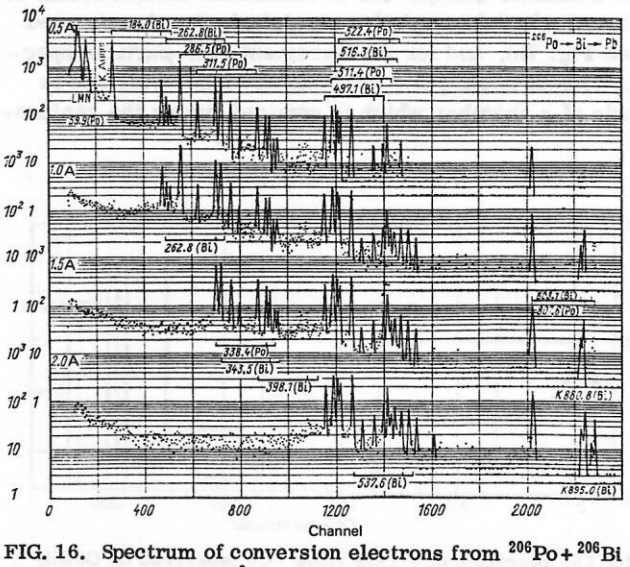

FIG. 16. Spectrum of conversion electrons from ^{206}Po + ^{206}Bi measured by an 80 mm^2 × 4 mm Si(Li) detector in a uniform magnetic field for various values of H.

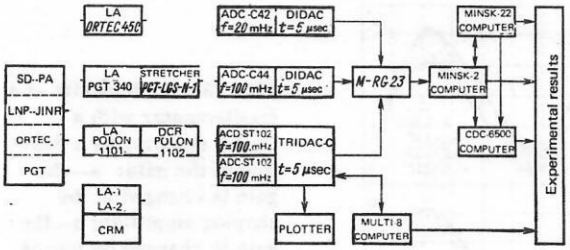

FIG. 17. Spectrometric apparatus for study of radiations of radioactive nuclides: f is the counting frequency of the ADC, t is the memory access time, and M is a magnetic tape.

periments, which has only a small influence on the accuracy of the results.

b) The temperature stability was checked under similar conditions; the results are shown in Fig. 19. It is evident that it is necessary to maintain the temperature in the room within ±1 °C during the measurements.

c) The high-counting-rate characteristics of the spectrometers have a substantial influence on the accuracy of determining the location of the maximum P and the area S of a spectral line if the measurement time is no less than $T_{1/2}$ of the nuclide under study. For illustration we have shown in Fig. 20 the dependence of P and σ on the spectrometer counting rate and the shaping constant. As can be seen, the limits of variation of the counting rate determine the maximum achievable accuracy in the determination of P and consequently also of the energy of the radiation. It follows from this that there are two means of reducing the influence of this effect: decrease of the value of τ if the complexity of the spectrum permits use of a poorer energy resolution, or use of a device which provides constancy of the counting rate by automatically changing the distance from the source to the detector.[5]

d) Nonlinearity of the spectrometric system. Analysis of the memory stage of the analog-to-digital converter (ADC) with intermediate linear conversion to a time interval shows[13] that the deviation from a linear characteristic of $\Delta U/U$ at large amplitudes of the input pulses increases as the rise time of the pulses is decreased (Fig. 21). For small pulse heights the sign of $\Delta U/U$ changes as the result of the increase in the contribution of transient processes due to the presence of a nonlinear element in the memory circuit. The sharp increase of $\Delta U/U$ in the high-voltage region (which is shown only for a sharper with $\tau = 2$ μsec) is determined by the limitation on the maximum in the amplifier of the charging circuit of the converter. The departure from linearity

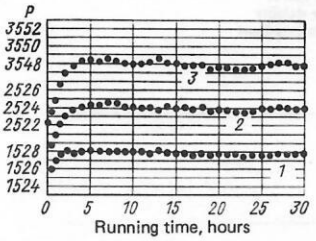

FIG. 18. Time stability of a spectrometer with a Ge(Li) detector and a TRIDAC-C system: 1—E = 122 keV, 2—E = 661 keV, 3—E = 1332 keV; P is the position of the peak of the spectral line.

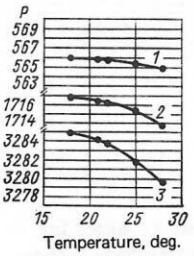

FIG. 19. Temperature stability of a spectrometer with a Ge(Li) detector and a TRIDAC-C system (the designations are the same as in Fig. 18).

due to the limitation of the pulse heights in the final stage of the linear amplifier shows up in a similar manner. The experimentally measured dependence of the nonlinearity on τ is shown in Fig. 22 for $\tau = 0.5$, 1.0, 1.5, and 2.0 μsec. The same effect is observed on adjustment of the gain if the transient characteristics of the shaping amplifier are changed (Fig. 23).

The factors affecting the energy resolution of spectrometers employing semiconductor detectors are shown in Table II.[39]

2. PROCESSING OF INFORMATION ON A SPECTRAL LINE BY COMPUTER

The accuracy in measurement of the energies and intensities of monoenergetic radiations of radioactive nuclides is determined by the characteristics of the semiconductor detector, the measurement technique, and to a considerable extent by the use of computers for processing of the information on the spectral lines. There are several means of modeling peaks.[14] However, for reasons of mathematical simplicity, directness of physical interpretation, and minimal requirements on memory size and computer speed, the most extensive use is made of approximation of the peak by a symmetric Gaussian.

For approximation of a spectral line we use a Gaussian distribution integrated over a single channel (the program Katok[15,16]):

$$N(k) = \frac{S}{\sigma\sqrt{2\pi}} \int_{k-1}^{k} \exp\left[-\left(\frac{K-p}{\sigma\sqrt{2}}\right)^2\right] dx + \sum_{i=0}^{l} a_i k^i, \qquad (6)$$

where $N(k)$ is the number of pulses in channel k, S is the number of pulses under the peak, $\sigma = h(2\sqrt{2\ln 2})^{-1}$, h is the width of the peak at half height, p is the location of the maximum at the peak, and $\sum_{i=0}^{l} a_i k^i$ is a polynomial of degree l describing the background under the peak. The value of l is chosen by analysis of σ (or h), whose dependence on energy must be investigated experimen-

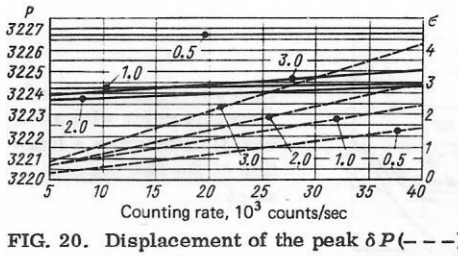

FIG. 20. Displacement of the peak δP (– – –) and width σ (———) of a spectral line as a function of counting rate for a spectrometer with a Ge(Li) detector (for various values of τ).

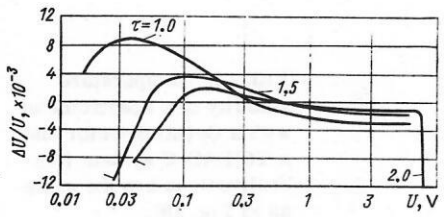

FIG. 21. Dependence of $\Delta U/U$ on U for various τ values for an analog-to-digital converter with linear intermediate transformation to a time interval.

tally (see, for example, Fig. 1). Regions where σ differs are processed again with other initial approximations.

Preparation of the initial material by the program Raxmetka[17] (marking) consists of specifying the initial approximations by means of a display with a light pen and recording them on a magnetic tape. In view of the smallness of the regions (less than 96 channels) we can assume that the condition of constancy of σ is correct. Exceptions are the region of characteristic radiation (x-ray structural lines) and the energy region 511 keV (the annihilation peak, naturally, is broadened). Processing of all the regions mentioned is carried out automatically. As the final results we print out the parameters θ^2, σ, $\Delta\sigma$, P, ΔP, S, ΔS, a_i, and Δa_i, where

$$\theta^2=\{\sum_{k_i}^{k_k}[N(k)-N^{\text{appr}}(k)]\}/(k_f-k_i-nm-l); \quad (7)$$

here N^{appr} is the approximated number of pulses in a channel, n is the number of peaks in the region, k_f and k_i are the channel numbers at the end and beginning of the spectrum, and m is the number of parameters. In addition, the values of P, ΔP, S, ΔS, and σ are sorted in the computer memory by means of a special program for the subsequent analysis. We note that the method used in the program is applicable to degenerate problems and permits determination of the number of peaks in a region.[18]

The values of ΔP and $\Delta S/S$ are investigated as a function of S, as well as the ratio of the maximum value of peak height in the absence of background to the height of the background under the peak and the dependence of $\Delta P/\sigma$ and $\Delta S/S$ on σ (Figs. 24–26). The measurements were made with a Ge(Li) detector and a ^{57}Co source (with energy 122 keV). The dependence of $\Delta S/S$ and $\Delta P/\sigma$ on σ were studied for $S=1.6\times10^5$ counts, so that the statistical spread has little influence on the accuracy of the results (see Fig. 25). In investigation of $\Delta S/S$ and ΔP as a function of the peak-to-background ratio the

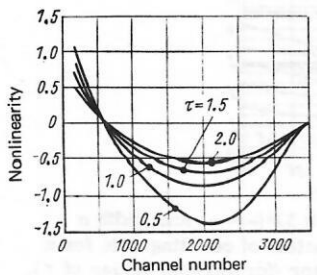

FIG. 22. Nonlinearity of a spectrometer with a Ge(Li) detector as a function of the shaping constant τ.

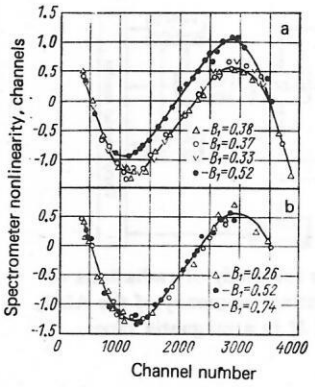

FIG. 23. Nonlinearity of a spectrometer with a Ge(Li) detector as a function of the gain: a—the gain is changed in the shaping amplifier; b—the gain is changed by means of a frequency-independent attenuator.

previously measured peak with energy 122 keV (^{57}Co, $S=1.6\times10^5$ counts) was raised by the continuous Compton distribution from the ^{60}Co source (the gain was chosen such that the peak from ^{57}Co lay on the smooth portion of the Compton distribution). In Fig. 26 we have shown also the stability of the analysis ($P\pm\Delta P, S\pm\Delta S$) as a function of the peak-to-background ratio. The results enable us to choose correctly the exposure time (see Fig. 24), the channel size (see Fig. 25), and the detector (see Fig. 26).

In processing spectra from semiconductor spectrometers with high energy resolution there are difficulties due to the asymmetry of a peak on the low-energy side

TABLE II. Factors affecting energy resolution of semiconductor spectrometers.

Radioactive source. Fluctuations of energy loss in source	Cause A. Insufficient source thickness B. Statistical fluctuations of energy loss in source thickness
Semiconductor detector	
1. Fluctuations of energy loss in detector entrance window	A. Variations in entrance-window thickness B. Statistical fluctuations of energy loss in entrance window C. Spread in angles of incidence
2. Fluctuations of number of liberated carrier pairs in detector	Transfer of energy to lattice as the result of: a) interaction with electrons; b) scattering by nuclei. Usually a) >> b)
3. Fluctuations of carrier collection efficiency	A. Statistics of recombination and attachment B. Inhomogeneities (local fluctuations of carrier lifetime) C. Edge effects Usually A << B
4. Detector noise	A. Inverse current: a) volume current–diffusion and generation; b) surface current B. Contact noise
Preamplifier	
1. Preamplifier noise	A. Thermal noise of resistors at FET input B. Shot noise of gate current C. Thermal noise of FET channel D. Microphonic noise E. Noise of elements following FET
2. Stability of gain	A. Stability of C_0 B. Temperature stability of preamp elements
Linear amplifier	
1. Linear amplifier characteristics	A. Reduced noise at linear-amplifier input B. Type of shaper C. Baseline stability D. Negative overshoot
2. High-counting-rate characteristics	
3. Stability of gain	
ADC	
1. Determines parameters of linear-amplifier output pulse	
2. Temperature stability	

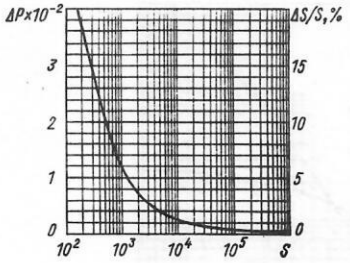

FIG. 24. Error in determination of the area $\Delta S/S$ and position of the maximum of the peak ΔP as a function of S with use of the program Katok (σ = 3.3 channels; peak/background = 100).

(see, for example, Fig. 12). The causes of asymmetry of a spectral line are as follows: poor collection of charge carriers in the semiconductor detector, presence of a thick exit window in the semiconductor detector in detection of charged particles, use of thick sources in spectrometry of charged particles, occurrence of escape of characteristic radiation in detection of low-energy radiations at the boundary of the sensitive layer, pileup of pulses at the output of the linear amplifier (Fig. 27a), poor DC restoration and consequently pileup of pulses in the linear amplifier (Fig. 27b), oscillation of the base line (Fig. 27c), high counting rate in the spectrometer for a given τ (pileup of pulses, Fig. 27d), instability of the spectrometric apparatus with time, and temperature stability. To evaluate the possibility of use of the program Katok in such problems, we obtained asymmetric peaks by changing the DC restoration at a constant counting rate. The results of this investigation are shown in Fig. 28; as the asymmetry parameter we took the ratio of the left and right half-baselines from the peak at 1/10 height, for the channel with the highest counting rate. As can be seen, the greatest permissible asymmetry f must be less than 1.5. However, if $f > 1.5$, the error rises rapidly but the value of S obtained coincides with the true value within the error.

3. EFFECTS DISTORTING THE SHAPE OF THE UNCORRECTED SPECTRUM

In measurement of the spectra of radiations from radioactive nuclides by means of semiconductor detectors it is possible to separate three groups of effects (the radioactive source, the semiconductor detector, and their relative arrangement) which distort the shape of the uncorrected spectrum. The necessity of a more detailed discussion of these effects is evident, for example, from analysis of the spectrum of γ rays from ^{139}Ce measured by means of a 200 mm^2×5 mm Ge(Li) detector (Fig. 29). The source was deposited on a copper substrate of thickness 500 μm. In the decay of ^{139}Ce there is only one γ transition. However, in the spectrum presented more than 20 different peaks are observed.

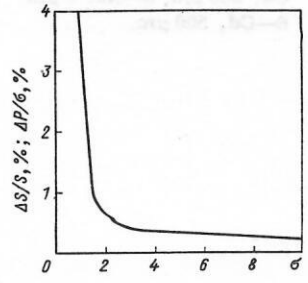

FIG. 25. Dependence of $\Delta S/S$ and $\Delta P/\sigma$ on σ with use of the program Katok ($S = 1.6 \times 10^5$ counts).

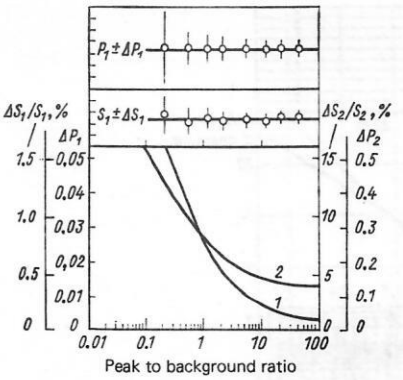

FIG. 26. Error and stability of determination of the area and position of the maximum of a peak as a function of peak to background ratio with use of the program Katok: 1—$S_1 = 1.2 \times 10^5$ counts, $\sigma_1 = 2.96$ channels; 2—$S_2 = 1.1 \times 10^4$ counts, $\sigma_2 = 3.05$ channels.

1. Gamma spectroscopy

The effects associated with the radioactive source are as follows.

1.1. *Scattering from the source backing.* The differential cross section per unit solid angle for photons scattered at an angle θ is shown in Fig. 30. It is evident that as the result of backscattering the choice of the material, atomic number, and thickness of the backing can substantially affect the behavior of the continuous distribution in the vicinity of a spectral line (Fig. 31) and this can lead to ambiguity in selection of the background parameters for data processing by computer.

1.2. *Accompanying radiations.* In the study of γ-ray spectra in detectors with a thin entrance window, difficulties arise as the result of incidence of β particles onto the sensitive region of the detector (see Fig. 9). In addition to deterioration of the background conditions, the effect leads to difficulties in the use of spectrome-

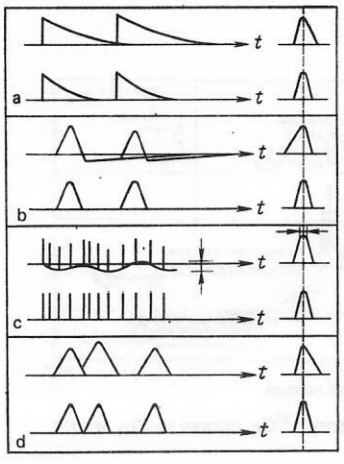

FIG. 27. Uncorrected spectra leading to asymmetry of a spectral line: a—pileup of pulses at the output of the preamplifier; b—poor dc restoration; c—baseline oscillation; d—pileup and linear amplifier for a given τ.

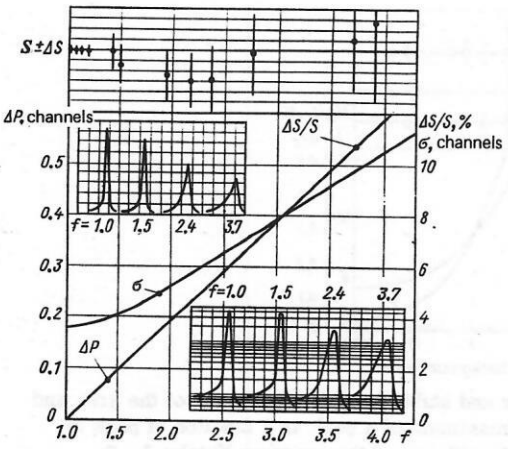

FIG. 28. Error and stability in determination of the area and maximum of the peak as a function of its asymmetry f (ratio of the left and right half-bases of the peak at 1/10 height) with use of the program Katok ($S = 10^5$ counts). For convenience in interpretation some of the uncorrected peaks are shown on both a linear and a logarithmic scale.

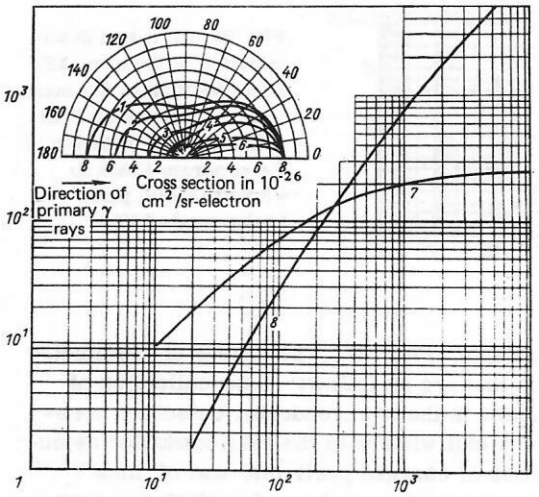

FIG. 30. Differential cross section for Compton scattering of photons at an angle θ: 1—0 KeV, 2—50 keV, 3—200 keV, 4—500 keV, 5—2000 keV, 6—5000 keV, 7—energy of backscattered γ rays, 8—maximum energy of Compton electrons.

ters with high resolution (<300 eV) as the result of accumulation of charge from higher-energy β particles on the gate of the FET.

1.3. *Scattering in the source.* This effect leads to distribution of the shape of the continuous distribution in the vicinity of a spectral line and to distortion of the intensity of the γ lines as the result of absorption. In particular, special caution must be observed in investigation of γ-ray spectra from sources with a carrier.

1.4. *Excitation of characteristic x rays in the backing (see Fig. 29) and in the source itself (Fig. 32).* It can be seen that in measurement of the γ-ray spectra of sources with a carrier the intensity of the x-ray lines can be distorted substantially as the result of fluorescence in the material of the source itself when a spectrometer with insufficient energy resolution is used.

The effects associated with the characteristics of the semiconductor detectors are as follows.

1.5. *Dependence of the cross sections for the photoeffect, Compton scattering, and pair production on the Z of the detector and the energy of the detected quanta.* These dependences are shown in Fig. 33. With increase

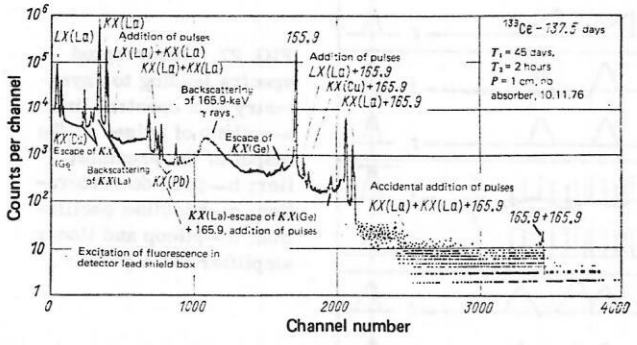

FIG. 29. Spectrum of γ rays from ^{139}Ce measured by a 200 mm^2 ×5 mm Ge(Li) detector.

of E the role of the photoeffect decreases but the total-absorption peak retains an appreciable value as the result of the multiple Compton scattering in the sensitive region of the detector. The choice of the geometrical dimensions of the crystal governs the energy resolution and the efficiency of the detector. As characteristics of a spectrometer for high-energy γ rays it is customary to give the ratio of the peak height p to the height of the Compton edge C for the 1332-keV transition of ^{60}Co; this ratio is a complex characteristic of the energy resolution and efficiency (see Fig. 10). However, the quality of a spectrometer for low-energy γ rays is characterized by its energy resolution and its sensitive area.

1.6. *Escape of annihilation radiation in pair production in the detector material* (E>1022 keV). The effect of pair production competes with multiple Compton scat-

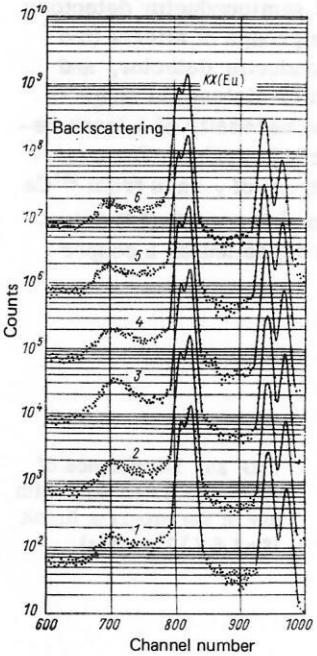

FIG. 31. Shape of uncorrected spectrum as a function of material and thickness of source backing: 1—Al, 18μm; 2—Al, 100 μm; 3—Al, 1000 μm; 4—Cu, 500 μm; 5—Au, 8 μm; 6—Cd, 500 μm.

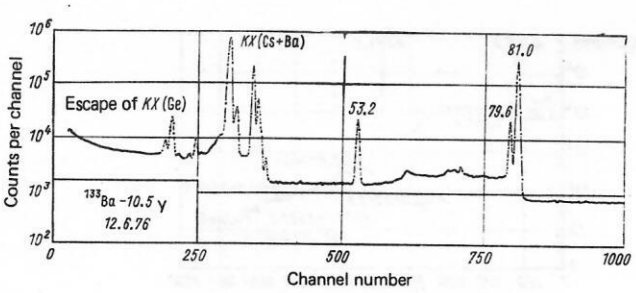

FIG. 32. Spectrum of low-energy γ rays from ^{133}Ba (source with carrier) measured by a 200 mm^2 ×5 mm Ge(Li) detector. The KX(Ba) peaks are due to fluorescence in the source; T_1 = 5 years, T_2 = 4 hours, P = 6 cm.

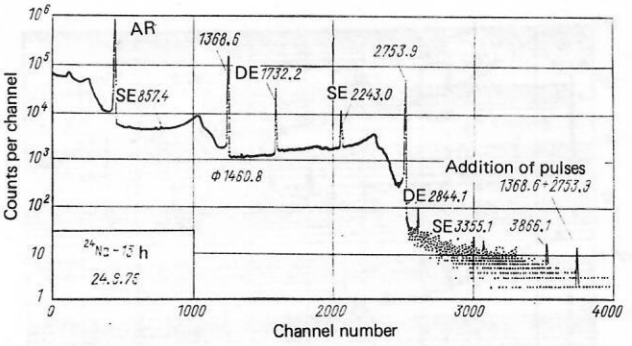

FIG. 34. Gamma-ray spectrum of ^{24}Na measured by a 38 cm^3 Ge(Li) detector: T_1 = 5 hours, T_2 = 5 hours, P = 10 cm.

tering; on observation of a number of precautions which take into account the kinematics of pair production and the pair-detection process, this effect can be used successfully to measure energies and intensities of γ rays. Let us consider the shape of the double-escape (DE) spectral line: the background pedestal of the right-hand portion of the peak is raised as the result of Compton scattering of annihilation γ rays before their escape from the detector (Fig. 34). In addition, the intensities of the single-escape (SE) and double-escape peaks depend strongly on the configuration and sensitive volume of the Ge(Li) detector.

1.7. *Escape of characteristic x rays from the detector sensitive volume.* This effect is important in the low-energy region where the photoeffect occurs at the boundary of the sensitive region and the probability of escape of the characteristic radiation is high (see Figs. 29 and 32).

1.8. *Scattering in the entrance window of the detector.* This effect is similar to that discussed in Sec. 1.3 above.

1.9. *Efficiency of charge collection in the detector sensitive volume.* If we assume that the conditions for high-quality measurements are satisfied (DC restoration, absence of scattering materials in the path from the source to the detector, and low counting rate), the broadening of a spectral line is determined mainly by the efficiency of charge collection. Then on the assumption of a Gaussian shape of the peak we should have the relations

$$a_1 \equiv \Delta E\,(1/100)/\Delta E\,(1/10) = 1.41; \quad a_2 \equiv \Delta E\,(1/10)/\Delta E\,(1/2) = 1.83, \tag{8}$$

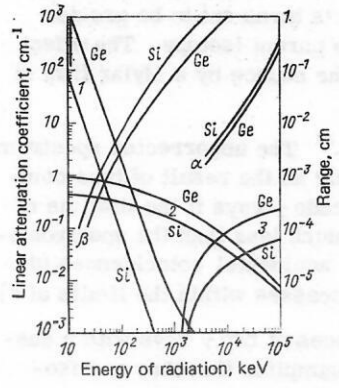

FIG. 33. Gamma-ray linear attenuation coefficient and range R for electrons and α particles as a function of energy for Si and Ge: 1—photoeffect, 2—Compton effect, 3—pair production.

where ΔE is the width of the peak at the height indicated in parentheses. For example, for Ge(Li) detectors of volume 1 and 37 cm^3 these values are respectively a_1 = 2.15 ± 0.10, a_2 = 1.86 ± 0.06 and a_1 = 2.15 ± 0.06, a_2 = 1.85 ± 0.05. It is evident that the coefficients a_2 agree with the theoretical values for a symmetric peak. A certain asymmetry of the peak on the low-energy side can result from escape of photoelectrons (or Compton electrons in the case of multiple scattering) from the detector sensitive volume. Of course, the contribution of this factor depends on the geometrical dimensions of the crystal and on the energy of the detected radiation.

The external effects are as follows.

1.10. *Scattering in the entrance window of the vacuum chamber (Al, Be, Mylar) and in the absorbers.* This effect determines the lower-energy threshold of the spectrometer (Fig. 35). Here the depression of the total-absorption peaks does not always remove the effects of addition (see below) and does not always decrease in proportion the spectrometer counting rate, since Compton scattering occurs in the absorbers with subsequent detection. We note that the solid angle for detection of the scattered radiation depends on the absorber-detector distance.

1.11. *Excitation of characteristic x rays in the materials surrounding the detector and source.* This discussion is similar to that in Sec. 1.4. Distortions arise most frequently as the result of fluorescence of brass (Cu+Zn) and indium used in making the detector mount.[2]

1.12. *Detection of annihilation γ rays* arising in interaction of high-energy quanta with the materials sur-

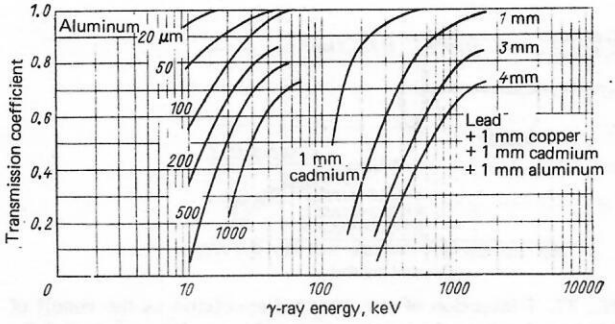

FIG. 35. Transmission coefficient of monoenergetic γ rays as a function of thickness and composition of absorbers.

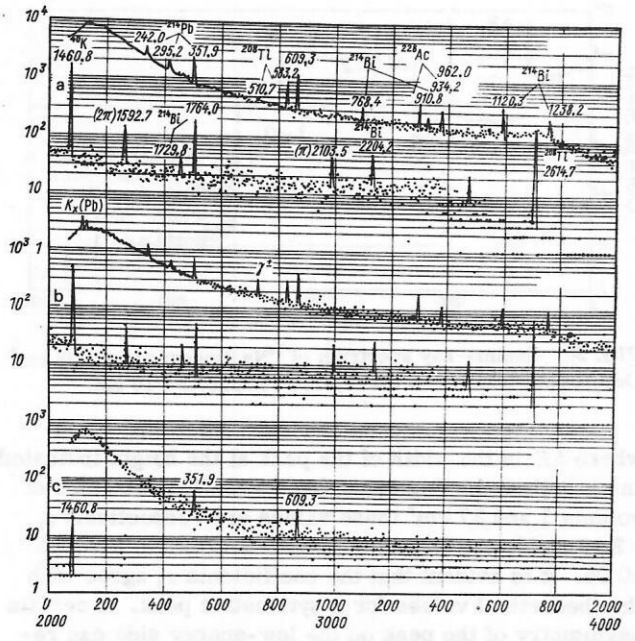

FIG. 36. Gamma-ray spectrum of the natural radioactive background, measured by a Ge(Li) detector (37 cm^3) without a shield (a) and with a lead shield (b) and with a 1 cm^3 Ge(Li) detector without a lead shield (c).

rounding the detector. The effects from the detector shielding box are shown in Fig. 36 (see Sec. 1.16).

1.13. *Scattering of γ rays in the materials surrounding the detector.* The design and material of the detector mounting lead to distortion of the uncorrected spectrum at the result of Compton scattering, for which the detection solid angle is large. This must be taken into account in the design of the spectrometer.[2,4]

1.14. *External bremsstrahlung.* This effect is important only in the study of low-intensity transitions in intense β radiation.

1.15. *Dependence of the position of the peak of a spectral line on the measurement geometry.* This effect has been investigated in Ref. 18 for various types of semiconductor detectors. For example, for planar detectors the effect is maximal if the direction of motion of the γ rays coincides with the direction of the applied field and is vanishingly small if the directions are mutually perpendicular. We chose the conditions for measurement of γ-ray energies in planar detectors with allowance for this fact (see Fig. 6b).

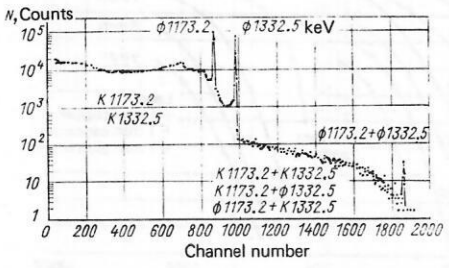

FIG. 37. Distortion of uncorrected spectrum as the result of addition of pulses due to true coincidences (37 cm^3 Ge(Li) detector, counting rate 10^3 counts per second, source-detector distance 7 cm; ϕ is the total absorption peak).

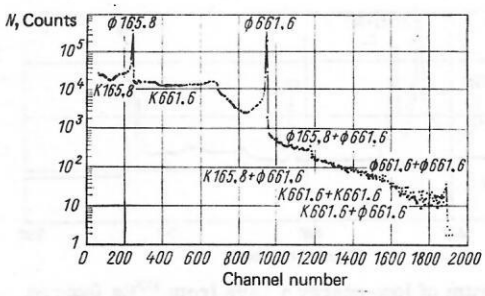

FIG. 38. Distortion of uncorrected spectrum as the result of addition of pulses due to accidental coincidences (37 cm^3 Ge(Li) detector, counting rate 2×10^4 counts per second).

In coaxial detectors the effect is important for crystals with one open end face and is negligible for crystals with two open ends. The effect of the field has been studied by us for a 37-cm^3 Ge(Li) detector with two open ends for $E = 1173$ keV (^{60}Co). If there is a geometry effect in measurement of the γ-ray energies, its value for the case investigated, which is 0.003 ± 0.008 keV for location of the source to one side of the detector and 0.004 ± 0.008 keV for variation of the distance along a frontal line from 6 to 39 cm, can be neglected.

1.16. *The natural radioactive background* can significantly affect the distortion of the intensities of weak γ lines during extended measurements. The principal sources of the background are ^{40}K and the decay products of ^{226}Ra and ^{232}Th. The uncorrected spectra for various measurement conditions are shown in Fig. 36. As can be seen, use of shielding of natural lead substantially depresses the radioactive background. Here there arise distortions due to excitation of the characteristic x rays of Pb (see Sec. 1.11) and Compton scattering and pair production in Pb (the 511-keV peak increases; see Sec. 1.12). In some situations in the study of low-intensity γ transitions the use of Ge(Li) detectors with a small sensitive volume turns out to be successful, since the background is proportional to the detector volume (Fig. 36c).

1.17. *Distortion of γ-ray intensities in study of chains of α-active nuclides as the result of recoil nuclei.* This effect is produced by the escape of the recoil nuclei from the source and their incidence on the lid of the spectrometer. As a result, the solid angle for detection of the daughter products turns out to be greater than the solid angle for the parent isotope. The effect is removed by screening the source by a Mylar film of thickness about 1 mg/cm^2.

1.18. *Addition of pulses.*[20] The uncorrected spectrum can be distorted appreciably as the result of true coincidences (detection of cascade γ rays if the lifetime of the intermediate state is much less than the spectrometer resolution time τ) and accidental coincidences (detection of uncorrelated processes within the limits of τ).

The number of coincidences of two γ rays with a cascade intensity A on the assumption that they are iso-

tropically distributed can be written as follows:

$$A_{\gamma_1\gamma_2}=\frac{A}{(1+\alpha_1)(1+\alpha_2)}\frac{\Omega\Phi_1}{4\pi}\frac{\Omega\Phi_2}{4\pi}\times\left[\frac{K_1}{\Phi_1}\frac{K_2}{\Phi_2}+\frac{K_1}{\Phi_1}+\frac{K_2}{\Phi_2}+1\right], \quad (9)$$

where α_i is the total conversion coefficient of the i-th transition, Ω is the detection solid angle, Φ_i is the detection efficiency of the i-th γ ray as the result of Compton scattering. It is easy to estimate from this the contribution of all effects: the term $(K_1/\Phi_1)(K_2/\Phi_2)$ corresponds to coincidence of the Compton distributions of E_1 and E_2 and is of no interest; the term K_i/Φ_i corresponds to coincidence of a Compton-scattered γ ray with another completely absorbed γ ray; the term unity corresponds to coincidence of completely absorbed cascade γ rays. For example, for a Ge(Li) detector (37 cm^3, ^{60}Co source, source-detector distance 7 cm; Fig. 37) the loss in I_γ (1332 keV) as the result of switching into the sum peak is 0.04%. At the same time the loss due to coincidences of K(1173 keV) and Φ(1332 keV) is 0.66%. It is assumed that there are no accidental coincidences (counting rate $<10^3$ counts/sec).

For monoenergetic γ rays with energy E_1 the following additions are possible as the result of accidental coincidences: K_1+K_1, $K_1+\Phi_1$, and $\Phi_1+\Phi_1$. In the case of detection of γ rays with energy E_2, in addition to analogous events it is also possible to have K_1+K_2, $K_1+\Phi_2$, $K_2+\Phi_1$, and $\Phi_1+\Phi_2$ (Fig. 38). Of these effects the important ones are Φ_i+K_j and $\Phi_1+\Phi_2$, since they lead to transfer of the pulses out of the total-absorption peak. For coincidences of the type $K_i+\Phi_j$ and K_i+K_j we can write $N_{ac}=2\tau_1 N_i N_j$; for $\Phi_i+\Phi_j$ we will have $N_{ac}=2\tau_2 N_i N_j$. Here τ_1 is the time shift between the added pulses if analysis of the distorted sum pulse still occurs in the ADC; τ_2 is the time within which the sum of two pulses from the total-absorption peak gives a peak with the instrumental width. For a 37-cm^3 Ge(Li) detector with a counting rate 2×10^4 counts/sec an experimental estimate gives $\tau_1=3$ and $\tau_2=0.8$ μsec. Hence the loss is intensity of the 661.6-keV line as the result of transfer into the distribution of accidental coincidences is 3.4%, while 0.05% is transferred to the accidental-coincidence peak.

2. Beta spectrometry

The effects associated with the radioactive source are as follows.

2.1. *Scattering from the source backing.* The scattering of β particles in the energy region from 10 keV to 10 MeV is determined mainly by elastic collisions with nuclei.[21] Distributions are made between single scattering, plural scattering, multiple scattering, and diffusion. All types of scattering can occur in the source backing, and this leads to an increase of the number of low-energy β particles. Inclusion of the backing effect is essential in investigation of continuous β spectra, but this involves great experimental difficulties.[22] However, in the study of internal-conversion electron spectra it is sufficient to observe the most general requirements: the lowest possible values of thickness and Z of the backing and use of electrically conducting materials. In particular, the sources used by us are prepared on a backing of aluminum 18 μm thick.

2.2. *Scattering in the source material.* In passage through a layer of matter, β particles lose energy as the result of collisions with electrons of the medium and emission of bremsstrahlung.[21] This effect leads to an increase of the number of low-energy particles and also to asymmetry of the peak and a shift toward lower energies. To reduce the contribution of these effects, sources are prepared by electromagnetic mass separation (the energy of implantation of the ions is 25 keV).

2.3. *Accompanying radiation.* A particularly complicated region for study of internal-conversion electron spectra is the region below 100 keV, where the characteristic radiation is intense and the internal-conversion coefficients are high. Difficulties also exist in the study of internal-conversion electron spectra in the background of intense positron and α-particle radiation, and in the study of weak positron spectra in a background of internal-conversion electrons, γ rays, and α particles. To remove the accompanying radiations we use a dispersionless magnetic apparatus (see Fig. 7e). It must be recalled that none of the methods of removing the accompanying radiations in the study of electron spectra permit complete removal of the spectrum distortion due to Compton electrons from γ rays.

2.4. *Excitation of characteristic radiation in the backing and in the source itself.* The discussion here is similar to that in Sec. 1.4.

The effects associated with the characteristics of the semiconductor detectors are as follows.

2.5. *Dependence of range on the Z of the detector material and the energy of the β particles recorded* (see Fig. 33). In investigation of the spectra of low-energy β particles ($E_\beta<1$ MeV) use is made of Si(Au) and Si(Li) detectors, which have a high efficiency for the radiation studied and a comparatively low sensitivity for the accompanying radiation. On the other hand, spectrometry of high-energy β particles (above 500 keV) is best carried out with thick Si(Li) and Ge(Li) detectors.

2.6. *Scattering in the detector entrance window.* The discussion here is similar to that in Sec. 1.3.

2.7. *Backscattering from the detector surface.* Experimental studies have shown that for normal incidence the backscattering coefficient does not depend on the initial energy of the electrons being scattered but depends on the Z of the scattering material; here[21] $p^-/p^+=1.3$ (the minus sign refers to an electron and the plus sign to a positron). This effect, however, depends strongly on the angle of incidence.[23]

2.8. *Bremsstrahlung of β particles and the escape of the bremsstrahlung from the detector sensitive region.* This effect has not yet been studied experimentally, but it is assumed that its contribution increases substantially for $E_\beta>1$ MeV.

2.9. *Escape of characteristic x rays from the detector sensitive volume.* In detection of β particles the absorption process occurs at the boundary of the sensitive region and the probability of escape of the characteris-

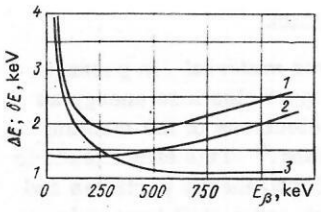

FIG. 39. Energy dependence of the energy resolution ΔE (1) and shift of maximum of spectral line δE (3) in measurement of a conversion-electron spectrum by an Si(Al) detector with a Mylar film (0.90 mg/cm^2) as vacuum-chamber entrance window, and energy resolution with an air lock (2).

tic radiation is high (see Fig. 13). In addition to the appearance of satellite peaks, the effect leads to appearance of an asymmetry of the spectral line on the low-energy side.

2.10. *The charge-collection efficiency of the detector* depends on the parameters of the initial material, the manufacturing technique, the type of detector, and also on edge effects (beam collimation). There is as yet no information in the literature on the contribution of these factors, although they apparently are involved in the shaping of the tail of the spectral line on the low-energy side.

2.11. *Dependence of the location of the maximum of a spectral line on the direction of biasing of the detector.* The design of the detector mounting and the means of connecting the bias voltage may be the causes of a shift in the maximum of a peak as the result of slowing down (or acceleration) of the β particles. Here it is assumed that the source is deposited on a substrate of conducting material and is grounded.

The external effects are as follows.

2.12. *Scattering in the material of the entrance window of the vacuum chamber.* In a number of problems it is possible to use a spectrometer with a thin entrance window. In Fig. 39 we have shown the energy dependence of the resolution and the shift of the peak with use of aluminized Mylar (0.90 mg/cm^2). It must be recalled that in such spectrometers it is necessary to shield the

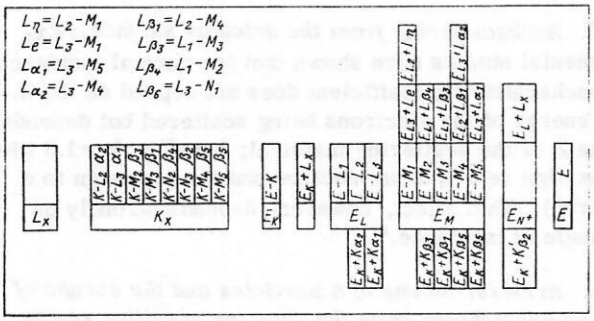

FIG. 40. Diagram of distortions of uncorrected spectrum due to true coincidences of $K(x)$ and $L(x)$ radiation with K, L, M, and N conversion electrons for a transition with energy E: the rectangles of the central band illustrate the energy distribution of the radiations; the distortions of the conversion-electron intensities as the result of coincidences with K_x radiation are illustrated by the rectangles of the lower band, and with L_x radiation—by the upper band. The Siegbahn designations have been used for the L_x radiation.

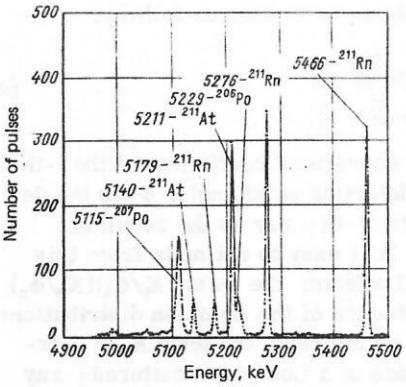

FIG. 41. Spectrum of α particles from ^{211}Rn measured by means of a $\pi\sqrt{2}$ magnetic α spectrograph.[70] The broadening of the 5115-keV α line (^{207}Po) is due to penetration of ^{207}Po recoil nuclei from decay of ^{211}Rn into the source backing.

window from light, since the photoeffect greatly affects the performance of the FET.

2.13. *Excitation of characteristic x-rays of materials surrounding the detector and source.* The discussion here is similar to that in Sec. 1.11.

2.14. *Detection of Compton electrons from scattering of γ rays in the materials surrounding the detector and source.*

2.15. *Radioactive background.* As a result of the small sensitive volume the natural radioactive background (see Sec. 1.16) does not play an important role in the study of internal-conversion electron spectra. However, in investigation of chains of α-active nuclides the background can be increased significantly as the result of radioactive recoil nuclei (see Sec. 1.17) which accumulate in the vacuum chamber and on the surface of the detector. The only method of suppressing this effect is the use of thin films which absorb the recoil nuclei.

2.16. *Addition of pulses.* Here the situation is similar to that in Sec. 1.18. However, special attention must be given to true coincidences of L_x and K_x radiation with K-conversion electrons, and also of L_x radiation with L-conversion electrons, which can greatly distort the resulting values of I_K and I_L (Fig. 40). This effect determines a limit on the solid angles used for a given accuracy in the determination I_K and I_L.

3. Alpha spectroscopy

The effects associated with the radioactive source are as follows.

3.1. *Scattering from the source backing.* The cross section for elastic scattering of α particles is given by the Rutherford formula and the contribution of this effect must be taken into account only for large values of the spectrometer solid angle ($\pi - 2\pi$). For spectroscopy of α particles ($\Omega \leq 0.04\pi$) the contribution of backscattering from the source backing can be neglected.

3.2. *Scattering in the source material.* This effect leads to an energy shift of the spectral lines toward low energies and to distortion of the intensities of the α lines as a result of scattering and absorption. To avoid

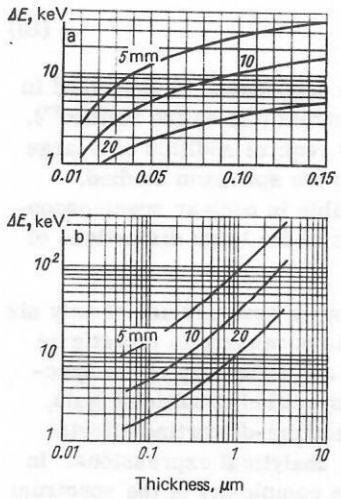

FIG. 42. Effect of entrance-window thickness on the energy resolution ΔE of a Si(Au) detector ($S = 1$ cm^2, source diameter 5 mm, $E_\alpha = 5$ MeV): a—ΔE as a function of thickness of Au entrance window on the assumption that there is no dead layer of Si; b—dependence on thickness of Si dead layer on the assumption that the Au entrance window thickness is 0.03 μm; the numbers in the curves are the distances from the source to the detector.

these effects we prepare sources by electromagnetic mass separation (ion-implantation energy 25 keV). However, in the study of chains of α-active nuclei the spectral lines of the daughter products are distorted as the result of penetration of recoil nuclei into the depth of the source backing (Fig. 41).

The effects associated with the characteristics of the detector are as follows.

3.3. *The dependence of range on Z of the detector material and on α-particle energy* is shown in Fig. 33. Although there have been significant advances in the preparation of Si(Li) and implanted Ge(Li) detectors, the greatest interest from the point of view of precision α spectroscopy is presented by Si(Au) detectors, which have a comparatively thin entrance window and which operate without cooling.

3.4. *Scattering in the entrance window.* Even before hitting the sensitive region of the detector, the α particle interacts with the material of the entrance window and this leads not only to energy loss (line shift) and broadening of the peak, but also to an increase of the continuous distribution in the spectrum (the tail). We note that the appearance of tails is due not only to the value and nonuniformity of the dead time but also to the

TABLE III. Effects distorting uncorrected spectrum.

Particle	Effects due to radioactive source	Effects due to detector characteristics	External effects
γ	Scattering from source backing Accompanying radiations Scattering in source Excitation of characteristic x rays in backing and in the source itself	Dependence of γ-ray interaction cross sections on detector Z and energy Satellite peaks due to escape of $\gamma^{\pm}$ in pair production in detector Satellite peaks due to escape of characteristic x rays from detector Scattering in detector entrance window Charge-collection efficiency in detector	Scattering in spectrometer entrance window, materials surrounding detector, and absorbers Excitation of characteristic x rays in materials surrounding detector and source Detection of $\gamma^{\pm}$ arising in pair production in materials surrounding detector Scattering of γ rays in materials surrounding detector External bremsstrahlung Dependence of position of spectral-line peak on measurement geometry Natural radioactive background Distortion of I_γ in study of chains of α-active nuclides Addition of pulses
β	Scattering from source backing Accompanying radiation Scattering in source Excitation of characteristic x rays in backing and in the source itself	Dependence of range on Z of detector material and on energy Scattering in detector entrance window Backscattering from detector Bremsstrahlung in detector Satellite peaks due to escape of characteristic x rays from detector Charge-collection efficiency in detector Dependence of position of spectral-line peak on bias voltage	Scattering in material of vacuum-chamber entrance window Excitation of characteristic x rays in materials surrounding the detector and source Detection of Compton electrons Radioactive background Addition of pulses
α	Scattering from source backing Scattering in source material	Dependence of range on Z of detector material and on energy Scattering in detector entrance window Charge-collection efficiency in detector	Spread of angles of incidence on detector surface Interaction of α particles with residual-gas molecules Addition of pulses Radioactive background

quality of processing of the surface and to the characteristics of the initial material (uniformity, carrier lifetime, dislocation density, etc.[3]). It is impossible at this time to formulate completely the technological conditions which would assure a good response function of an α spectrometer.

3.5. *Efficiency of charge-carrier* collection is one of the main sources of asymmetry of a spectral line.[24] Evidently this phenomenon is associated with the loss of charge carriers in the sensitive region of the detector as a consequence of their capture by traps and of recombination losses.[3] In distortion of a spectral line and the increase of the low-energy tail, an important role is played also by edge effects arising when an α particle hits the edge of the detector, where nonuniformities are possible. As the result of beam collimation, edge effects are greatly reduced, but as a result of the effect of the ends of the collimator they do not disappear.

The external effects are as follows.

3.6. *Distortion of the uncorrected spectrum as the result of spread in the angles of incidence and consequently of the traversal of different thicknesses of entrance window in measurement under conditions of large solid angle* Ω (Fig. 42). This effect leads to an increase of the low-energy tail and to reduction of the achievable energy resolution.[25]

3.7. *Distortion of the uncorrected spectrum as the result of loss due to interaction of* α *particles with residual-gas molecules.* In order that the displacement and broadening of a spectral line not exceed 10 keV for 5-MeV α particles on variation of the source-detector distance from 3 to 37 mm, the pressure in the spectrometer chamber[26] must be less than 210 newton/meter^2.

3.8. *Addition of pulses.* This effect is due to accidental coincidences (which depend on the counting rate) and to true coincidences of accompanying cascade α, β, and γ radiations (which depend on the solid angle) and leads not only to distortion of the spectral line (asymmetry and broadening) but also to an increase of the continuous distribution.

3.9. *Radioactive background.* The discussion here is similar to that in Sec. 2.15.

In conclusion we give in Table III a summary of the effects which distort the shape of the uncorrected spectrum.

4. TECHNIQUE OF MEASUREMENT OF ENERGY AND RELATIVE INTENSITY OF MONOENERGETIC RADIATIONS

The technique of measuring the energies of monoenergetic radiations by means of semiconductor detectors is based on comparison with energy standards. Here two approaches are distinguished in the development of programs for calibration by means of computers: in the first case the dependence of E on channel number for the entire spectrum is described by a polynomial of degree n:

$$E=\sum_{i=0}^{n} A_i P^i; \tag{10}$$

in the second case the same dependence is described in a limited portion of the spectrum (the spline method[27]). Consequently, both methods require addition of a large number of standard peaks to the spectrum studied, which is practically impossible in nuclear spectroscopic experiments as the result of the large distortions of the uncorrected spectrum.

The technique developed by us assumes use of only six energy standards. Here it is necessary to investigate beforehand the nonlinearity and efficiency of the spectrometer under previously specified conditions (gain, solid angle, absorbers, spectrum-distorting effects) and to approximate them by analytical expressions. In the particular case when the complexity of the spectrum permits addition of a large number of standards, the method goes over to one of the approaches mentioned above.

The technique for measurement of relative intensities of monoenergetic radiations is based on the preliminary study of the spectrometer efficiency by means of calibrated sources.

Spectrometer linearity[28-30]

Nonlinearity is investigated on the assumption that two arbitrary reference peaks of different energies lie on a straight line whose coefficients B_1 and B_2 are found from from the equations

$$\left.\begin{aligned} E=B_1+B_2P;\ B_1=(E_1P_2-E_2P_1)/(P_2-P_1);\\ B_2=(E_1-E_2)/(P_1-P_2). \end{aligned}\right\} \tag{11}$$

It is easy to show that the choice of the difference $|P_2-P_1|$ governs the accuracy of constructing the nonlinearity and consequently the error in energy measurement (usually $|P_2-P_1|>3500$). Then Eq. (11) is used to calculate the locations of the peaks with known energy and the quantity $\delta_j=P_j-P_{j\text{-theor}}$ is found as a function of the channel number P. Then values of δ_j are approximated by the method of least squares (the Fumili program[28]) by the polynomial

$$\delta_j=\sum_{i=1}^{M} A_i P_j^{i-1}, \tag{12}$$

where $M=2$–5. The choice $M\leqslant 5$ is due to the assumption of a smooth dependence of the nonlinearity on channel number (for larger M, oscillations between the experimental points are possible).

When this technique was first developed in 1972, a complicated dependence $\delta_j(P)$ was observed and this led to the necessity of breaking the response up into portions for approximation ($\leqslant 5$). Although the present state of the art no longer requires this procedure, the program organization of the technique allows for its use also with less perfected spectrometers. The choice of the optimum M value and region of approximation is made by analysis of the quantity

$$\frac{1}{n}\sum_{j=1}^{n}|(\delta_j-\delta_{j\,\text{exp}})|=\bar{\Delta}, \tag{13}$$

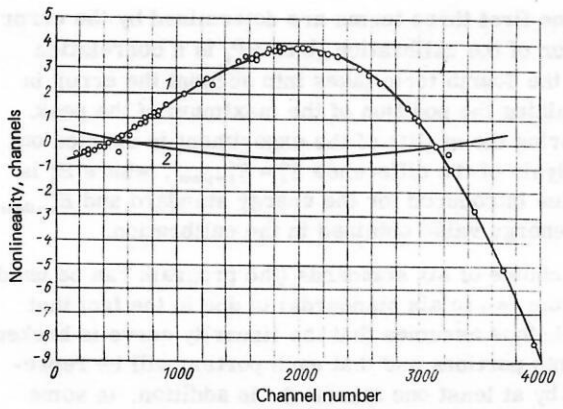

FIG. 43. Nonlinearity of a spectrometer with a 38 cm^3 Ge(Li) detector (1) and a 200 $mm^2 \times 5$ mm Ge(Li) detector (2): the points are experimental values; the continuous line is a fit by a polynomial (see the text).

where n is the number of experimental points. The quantity $\bar{\Delta}$ obviously characterizes the limiting error attainable in a given experiment. Usually $\bar{\Delta} \leq 0.05$ channel, and the value depends on the spectrometer quality, the accuracy of the experimenter, and the internal consistency of the set of energy standards used. The regions of approximation are matched over an interval containing at least four experimental points and with the necessary requirement

$$|\delta_j^{(1)} - \delta_j^{(2)}| < \bar{\Delta}_{1,2},$$

where $j = 1, \ldots, 4$; the superscripts (1) and (2) refer to the calculated values of the first and second regions; $\bar{\Delta}_{1,2}$ is the smaller of Δ_1 and Δ_2.

The program for construction of the spectrometer nonlinearity and approximation of the experimental data is described in Refs. 28 and 30. An example of a plot of the nonlinearity of a spectrometer with a Ge(Li) detector and its approximation by the polynomial (12) is given in Fig. 43. For comparison we have shown in the same figure the linearity of a spectrometer with a linear amplifier of higher quality.

Spectrometry efficiency [29-30]

In the study of efficiency it is necessary to consider two approaches: with use of sources whose activities have been calibrated, or with use of data on the relative intensities of transitions for nuclides with a complex decay scheme.

Absolute efficiency. Measurements with sources of calibrated activity are carried out under conditions of a previously chosen standard geometry with allowance for effects distorting the uncorrected spectrum. Here measures must be taken to reduce the contribution of errors associated with geometrical reproducibility, dead time, measurement time, $\Delta S/S$, and half-life. Calculation of efficiency values is carried out with the formula

$$\varepsilon_{abs} = (S/\tau)/[I \exp(-\lambda t)], \quad (14)$$

where S is the area of a peak at a given energy, τ is the measurement time, I is the number of monoenergetic particles of a given energy emitted by the source into an angle 4π per second, $(\ln 2)/T_{1/2}$ is the radioactive decay probability per day, and t is the time elapsed from the moment of standardization to the time of measurement, in days. Then the method of least squares (the Fumili program) is used to approximate the values by the polynomial

$$\ln \varepsilon_j = \sum_{i=1}^{M} C_i (\ln E_j)^{i-1}. \quad (15)$$

where $M = 2-5$. As in the case of the nonlinearity, the choice $M \leq 5$ is due to the assumption of a smooth dependence of the efficiency of the semiconductor spectrometer on energy. The optimum value of M is chosen from analysis of the values of

$$\Delta = (\varepsilon_{abs} - \varepsilon_{theor})/\varepsilon_{abs} \mid_{E_j}. \quad (16)$$

The number of regions for the approximation is ≤ 5. This choice is due to the complex dependence of the detector efficiency on energy, on the one hand, and to the absence of a sufficient number of experimental points uniformly distributed over the entire energy range, on the other hand. In particular, with use of the standards set SSGS (standard spectrometric gamma sources) for Ge(Li) detectors in the region 165–661 keV there are only two experimental points, although the efficiency in this region changes by a factor of 5–10. Control of each experimental point ε_{abs} is carried out from the analysis of

$$\frac{\Delta\varepsilon}{\varepsilon} = \left\{\left(\frac{\Delta I}{I}\right)^2 + \left(\frac{\Delta S}{S}\right)^2 + \left(\frac{\Delta\tau}{\tau}\right)^2 + \left(\frac{0.693\,\Delta t}{T_{1/2}}\right)^2 + \left(\frac{0.693 t\,\Delta T_{1/2}}{T_{1/2}^2}\right)^2\right\}^{1/2}. \quad (17)$$

Relative efficiency. In a number of problems it is sufficient to know just the relative efficiency of the spectrometer, which is easily calculated by means of the relative intensities of monoenergetic radiations of calibrated sources according to the formula

$$\varepsilon_{rel} = S/I. \quad (18)$$

In the case where several sources are used, the problem arises of matching their values. For this purpose a basic nuclide is chosen, with respect to which the values $\varepsilon_{rel}(E)$ obtained for different nuclides are normalized. In particular values of ε_{abs} can be used as the basic points. Conversion of values of $\varepsilon_{rel}(E)$ for each nuclide to the basic values is accomplished by means of a normalization factor and parabolic interpolation. Then all values $\varepsilon(E)$ are arranged in order of increasing E. The approximation of the experimental points is then carried out.

Construction of the absolute efficiencies of spectrometers will be discussed below. Here we give an illustration of the relative efficiency of spectrometers with Ge(Li) detectors (Fig. 44). The results were obtained with use of the relative intensities of the γ rays of ^{75}Se, ^{173}Lu, ^{182}Ta, ^{152}Eu, ^{160}Tb, ^{192}Ir, ^{110}Ag, and ^{56}Co.[29] The basic source was ^{152}Eu. The programs for plotting and fitting the spectrometer efficiency have been described in Refs. 28 and 30.

Processing of the results of single measurements

The structural scheme of the program for processing of single measurements is given in Fig. 45. After tak-

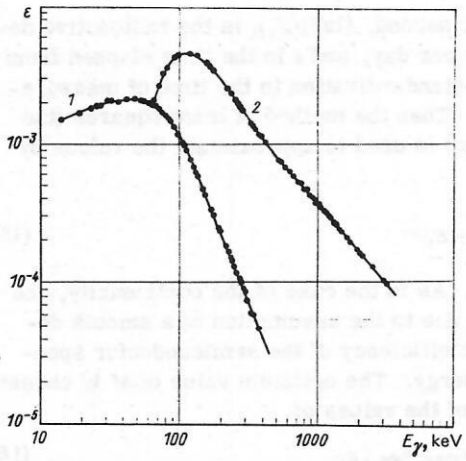

FIG. 44. Efficiency of a spectrometer with a 38 cm^3Ge(Li) detector: the points are experimental values; the continuous lines are fits by polynomials; the arrows show the limits of the approximation fields.

ing into account spectrometer linearity (the correction $p_i^e \to p_i^{e\prime}$) by the method of least squares with six standard lines, the coefficients of the calibration line are calculated:

$$E_i^e = B_1 + B_2 P_i^e. \tag{19}$$

The weights used are $\{(\Delta E_i^e)^2 + (B_2 \Delta P_i^e)^2\}^{-1}$, where ΔE_i^e is the error in the standard, excluding the systematic part of the error. The error in the energy of a single measurement is calculated by the formula

$$\Delta E_i = \{(\Delta B_1)^2 + (\Delta B_2)^2 P_i^2 + rP_i + (B_2 \Delta P_i)^2\}^{1/2}. \tag{20}$$

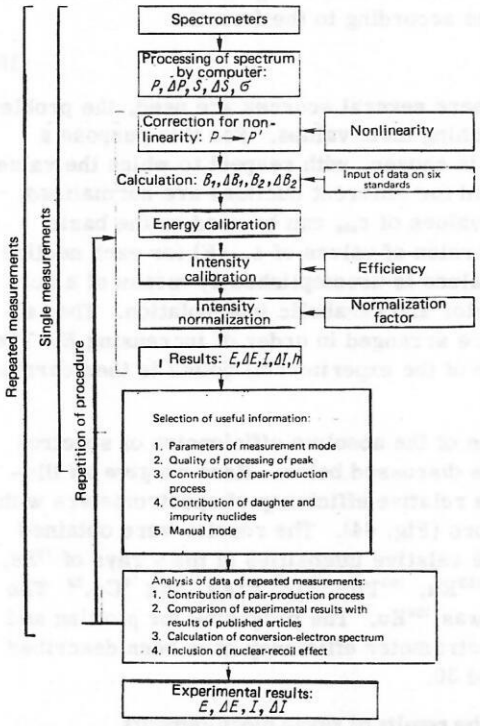

FIG. 45. Structural arrangement of an experiment to measure the energies and relative intensities of monoenergetic radiations.

Here the first three terms are determined by the error corridor of the calibration line; rP_i is a correlation term; the fourth term takes into account the error in determining the position of the maximum of the peak. Monitoring the quality of the experiment is carried out by analysis of the difference $E_i^e - E_{i\text{-theor}}^e$, where E_i^e is the value introduced for the energy standard and $E_{i\text{-theor}}^e$ is the energy value obtained in the calibration.

The choice of six standards (the program can be used with from two to six standards) is due to the fact that the technique assumes that the linearity curve is broken down into portions and that each portion will be represented by at least one standard. In addition, in some cases distortions of the values of P_i^e are possible as the result of various instrumental effects (unknown transitions, impurities, addition of pulses, escape of characteristic x rays from the detector, etc.). The chosen number of standards permits the contribution of such effects to be observed.

The relative intensities and their errors are calculated by the formulas

$$I_i = \frac{S_i}{\varepsilon_i}\frac{I_n}{S_n/\varepsilon_n}; \qquad \Delta I_i = I_i \sqrt{\left(\frac{\Delta S_i}{S_i}\right)^2 + \left(\frac{\Delta S_n}{S_n}\right)^2}, \tag{21}$$

where ε_i is the spectrometer efficiency for monoenergic particles with energy E_i, I_n and S_n are the intensity and area of the peak chosen for normalization, and S_i is the area of the peak being calibrated.

As a result of the above processing, the following quantities are fed to the ADC: P_i, ΔP_i, $\delta_{j\text{-theor}}$, S_i, ΔS_i, $\varepsilon_{i\text{-theor}}$, E_i, ΔE_i, I_i, ΔI_i, and $h_i = 2.354\sigma_i B_2$. The experimental results (E, ΔE, I, ΔI, and h) are recorded on magnetic tape, punched tape, or cards for further processing.

Criteria for evaluation of quality of experimental data in single measurements, and selection of useful information

The basis of precision spectrometry of monoenergetic radiations is the processing of a spectral line by computer. Unfortunately, this process is quite subjective, since it is necessary to specify beforehand the initial approximations (to mark out the spectrum) and, of great importance, the number of peaks. As yet it has not been possible to write an automatic processing program, as the result of the complicated response function of spectrometers with semiconductor detectors and the necessity of extracting information on low-intensity transitions in an intense background pedestal.

We shall formulate criteria for γ-ray spectrometry, which is the most complete class of problems. Spectrometry of internal-conversion electrons and α particles is a particular case of this formulation.

a. *Parameters of the measurement region.* Spectral lines whose energies lie outside the region of approximation of the nonlinearity (criterion 1) and efficiency (criterion 2) on the basis of the total-absorption peak are discarded and printed out as a separate group.

b. *Quality of processing of a spectral line by computor.* For intense single peaks (for example, $I>1$) the half-width of the line $h_{exp}(E)$ is fitted by the polynomial

$$h(E)=a_1+a_2E+a_3E^2. \tag{22}$$

In our measurements the most intense line is taken as 100 units. Spectral lines whose $h_{exp}(E)$ values do not satisfy the inequality

$$|h_{exp}(E)-h(E)|\leqslant\Delta h \tag{23}$$

are discarded and printed out as a separate group (criterion 3). The values of Δh depend on the spectrometer quality and especially on the energy resolution. The discarded peaks are processed again with new initial approximations. Note that an exaggerated value of h may be an indication of multiplet structure of a peak.

c. *Contribution of pair production in the detector.* Experimental values of the efficiencies based on the single-escape and double-escape peaks are approximated by the polynomial

$$\ln\varepsilon_j\,(\mathrm{SE,DE})=\sum_{i=1}^{M}k_j(\ln E_j)^{i-1}, \tag{24}$$

and then for each value $E>1022$ keV we have

$$[E-E\,(\mathrm{SE,DE})]\pm[(\Delta E)^2+(\Delta E\,(\mathrm{SE,DE}))^2]^{1/2}. \tag{25}$$

If there is a transition whose energy $E\pm\Delta E$ coincides within experimental error with this difference, its intensity is corrected by means of the corresponding efficiency:

$$[S_i-S_i\,(\mathrm{SE,DE})]\pm[(\Delta S_i)^2+(\Delta S_i\,(\mathrm{SE,DE}))^2]^{1/2}. \tag{26}$$

Here S_i is the area of the peak with energy E_i, S_i(SE, DE) is the calculated area of the single-escape or double-escape peak, and ΔS_i and ΔS_i(SE, DE) are the corresponding errors. The error ΔS_i(SE, DE) is specified by means of a parameter[28,29] similar to $\varkappa$. Obviously in this processing there is a conversion: intensity → area → intensity. For monitoring purposes the sets of corrected intensities (criterion 4) are printed out by the ADC.

d. *Contribution of daughter or impurity nuclides to distortion of the intensities of the γ transitions studied.* The most intense lines of a daughter or impurity nuclide are used to find the normalization coefficient

$$q=(1/n)\sum_{i=1}^{n}(I_i/I_i'), \tag{27}$$

where I_i are the intensities obtained in a given experiment for transitions of a daughter or impurity nuclide with relative intensities I_i'; n is the number of specified peaks. For transitions which coincide within the limits

$$[(\Delta E_i')^2+(\Delta E_i)^2]^{1/2} \tag{28}$$

in energy with a transition of a daughter or impurity nuclide, a correction (criterion 5) is made to the intensities by the formula

$$[I_i-I_i'q]\pm[(\Delta I_i)^2+(\Delta I_i'q)^2]^{1/2}. \tag{29}$$

For monitoring purposes, sets of corrected γ-ray intensities are printed out by the ADC.

e. *Manual mode of information selection* (criterion 6). By this means it is possible to discard transitions which have been repeatedly processed with different initial approximations, and also possible background, instrumental, and impurity peaks. The selection is accomplished by specifying the number of the γ transition.

The program is organized so that various criteria can be applied repeatedly or not applied at all. The corrected results are written on magnetic tape or punched cards for subsequent processing.

Processing of results of repeated measurements

The results of single measurements in different detectors, spectrometer circuits, and with different gain settings are processed in accordance with the following formulas:

$$\left.\begin{aligned}
&E=\frac{\sum_{i=1}^{n}E_i(1/\Delta E_i)^2}{\sum_{i=1}^{n}(1/\Delta E_i)^2};\quad \Delta E_1=[\alpha_1^2+\alpha_3^2+\alpha_4^2+\alpha_5^2]^{1/2};\\
&\qquad\qquad\qquad\qquad\qquad\qquad\quad \Delta E_2=[\alpha_2^2+\alpha_3^2+\alpha_4^2+\alpha_5^2]^{1/2};\\
&I=\frac{\sum_{i=1}^{n}I_i(1/\Delta I_i)^2}{\sum_{i=1}^{n}(1/\Delta I_i)^2};\quad \Delta I_1=[\beta_1^2+\beta_3^2]^{1/2};\\
&\qquad\qquad\qquad\qquad\qquad\qquad\quad \Delta I_2=[\beta_2^2+\beta_3^2]^{1/2};\\
&\alpha_1^2=\frac{1}{\sum_{i=1}^{n}(1/\Delta E_i)^2};\quad \alpha_2^2=\frac{\sum_{i=1}^{n}(1/\Delta E_1)^2(E-E_i)^2}{(n-1)\sum_{i=1}^{n}(1/\Delta E_i)^2};\\
&\alpha_3^2=\rho^2E^2;\quad \begin{cases}\alpha_5^2=1/3B_2^2\bar{\Delta}^2;\\ \alpha_5^2=0;\end{cases}\\
&\alpha_4^2=\mu^2E^2;\\
&\beta_3^2=\varkappa^2I^2.
\end{aligned}\right\} \tag{30}$$

Here n is the number of measurements, E is the energy in keV, α_3 is the error of the tertiary standards relative to which the set of energy standards is constructed on the assumption $E_\gamma(411.8-{}^{198}\mathrm{Hg})=411.794\pm0.000$ keV (Ref. 19) ($\rho=10\times10^{-6}$), α_4 is the error of the secondary standard $E_\gamma(411.8-{}^{198}\mathrm{Hg})=411.794\pm0.007$ keV ($\mu=17\times10^{-6}$), α_5 is the error associated with approximation of the nonlinearity for measurement in one spectrometer (for different spectrometers this error goes over from a systematic error to a random error, i.e., $\alpha_5=0$), the errors β_1 and β_2 are calculated similarly to α_1 and α_2, $\varkappa$ characterizes the limiting error which can be achieved in a given spectrometer (for certain spectrometers $\varkappa$ is taken to be the best value). As ΔE and ΔI one takes the error which is the greater of ΔE_1, ΔE_2 and ΔI_1, ΔI_2, respectively.

The principle of operation of the program for automatic processing of the results of repeated measurements is shown in Fig. 45.[28,30] After selection of the useful information, the sets of single measurements ($E, \Delta E, I, \Delta I$) are transmitted to the computer and the data are arranged in order of increasing E. Then the energies whose values coincide within experimental error are systematically selected and the results are processed in accordance with the equations (30). The input data and the calculated values are printed out by the ADC.

The results obtained are subjected to the following analysis.

Contribution of pair production in the detector. This effect has been discussed above, where we assumed

measurement in an energy region encompassing the complete γ-ray spectrum. On the other hand, we note that each spectrometer must be used in some optimal region. Thus, the program of automatic inclusion of the effect of pair production in the detector will not be effective when a limited energy region is investigated. Therefore, after the processing of repeated measurements for $E > 1022$ keV, the energies of the single-escape and double-escape peaks are calculated. Then the single-measurement data are analyzed again and spurious peaks are removed (criterion 6).

Comparison of experimental results with data in the literature. We consider transitions whose energies coincide within experimental error. When necessary the intensity renormalization coefficient is taken into account. The energies and intensities of transitions observed either only in our experiments or only in published work are printed out as individual groups. In the case of inconsistencies, a repeated analysis of individual measurements is made.

Calculation of the internal conversion electron spectrum. In order to plan and carry out correctly an experiment to study internal-conversion electron spectra, provision is made for plotting the calculated spectrum on the basis of data on γ-ray energies. Two tables are printed out by the ADC: (1) the energies of the γ transitions and the energies of the corresponding conversion lines (K, L, M, etc.) and their errors, (2) the energies of the conversion lines in order of increasing value.

In constructing decay schemes with use of the Ritz rules, the correction to the energy for nulcear recoil is important in determination of the transition energy. In the program the transition energy is calculated by adding the correction for nuclear recoil:

for γ rays

$$E_0 = \frac{1}{2}\left(\frac{E}{mc^2}\right)^2 \frac{m}{M(A,Z)}\, mc^2; \tag{31}$$

for internal-conversion electrons

$$E_0 = E\left(\frac{E}{mc^2}+2\right)\frac{m}{2M(A,Z)}. \tag{32}$$

These expressions refer to a free stationary nuclide.

5. SPECTROMETRY OF γ RAYS

The technique of measuring the energies and relative intensities of γ rays by means of semiconductor detectors is based on comparison of the uncorrected spectra of the nuclide under study and of standard nuclides; in the course of this comparison there are many factors which reduce the accuracy achievable. Consequently the process of comparison of the location of the peak of a spectral line (P) and its energy (E), and also of the area (S) and intensity (I) of a line, must be systematic from the point of view of taking into account the given standard nuclides and definite in regard to the calculation of errors. When we consider that at the present time spectrometers employing silicon and germanium have characteristics close to the limiting possible values, a change in the data on standard nuclides leads only to simple corrections of the results without repetition of the experiment.

Gamma-ray energy standards

The only natural γ-ray energy standard, whose value is completely determined by fundamental constants, is the energy of annihilation radiation[31]:

$$mc^2 = 511.0041 \pm 0.0016\,\text{keV}. \tag{33}$$

The energy of annihilation of a stationary positron with inclusion of half of the binding energy of the $^1S_0$ state is

$$\gamma^{\pm} \equiv h\nu^{\pm} = mc^2 - mc^2/8h^2 = 511.0007 \pm 0.0016\,\text{keV}. \tag{34}$$

Unfortunately, use of this value is hindered as a result of the complex shape of the spectral line,[32] which sets a limit of the achievable accuracy. Therefore the secondary standard, whose spectral line shape does not depend on secondary effects, has been taken as the 411.8-keV γ transition of ^{198}Hg (the selection is discussed, for example, in Ref. 32). The accurate value

$$E_\gamma(411.8\,\text{keV} - {}^{198}\text{Hg}) = 411.794 \pm 0.007\ \text{keV} \tag{35}$$

was determined by means of an iron-free β spectrometer in a comparison of the L_3 line of photoelectrons from external conversion, $\gamma = 411.8$ keV, and the K line $\gamma^{\pm}$ in a uranium radiator.[33]

Another approach is also possible. As a primary energy standard one can use the energy of the x-ray line WK_{α_1} (Ref. 31):

$$E(WK_{\alpha 1}) = 59.31918 \pm 0.00036\ \text{keV}. \tag{36}$$

Analyzing the data of various experiments, B. S. Dzhelepov suggests[32]

$$E_\gamma(411.8 - {}^{198}\text{Hg}) = 411.803 \pm 0.014\,\text{keV}. \tag{37}$$

At the present time considerable attention is devoted to the energy value of the 411.8-keV γ rays (^{198}Hg). In particular, the following values are given:

$$\begin{aligned} &E_\gamma(411.8 - {}^{198}\text{Hg}) = 411.8007 \pm 0.0027\ \text{keV}\ [\text{Ref. 34}];\\ &E_\gamma(411.8 - {}^{198}\text{Hg}) = 411.805 \pm 0.0015\ \text{keV}\ [\text{Ref. 35}]. \end{aligned} \tag{38}$$

Apparently the discussion will be continued.

In our experiments we shall take the value (35). This is due to the fact that with this value: a) in Ref. 33 measurements have been made of the transition energies which are frequently used as standards; b) in Ref. 36, Heath gives the data of Helmer, Greenwood, and Gerhke on γ-ray energies, which are used for calibration of γ spectrometers; c) in Ref. 37 a crystal diffraction spectrometer has been used to measure the γ-ray energies of ^{182}Ta and ^{192}Ir, i.e., these data can be considered as tertiary standards (Table IV); d) in the case that a new value is adopted for $E_\gamma = 411.8$ keV, the correction procedure becomes simple:

$$E_2 = E_1[E_2(411.8)/E_1(411.8)], \tag{39}$$

where E_1 are the energy values obtained on the assumption (35) and E_2 are the same on the assumption of the new value of the secondary standard.

Gamma-ray intensity standards

At the present time there are a number of nuclides whose activity, in view of the simplicity of the decay scheme, can be measured by various methods, with an

TABLE IV. Energy of ^{182}Ta and ^{192}Ir γ rays.

Nuclide	[37]			[32]		[36]		[58]		[29]	
	E	$\Delta E'$	ΔE	E	ΔE	E	ΔE	E	ΔE	E	ΔE
^{182}Ta	31.7370	0.0004	0.0007	31.736	0.001	—	—	—	—	—	—
	42.7143	0.0006	0.0009	42.715	0.002	—	—	—	—	—	—
	65.7219	0.0006	0.0013	65.722	0.002	—	—	—	—	—	—
	67.7496	0.0006	0.0013	—	—	67.750	0.001	—	—	—	—
	84.6802	0.0008	0.0016	84.680	0.003	84.680	0.002	—	—	84.681	0.003
	100.1067	0.0009	0.0019	100.103	0.002	100.105	0.001	—	—	100.105	0.002
	113.6677	0.0011	0.0022	113.673	0.003	113.673	0.002	—	—	113.672	0.008
	116.4172	0.0011	0.0023	116.416	0.004	116.418	0.002	—	—	116.413	0.003
	152.4298	0.0013	0.0029	152.431	0.003	152.434	0.002	—	—	152.427	0.003
	156.3819	0.0014	0.0030	156.391	0.004	156.387	0.002	—	—	156.380	0.005
	179.3895	0.0016	0.0034	179.395	0.005	179.393	0.003	—	—	179.388	0.003
	198.3478	0.0017	0.0038	198.361	0.008	198.356	0.002	—	—	198.349	0.007
	222.1037	0.0019	0.0042	222.107	0.005	222.110	0.003	—	—	222.102	0.006
	229.3162	0.0035	0.0052	229.321	0.008	229.322	0.006	—	—	229.316	0.005
	264.0697	0.0022	0.0050	264.072	0.009	264.072	0.006	—	—	264.069	0.005
^{192}Ir	136.3400	0.0007	0.0024	—	—	—	—	—	—	—	—
	295.9483	0.0014	0.0052	295.942	0.009	295.949	0.006	295.949	0.004	295.946	0.005
	308.4464	0.0014	0.0054	308.430	0.010	308.445	0.007	308.444	0.005	308.445	0.006
	316.4977	0.0014	0.0056	316.487	0.010	316.497	0.007	316.496	0.005	316.495	0.006
	416.4501	0.0035	0.0079	—	—	416.450	0.008	—	—	416.454	0.014
	468.0546	0.0021	0.0082	468.059	0.014	468.062	0.010	—	—	468.056	0.009
	588.5562	0.0034	0.0106	588.567	0.017	588.572	0.012	588.566	0.008	588.572	0.012
	604.3942	0.0026	0.0106	604.396	0.017	604.401	0.012	604.393	0.008	604.394	0.012
	612.4460	0.0026	0.0106	612.446	0.017	612.450	0.013	612.445	0.008	612.446	0.013
	884.5037	0.0044	0.0156	—	—	884.523	0.018	884.514	0.012	—	—

Note. $\Delta E'$ is the error without inclusion of the error in the secondary standard ($\alpha_4 = 0$); ΔE is the total error ($\alpha_4 = 17 \times 10^{-6}$ E keV).

TABLE V. Radioactive sources, activity measurement errors ΔA, γ-ray yield per 100 decays, and minimum values obtainable in measurement of spectrometer efficiency.

Nuclide	Reference	$T_{1/2}$, days	ΔA, %	E	I	ΔI	$\Delta\varepsilon_1$	$\Delta\varepsilon_2$	$\Delta\varepsilon_3$
^{241}Am	[28]	432.9 (8) years	1	59.54	35.9	0.6	1.7	1.9	2.3
^{109}Cd	[60]	453.2 (18)	2.5	22.1 *KX*	83.00	3.00	3.6	4.4	—
				25.0 *KX*	17.81	0.64	3.6	4.4	—
				88.03	3.79	0.07	1.8	3.1	—
^{57}Co	[28]	269.8 (4)	1	6.5 *KX*	55.3	1.5	2.7	2.9	3.1
				14.41	9.5	0.2	2.1	2.3	2.6
				122.06	85.6	0.4	0.5	1.1	1.6
				136.47	10.75	0.30	2.8	3.0	3.2
^{139}Ce	[28]	137.2 (4)	1	33.4 *KX*	62.53	0.57	3.8	3.9	4.1
				37.8 *KX*	15.13	0.14	3.8	3.9	4.1
				165.85	80.35	0.08	0.1	1.0	1.5
^{203}Hg	[28]	46.76 (8)	1.5	10.3 *LX*	5.63	0.08	1.4	2.1	2.1
				72.9 *KX*	9.77	0.50	5.1	5.3	5.3
				82.5 *KX*	2.73	0.20	7.3	7.5	7.5
				279.19	81.55	0.15	0.2	1.5	1.5
^{113}Sn	[28]	115.2 (8)	1.5	3.3 *LX*	13.5	0.1	0.7	1.7	1.7
				24.7 *KX*	96.6	0.3	0.3	1.5	1.5
				255.12	1.9	0.1	5.3	5.5	5.5
				391.69	64.4	0.3	0.5	1.6	1.6
^{137}Cs	[28]	30.18 (10) years	1	4.5 *LX*	1.25	0.01	0.8	1.3	1.7
				32.1 *KX*	5.67	0.18	3.2	3.3	3.5
				36.5 *KX*	1.34	0.05	3.7	3.9	4.0
				661.65	85.1	0.5	0.6	1.2	1.6
^{54}Mn	[28]	312.5 (3)	0.5	5.5 *KX*	25.0	0.2	0.8	0.9	1.7
				834.86	100	—	—	0.5	1.5
^{88}Y	[28]	107.4 (8)	1.5	14.4 *KX*	63.40	0.32	0.5	1.6	1.6
				898.01	91.40	0.07	0.1	1.5	1.5
				1836.07	99.40	0.07	0.1	1.5	1.5
^{65}Zn	[28]	245.7 (11)	1	8.1 *KX*	35.2	0.3	0.9	1.3	1.7
				1115.56	50.6	0.4	0.8	1.3	1.7
^{60}Co	[28]	5.275 (5) years	0.5	1173.24	99.74	0.05	0.1	0.5	1.5
				1332.49	99.85	0.03	0.1	0.5	1.5
^{22}Na	[28]	2.602 (5) years	1	1274.53	99.95	0.02	0.1	1.0	1.5
^{24}Na	[61] [62]	15.030 (3) hours	—	1368.60	100	—	—	—	—
				2753.97	99.85	0.02	0.02	—	—

Note. $\Delta\varepsilon_1 = \Delta I/I$; $\Delta\varepsilon_2 = [(\Delta I/I)^2 + (\Delta A)^2]^{1/2}$; $\Delta\varepsilon_3 = [(\Delta I/I)^2 + (\Delta A = 1.5\%)^2]^{1/2}$.

error 0.5–3% (Table V). These data are also used for investigation of the experimental dependence of the efficiency of Ge(Li) spectrometers as a function of the energy for a given geometry.[28] In addition, one frequently uses data on the relative intensities of the γ transitions arising in the decay of ^{182}Ta, ^{152}Eu, ^{110m}Ag, ^{56}Co, etc. Here, however, it must be remembered that these data were obtained by means of the data of Table V and that the comparison procedure is frequently erroneous.

Construction of a set of energy standards[29]

As tertiary standards we have used the energies of the ^{182}Ta and ^{192}Ir γ rays, measured by means of a crystal diffraction spectrometer (see Table IV, column 1). For comparison we have given in the same table the energies recommended by various authors. These data give rise to speculation on the choice of energy standards. A number of discrepancies indicate the existence of errors in the experiments with a crystal diffraction spectrometer (see Table IV, columns 1–3). In particular, the value of the energy 588 keV (^{198}Ir) (Ref. 37) can be considered as a blunder.

Energy standards above 600 keV are created by use of transition energy values obtained by addition of concurrent cascade transitions with inclusion of nuclear recoil for nuclides with well investigated decay schemes (Table VI). The upper energy limit 600 keV (see Table IV) imposes a limitation of 1200 keV for two-cascade transitions. Consequently, the possible energy ranges are ~1000, ~2000, and ~4000 keV. Unfortunately, the number of concurrent cascades for nuclides with sufficiently simple spectra and convenient half-lives is limited. Therefore we have used also the fact of retention of spectrometer nonlinearity with change of the gain by means of a frequency-independent attenuator.[5]

The procedure of constructing a complete set of energy standards has been as follows:

a) *The range up to 260 keV.* The choice of this ener-

TABLE VI. γ-ray energy obtained by means of concurrent cascade transitions.

Nuclide	E (1)	Φ (1)	E (2)	Φ (2)	E (C)	Φ (C)	E (D)	Φ (D)	E	Φ
^{173}Lu	285.369	0.003	350.750	0.005	636.119	0.006				
	179.363	0.001	456.771	0.006	636.134	0.006				
	78.651	0.006	557.482	0.004	636.133	0.007	—	—	636.129	0.006
^{95m}Tc	204.119	0.003	582.068	0.005	786.184	0.006	786.194	0.007	786.188	0.015
	204.119	0.003	616.497	0.019	820.614	0.023	820.640	0.013	820.632	0.019
^{134}Cs	569.322	0.003	795.856	0.003	1365.177	0.004				
	563.231	0.004	801.943	0.004	1365.173	0.006	1365.180	0.011	1365.177	0.003
^{110m}Ag	620.353	0.006	763.936	0.005	1384.285	0.008				
	677.613	0.002	706.672	0.003	1384.280	0.004				
	446.802	0.005	937.507	0.003	1384.305	0.006	1384.274	0.007	1384.285	0.007
	657.744	0.002	818.028	0.007	1475.777	0.007	1475.781	0.010	1475.778	0.006
	687.001	0.004	818.028	0.007	1505.024	0.008				
	620.353	0.006	884.695	0.002	1505.043	0.006	1505.043	0.023	1505.036	0.006
	677.613	0.002	884.695	0.002	1562.293	0.003				
	744.271	0.004	818.028	0.007	1562.302	0.008	1562.319	0.020	1562.295	0.007
^{144}Ce	696.492	0.004	1489.132	0.005	2185.617	0.007	—	—	2185.617	0.007
^{56}Co	1238.271	0.003	1360.209	0.005	2598.450	0.006	2598.429	0.013	2598.444	0.008
^{88}Y	898.048	0.005	1836.074	0.008	2734.103	0.004	—	—	2734.103	0.009
^{56}Co	1238.271	0.003	2015.196	0.018	3253.423	0.018	3253.410	0.019	3253.414	0.013

Note. E(C) is the energy found by addition of cascade transitions with inclusion of nuclear-recoil energy; E(D) is the energy obtained in direct measurement by means of other energy standards; E is the average value of the energies E(C) and E(D).

gy region is due to the attempt to reduce the errors with optimal choice of the gain for spectrometers with high energy resolution.

b) *The range up to 600 keV.* A complete set of data has been used (see Table IV). A typical uncorrected spectrum is shown in Fig. 46. By means of concurrent cascade transitions the energies of three direct transitions have been determined: 636, 786, and 820 keV (see Table VI).

c) *The range up to 820 keV.* Gamma rays up to 612 keV have been measured in the working region of spectrometer channels (see Table VI), the nonlinearity studied, and its behavior fitted by a polynomial.[12] Then the gain was changed in such a way that the energy range of the calculated direct transitions up to 820 keV was placed in the working region (see Table VI). Completion of this step made possible determination of the energy of four direct transitions (1365, 1384, 1475, and 1505 keV).

d) *The range up to 1505 keV.* The energies of nine direct transitions have been determined and improved: 786, 820, 1365, 1384, 1475, 1505, 1562, 2185, and 2598 keV (see Table VI). Then all measurements carried out up to this moment were recalibrated by means of the improved data on Table VI. A typical uncorrected spectrum is shown in Fig. 47.

e) *The range above 1500 keV.* The measurements were made in three stages: up to 2185, 2598, and 3500 keV (see Table VI). A typical uncorrected spectrum is shown in Fig. 48.

More than 800 series of measurements have been made in various detectors, spectrometer circuits, and gain settings. The results of the experiments are given in Table VII. Following Ref. 32, we give the orders of the standards. The quaternary standards were obtained in a direct comparison with the data of Ref. 37. The fifth-order standards were obtained in comparison with

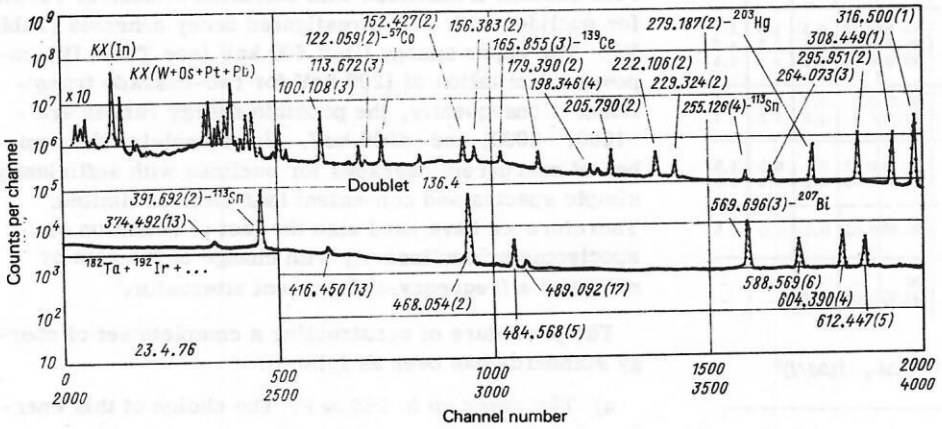

FIG. 46. Uncorrected γ spectrum in the range up to 600 keV (200 mm^2 × 5 mm Ge(Li) detector): the energy values and (in parentheses) their relative errors obtained in the present experiment are given; T_2 = 6 hours, P = 10 cm, no absorber.

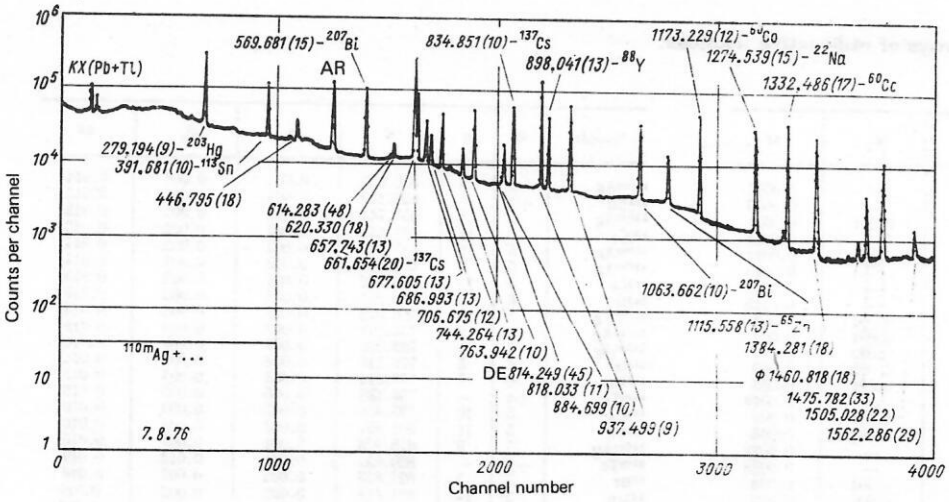

FIG. 47. Uncorrected γ spectrum in the range up to 1505 keV (38 cm^3 Ge(Li) detector): $T_2 = 9$ hours, $P = 25$ cm, absorber—1 mm Cd.

the tertiary and quaternary standards. The + sign indicates that the energy value was obtained by addition of the energies of concurrent cascade transitions.

A check of energy standards up to 600 keV is carried out by solution of the inverse problem—measurement of the energies of the ^{182}Ta and ^{192}Ir γ rays by means of the data of Table VII. The results of three series of measurements are given in Table IV (column 5). They indicate a good convergence of our data with the recommended values. A check of the reliability over a wider region was carried out by means of concurrent direct and cascade transitions (within the limits of α_1 or α_2) for nuclides with well investigated decay schemes (Table VIII). The fact of agreement of the results within the listed errors can be interpreted as a confirmation of the correctness of the model for calculation of the errors.

We note that previously it was proposed to use the single-escape and double-escape peaks for precision measurements of the energies of high-energy γ transitions. We carried out six series of measurements of the γ-ray spectrum of ^{56}Co (Table IX). It is evident that complicated kinematical processes in the electric field of the detector in detection of an electron-positron pair are the source of systematic errors. Incidentally, the γ-transition energy values obtained by means of double-escape peaks for ^{56}Co agree with the values recommended in Ref. 38.

The values of certain energy standards recommended by various authors are compared in Table X. The data of Refs. 32 and 36 were obtained by analysis of various experimental studies and corrected with inclusion of the newest values of the fundamental constants. The data of Refs. 54 and 57 were obtained by means of new experiments in crystal diffraction spectrometers. In general we observe good agreement of the results within the errors. At the same time the energies of certain ^{152}Eu transitions from Ref. 57 differ from those obtained by us. Analysis of a larger number (than in Ref. 57) of concurrent and cascade transitions (see Table VIII) indicates good internal consistency of our results. Here we must keep in mind that the 443.9-keV transition may be a doublet. The relation of the two complete sets of energy standards proposed in the present work and in Ref. 36 is illustrated in Fig. 49. As can be seen, with increase of E an increase is observed in the difference between our energy values and those from Ref. 36, which at $E \sim 3000$ keV reaches 100 eV. In the same figure we have given also the differences in the ^{56}Co γ-ray energy values proposed by us and in Ref. 38.

It is of particular interest to compare our results with the tertiary standards measured in an iron-free mag-

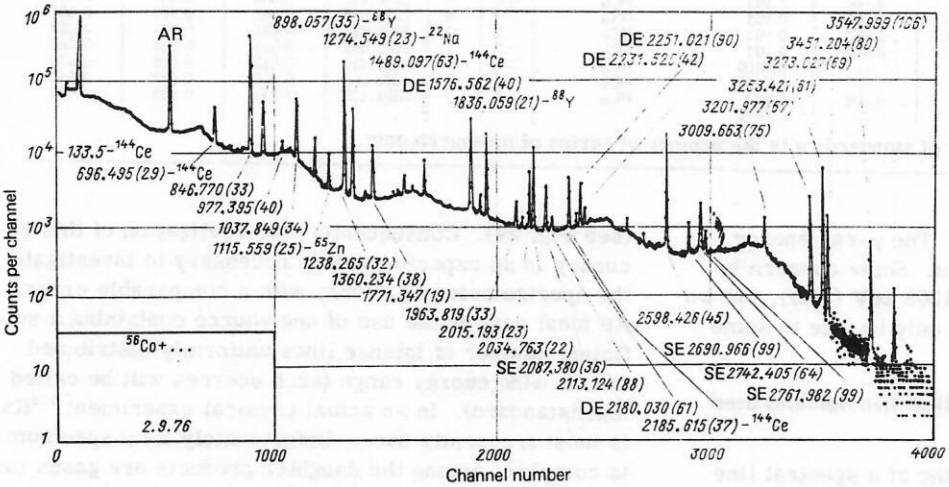

FIG. 48. Uncorrected γ spectrum in the range up to 3500 keV (50 cm^3 Ge(Li) detector): $T_2 = 12$ hours, $P = 25$ cm, absorber—1 mm.

TABLE VII. Energy standards for γ rays of radioactive nuclides.

Nuclide	Q	q	E	Φ_1	Φ_2	ΔE
^{182}Ta	3	—	31.7370	—	—	0.0007
^{182}Ta	3	—	42.7143	—	—	0.0009
^{241}Am	5	6	59.538	0.002	0.001	0.002
^{169}Yb	3	—	63.1182	—	—	0.0011
^{182}Ta	3	—	65.7219	—	—	0.0013
^{182}Ta	3	—	67.7496	—	—	0.0013
^{170}Tm	3	—	84.2517	—	—	0.0015
^{182}Ta	3	—	84.6802	—	—	0.0016
^{160}Tb	4	6	86.790	0.001	0.001	0.002
^{109}Cd	4	14	88.032	0.001	0.001	0.002
^{176m}Lu	5	4	88.367	0.002	0.002	0.003
^{75}Se	4	6	96.734	0.002	0.002	0.003
^{153}Gd	4	12	97.432	0.001	0.001	0.003
^{182}Ta	3	—	100.1067	—	—	0.0019
^{153}Gd	4	12	103.181	0.001	0.001	0.002
^{169}Yb	5	9	109.784	0.001	0.001	0.003
^{182}Ta	3	—	113.6677	—	—	0.0022
^{182}Ta	3	—	116.4172	—	—	0.0023
^{169}Yb	5	9	118.191	0.001	0.001	0.003
^{75}Se	4	12	121.117	0.001	0.001	0.003
^{152}Eu	4	14	121.782	0.001	0.001	0.003
^{57}Co	4	15	122.060	0.001	0.001	0.002
^{169}Yb	5	9	130.525	0.001	0.002	0.003
^{144}Ce	4	9	133.518	0.001	0.001	0.003
^{75}Se	4	12	136.000	0.001	0.001	0.003
^{57}Co	4	6	136.475	0.001	0.002	0.005
^{141}Ce	6	4	145.443	0.001	0.001	0.003
^{182}Ta	3	—	152.4298	—	—	0.0029
^{182}Ta	3	—	156.3819	—	—	0.0030
^{139}Ce	4	32	165.854	0.001	0.001	0.003
^{173}Lu	5	10	171.402	0.001	0.001	0.004
^{169}Yb	5	9	177.208	0.001	0.001	0.004
^{173}Lu	5	9	179.363	0.001	0.001	0.004
^{182}Ta	3	—	179.3895	—	—	0.0034
^{160}Tb	5	4	197.026	0.003	0.002	0.004
^{169}Yb	5	9	197.948	0.001	0.001	0.004
^{182}Ta	3	—	198.3478	—	—	0.0038
^{75}Se	5	6	198.603	0.002	0.002	0.005
^{167}Tm	6	4	207.797	0.001	0.001	0.004
^{160}Tb	4	6	215.641	0.001	0.001	0.004
^{82}Br	6	5	221.476	0.002	0.001	0.006
^{182}Ta	3	—	222.1037	—	—	0.0042
^{182}Ta	3	—	229.3162	—	—	0.0052
^{173}Lu	5	9	233.603	0.002	0.001	0.005
^{152}Eu	4	14	244.691	0.001	0.001	0.005
^{113}Sn	4	15	255.132	0.007	0.002	0.008
^{169}Yb	5	9	261.069	0.007	0.004	0.009
^{182}Ta	3	—	264.0711	—	—	0.0050
^{75}Se	5	6	264.652	0.001	0.001	0.005
^{173}Lu	5	6	272.111	0.001	0.001	0.005
^{133}Ba	4	7	276.397	0.003	0.003	0.005
^{203}Hg	4	10	279.189	0.001	0.001	0.006
^{75}Se	5	9	279.535	0.001	0.001	0.006
^{173}Lu	5	5	285.369	0.002	0.003	0.006
^{192}Ir	3	—	295.9483	—	—	0.0052
^{160}Tb	5	5	298.571	0.002	0.002	0.006
^{133}Ba	4	7	302.850	0.002	0.002	0.006
^{75}Se	5	7	303.908	0.004	0.003	0.010
^{169}Yb	+5	—	307.732	0.002	0.003	0.006
^{192}Ir	3	—	308.4464	—	—	0.0054
^{192}Ir	3	—	316.4977	—	—	0.0056
^{152}Eu	4	11	344.267	0.001	0.001	0.007
^{133}Ba	4	7	356.005	0.002	0.002	0.007
^{133}Ba	4	7	383.831	0.003	0.004	0.008
^{113}Sn	4	17	391.688	0.002	0.002	0.007
^{75}Se	+5	9	400.650	0.002	0.003	0.008
^{152}Eu	5	5	411.084	0.006	0.007	0.010
^{198}Hg	2	—	411.794	—	—	0.007
^{192}Ir	3	—	416.4501	—	—	0.0079
^{152}Eu	5	5	443.940	0.005	0.003	0.009
^{110m}Ag	5	9	446.802	0.004	0.005	0.011
^{192}Ir	3	—	468.0546	—	—	0.0082
^{82}Br	6	5	554.330	0.004	0.005	0.011
^{134}Cs	5	6	563.231	0.004	0.003	0.011
^{134}Cs	5	6	569.322	0.003	0.002	0.012
^{207}Bi	4	16	569.683	0.001	0.002	0.011
^{192}Ir	3	—	588.5562	—	—	0.0106
^{192}Ir	3	—	604.3942	—	—	0.0106
^{134}Cs	5	11	604.707	0.001	0.002	0.012
^{192}Ir	3	—	612.4460	—	—	0.0106
^{110m}Ag	5	9	620.353	0.005	0.006	0.014
^{173}Lu	+4	—	636.129	0.004	0.006	0.013
^{110m}Ag	5	8	657.744	0.002	0.002	0.013
^{137}Cs	5	11	661.648	0.002	0.002	0.013
^{110m}Ag	5	9	677.613	0.002	0.002	0.014
^{110m}Ag	5	9	687.001	0.003	0.004	0.014
^{144}Ce	5	10	696.492	0.004	0.003	0.013
^{82}Br	6	5	698.361	0.004	0.003	0.013
^{110m}Ag	5	10	706.672	0.002	0.003	0.014
^{110m}Ag	5	9	744.271	0.003	0.004	0.015
^{110m}Ag	5	9	763.936	0.003	0.005	0.016
^{82}Br	6	5	776.516	0.004	0.003	0.014
^{152}Eu	6	7	778.914	0.003	0.004	0.015
^{95m}Tc	+4	—	786.188	0.005	0.005	0.015
^{134}Cs	5	10	795.856	0.002	0.003	0.016
^{134}Cs	5	11	801.957	0.003	0.004	0.016
^{110m}Ag	5	9	818.028	0.004	0.007	0.015
^{95m}Tc	+4	—	820.632	0.011	0.012	0.019
^{82}Br	7	5	827.828	0.005	0.007	0.016
^{54}Mn	5	14	834.858	0.002	0.002	0.015
^{56}Co	6	13	846.777	0.004	0.001	0.016
^{152}Eu	6	5	867.383	0.006	0.003	0.016
^{160}Tb	6	5	879.387	0.005	0.005	0.017
^{110m}Ag	5	9	884.695	0.002	0.002	0.016
^{88}Y	6	11	898.048	0.004	0.005	0.019
^{110m}Ag	5	9	937.507	0.003	0.002	0.017
^{160}Tb	6	5	962.347	0.007	0.003	0.018
^{152}Eu	6	8	964.070	0.003	0.002	0.018
^{160}Tb	6	5	966.163	0.005	0.002	0.019
^{56}Co	6	18	1037.841	0.003	0.002	0.018
^{82}Br	7	5	1043.996	0.005	0.008	0.020
^{207}Bi	6	14	1063.660	0.002	0.001	0.019
^{152}Eu	6	7	1085.835	0.004	0.004	0.019
^{152}Eu	6	8	1112.065	0.008	0.004	0.022
^{65}Zn	6	12	1115.555	0.004	0.001	0.020
^{182}Ta	6	8	1121.290	0.004	0.002	0.020
^{60}Co	6	8	1173.236	0.005	0.004	0.021
^{56}Co	6	11	1175.095	0.006	0.008	0.023
^{160}Tb	6	5	1177.970	0.007	0.001	0.022
^{182}Ta	6	8	1189.034	0.004	0.002	0.021
^{160}Tb	6	5	1199.904	0.008	0.006	0.023
^{152}Eu	6	8	1212.895	0.008	0.004	0.023
^{182}Ta	6	8	1221.391	0.004	0.002	0.022
^{182}Ta	6	8	1230.988	0.004	0.003	0.023
^{56}Co	6	18	1238.271	0.003	0.002	0.022
^{182}Ta	6	8	1257.416	0.007	0.006	0.023
^{160}Tb	6	5	1271.896	0.007	0.003	0.024
^{182}Ta	6	8	1273.711	0.010	0.005	0.024
^{22}Na	6	8	1274.531	0.004	0.002	0.023
^{182}Ta	6	8	1289.119	0.007	0.015	0.024
^{152}Eu	6	5	1299.108	0.009	0.007	0.024
^{160}Tb	6	5	1312.174	0.007	0.011	0.026
^{82}Br	7	5	1317.459	0.007	0.007	0.025
^{60}Co	6	8	1332.485	0.005	0.003	0.025
^{56}Co	6	15	1360.209	0.005	0.005	0.024
^{134}Cs	+5	—	1365.177	0.003	0.002	0.024
^{24}Na	6	8	1368.615	0.006	0.003	0.026
^{110m}Ag	+5	—	1384.285	0.005	0.007	0.026
^{152}Eu	6	8	1407.974	0.006	0.004	0.026
^{110m}Ag	+5	—	1475.778	0.009	0.006	0.027
^{144}Ce	6	10	1489.132	0.009	0.006	0.027
^{110m}Ag	+5	—	1505.036	0.005	0.006	0.028
^{110m}Ag	+5	—	1562.303	0.004	0.006	0.029
^{207}Bi	7	6	1770.253	0.013	0.006	0.034
^{56}Co	7	13	1771.347	0.006	0.007	0.032
^{56}Co	7	9	1810.768	0.018	0.018	0.037
^{88}Y	7	10	1836.074	0.008	0.003	0.034
^{56}Co	7	13	1963.760	0.019	0.017	0.038
^{56}Co	7	13	2015.196	0.018	0.008	0.040
^{56}Co	7	13	2034.772	0.007	0.006	0.037
^{56}Co	7	7	2113.154	0.030	0.015	0.048
^{144}Ce	6	—	2185.607	0.007	—	0.041
^{56}Co	7	7	2212.859	0.036	0.038	0.055
^{56}Co	+6	—	2598.444	0.006	0.008	0.047
^{24}Na	7	6	2753.989	0.012	0.012	0.051
^{56}Co	7	7	3009.587	0.023	0.017	0.059
^{56}Co	7	7	3201.987	0.019	0.009	0.060
^{56}Co	+6	—	3253.414	0.013	0.006	0.060
^{56}Co	7	7	3273.000	0.020	0.022	0.062
^{56}Co	7	7	3451.173	0.024	0.018	0.070

Note. $\Phi_1 = \alpha_1$; $\Phi_2 = \alpha_2$; Q is the order of standard; q is the number of series of measurements.

netic β spectrometer (Table XI). The γ-ray energy values are in excellent agreement. Some concern is caused by the transition energy 1368 keV (^{24}Na), but we assume that the discrepancy can only be due to some error in Ref. 33.

Relative intensities of γ rays of radioactive nuclides used for spectrometer calibration[29]

Use of computers for processing of a spectral line permits determination of the area S with an error < 1% (see Fig. 24). Consequently, for realization of this accuracy in an experiment it is necessary to investigate the spectrometer efficiency with a comparable error. An ideal case is the use of one source containing a sufficient number of intense lines uniformly distributed over a wide energy range (such sources will be called multistandard). In an actual physical experiment ^{226}Ra is most frequently used. Unfortunately its γ spectrum is complex, among the daughter products are gases (so that it is difficult to observe equilibrium conditions),

TABLE VIII. γ-ray energy obtained by means of concurrent cascade transitions and measured by means of energy standards (see Table VII).

Nuclide	$E(1)$	$\Phi(1)$	$E(2)$	$\Phi(2)$	$E(C)$	$\Phi(C)$	$E(D)$	$\Phi(D)$	Difference
^{56}Co	1238.271	0.003	1360.209	0.005	2598.450	0.006	2598.429	0.013	−0.021±0.014
	1238.271	0.003	2015.196	0.018	3253.423	0.018	3253.410	0.019	−0.013±0.026
	1238.271	0.003	2034.772	0.007	3272.995	0.008	3273.000	0.022	+0.005±0.023
^{75}Se	96.734	0.002	303.908	0.004	400.642	0.005	400.646	0.006	+0.004±0.008
	121.117	0.001	279.535	0.001	400.652	0.002	400.646	0.006	−0.006±0.007
	136.000	0.001	264.652	0.001	400.652	0.002	400.646	0.006	−0.006±0.007
^{82}Br	221.476	0.002	606.344	0.012	827.819	0.012	827.828	0.007	+0.009±0.014
	698.361	0.004	619.100	0.009	1317.456	0.010	1317.459	0.007	+0.003±0.012
	698.361	0.004	776.516	0.004	1474.865	0.006	1474.867	0.009	+0.002±0.011
^{95m}Tc	204.119	0.003	582.068	0.005	786.184	0.006	786.194	0.007	+0.010±0.009
	204.119	0.003	616.497	0.019	820.640	0.013	820.640	0.013	0.000±0.018
^{110m}Ag	446.802	0.005	937.507	0.003	1384.305	0.006	1384.274	0.007	−0.031±0.009
	677.613	0.002	706.672	0.003	1384.280	0.004	1384.274	0.007	−0.006±0.008
	620.353	0.006	763.936	0.005	1384.285	0.008	1384.274	0.007	−0.011±0.011
	657.744	0.002	818.028	0.007	1475.777	0.007	1475.781	0.010	+0.004±0.012
	620.353	0.006	884.695	0.002	1505.024	0.006	1505.028	0.011	+0.004±0.013
	687.001	0.004	818.028	0.007	1505.043	0.008	1505.028	0.011	−0.015±0.014
	677.613	0.002	884.695	0.002	1562.293	0.003	1562.319	0.020	+0.026±0.022
	744.271	0.004	818.028	0.007	1562.302	0.008	1562.319	0.020	+0.048±0.022
^{131}Ba	54.889	0.005	78.733	0.003	133.622	0.006	133.609	0.006	−0.013±0.008
	92.284	0.003	123.805	0.002	216.089	0.004	216.085	0.010	−0.004±0.011
	157.148	0.020	216.085	0.010	373.232	0.022	373.221	0.019	−0.011±0.029
	246.897	0.032	373.221	0.019	620.118	0.037	620.090	0.010	−0.028±0.039
^{140}Ba	328.763	0.004	487.012	0.010	815.773	0.011	815.770	0.015	−0.003±0.019
^{144}Ce	696.492	0.004	1489.132	0.009	2185.617	0.010	2185.607	0.013	−0.010±0.016
^{149}Gd	149.733	0.006	346.660	0.006	496.392	0.008	496.403	0.010	+0.011±0.013
	346.660	0.006	298.617	0.007	645.276	0.009	645.288	0.008	+0.012±0.012
	272.317	0.006	516.558	0.008	788.874	0.010	788.857	0.008	−0.017±0.013
	149.733	0.006	788.857	0.008	938.589	0.010	938.591	0.011	+0.002±0.015
	272.317	0.010	666.293	0.008	938.608	0.013	938.591	0.011	−0.017±0.017
^{152}Eu	244.691	0.001	443.940	0.005	688.630	0.005	688.655	0.048	+0.025±0.048
	367.768	0.014	411.084	0.007	778.850	0.016	778 914	0.009	+0.064±0.019
	121.782	0.001	964.070	0.003	1085.851	0.003	1085.835	0.009	−0.016±0.011
	678.639	0.020	411.084	0.007	1089.722	0.021	1089.726	0.028	+0.004±0.035
	244.691	0.001	867.383	0.006	1112.073	0.006	1112.065	0.010	−0.008±0.012
	443.940	0.005	964.070	0.003	1408.008	0.006	1407 974	0.009	−0.034±0.011
	244 691	0.001	1212 895	0.008	1457.592	0.008	1457.590	0.034	−0.002±0.036
^{160}Tb	86.790	0.001	879.387	0.005	966.177	0.005	966.163	0.005	−0.014±0.007
	197.026	0.003	765.311	0.009	962.337	0.010	962.347	0.007	+0.010±0.012
	298.571	0.002	879.387	0.005	1177.958	0.006	1177.970	0.007	+0.012±0.009
	215.641	0.001	962.347	0.007	1177.988	0.007	1177.970	0.007	−0.018±0.010
	197.026	0.003	1002.865	0.007	1199.891	0.008	1199.904	0.008	+0.013±0.011
	392.480	0.032	879.387	0.005	1271.867	0.032	1271.896	0.007	+0.029±0.033
	309.562	0.016	962.347	0.007	1271.909	0.018	1271.896	0.007	−0.013±0.019
	197.026	0.004	1115.156	0.018	1312.182	0.018	1312.174	0.011	−0.008±0.021
^{172}Lu	410.300	0.014	399.750	0.020	810.051	0.024	810.084	0.029	+0.033±0.038
	410.300	0.014	490.451	0.017	900.751	0.022	900.730	0.028	−0.021±0.036
	203.436	0.003	697.298	0.029	900.734	0.029	900.730	0.028	−0.004±0.040
	112.793	0.005	816.339	0.021	929.132	0.022	929.106	0.026	−0.006±0.034
	181.530	0.002	912.085	0.022	1093.615	0.022	1093.609	0.006	−0.006±0.033
	528.266	0.022	584.727	0.020	1112.991	0.030	1113.010	0.019	+0.019±0.049
	490.451	0.017	912.085	0.022	1402.536	0.028	1402.510	0.016	−0.024±0.032
	528.266	0.022	912.085	0.022	1440.349	0.031	1440.347	0.026	−0.002±0.035
^{173}Lu	78.651	0.006	100.719	0.006	179.370	0.008	179.363	0.004	−0.007±0.009
	100.719	0.006	171.402	0.003	272.120	0.007	272.111	0.002	−0.009±0.007
	171.402	0.003	179.363	0.004	350.764	0.005	350.750	0.005	−0.014±0.007
	171.402	0.003	285.369	0.003	456.771	0.004	456.769	0.013	−0.002±0.014
	100.719	0.006	456.769	0.013	557.488	0.014	557.485	0.016	−0.003±0.021
	285.369	0.003	350.750	0.005	636.120	0.007	636.129	0.007	+0.009±0.010
	456.769	0.013	179.363	0.004	636.132	0.014	636.129	0.007	−0.003±0.016
	557.485	0.016	78.651	0.006	636.136	0.017	636.129	0.007	−0.007±0.018
^{182}Ta	100.105	0.002	1189.034	0.004	1289.139	0.005	1289.119	0.014	−0.020±0.015
	100.105	0.002	1157.308	0.022	1257.410	0.022	1257.416	0.015	+0.006±0.027
	229.316	0.005	928.023	0.042	1157.338	0.043	1157.308	0.022	−0.030±0.048
	229.316	0.005	1001.705	0.006	1231.018	0.008	1230.988	0.004	−0.020±0.009
	84.681	0.003	1189.034	0.004	1273.714	0.005	1273.711	0.010	−0.003±0.012
	116.413	0.003	1157.308	0.022	1273.716	0.022	1273.711	0.010	−0.005±0.026
	152.427	0.003	1121.290	0.004	1273.717	0.005	1273.711	0.010	−0.006±0.011

Note. The designations are the same as in Table VI. Nuclear-recoil energy is taken into account.

TABLE IX. γ-ray energy obtained from total-absorption peaks (TA), single-escape peaks (SE), and double-escape peaks (DE).

E (DE)	Φ (DE)	E (SE)	Φ (SE)	E	Φ	Escape
749.448	0.041	1260.320	0.052	1771.450	0.041	DE
				1771.321	0.052	SE
				1771.347	0.023	TA
1576.530	0.042	2087.424	0.046	2598.532	0.042	DE
				2598.425	0.046	SE
				2598.435	0.011	TA
2180.148	0.105	2690.970	0.070	3202.150	0.105	DE
				3201.971	0.070	SE
				3201.987	0.019	TA
2231.572	0.031	2742.399	0.055	3253.574	0.031	DE
				3253.400	0.055	SE
				3253.414	0.016	TA
2251.179	0.047	2761.987	0.107	3273.181	0.047	DE
				3272.988	0.107	SE
				3273.000	0.022	TA

and there is not an adequate number of intense γ transitions uniformly distributed in energy. Therefore we shall investigate a set of radionuclides which represent such a hypothetical source.

For calibration of a set of multistandard sources, three approaches are possible.

1. *Calculation of detector efficiency on the basis of the total-absorption peak.* The method is based on the dependence of the photoeffect and Compton scattering on the Z of the detector and on the γ-ray energy. Sources calibrated in activity are used to determine those parameter values which best satisfy the experimental points. An example of this approach is shown in Fig. 50.[40] Let us consider the break in the theoretical curve in the region 200–600 keV. As a rule, authors who have studied

TABLE X. γ-ray energy standards.

Nuclide	[29]			[32]		[36]		[56]		[57]		
	E	$\Delta E'$	ΔE	E	ΔE	E	ΔE	E	ΔE	E	$\Delta E'$	ΔE
^{109}Cd	88.032	0.002	0.002	88.035	0.006	88.037	0.005	88.032	0.002	—	—	—
^{153}Gd	97.432	0.002	0.003	97.429	0.003	97.432	0.003	—	—	97.42920	0.00026	0.00168
^{153}Gd	103.181	0.002	0.002	103.179	0.004	103.180	0.002	—	—	103.17804	0.00021	0,00177
^{152}Eu	121.782	0.002	0.003	121.780	0.004	—	—	—	—	121.7793	0.0003	0.0021
^{57}Co	122.060	0.001	0.002	—	—	122.063	0.004	—	—	122.05826	0.00012	0.0021
^{57}Co	136.475	0.002	0.004	—	—	136.473	0.004	—	—	136,47089	0.00030	0.0023
^{139}Ce	165.854	0.002	0.003	—	—	165.857	0.007	165.853	0.007	—	—	—
^{160}Tb	215.641	0.002	0.004	—	—	215.641	0.004	—	—	—	—	—
^{152}Eu	244.691	0.002	0.005	244.693	0.010	—	—	—	—	244.6927	0.0008	0.0042
^{203}Hg	279.189	0.003	0.006	279.190	0.009	279.188	0.006	279.190	0.006	—	—	—
^{160}Tb	298.571	0.003	0.006	—	—	298.572	0.006	—	—	—	—	—
^{152}Eu	344.267	0.003	0.007	344.267	0.010	—	—	—	—	344.2724	0.0017	0.0061
^{152}Eu	367.768	0.014	0.016	—	—	—	—	—	—	367.779	0.004	0.007
^{113}Sn	391.688	0.003	0.007	—	—	391.688	0.010	—	—	—	—	—
^{152}Eu	411.084	0.007	0.010	—	—	—	—	—	—	411.107	0.007	0,010
^{152}Eu	443.940	0 005	0.009	—	—	—	—	—	—	443.979	0.006	0.010
^{207}Bi	569.683	0.004	0.011	—	—	569.689	0.013	—	—	—	—	—
^{134}Cs	604.707	0.004	0.012	604.748	0.030	—	—	—	—	—	—	—
^{137}Cs	661.648	0.004	0.013	661.633	0.012	661.638	0.019	—	—	661.6492	0.0052	0.012
^{110m}Ag	763.936	0.007	0.016	—	—	763.928	0.019	—	—	—	—	—
^{152}Eu	778.914	0.006	0.015	—	—	—	—	—	—	778.905	0.013	0.019
^{54}Mn	834.858	0.006	0.015	—	—	834.827	0.021	—	—	—	—	—
^{88}Y	898.048	0.006	0.019	—	—	898.021	0.019	—	—	—	—	—
^{152}Eu	964.070	0.006	0.018	—	—	—	—	—	—	964.007	0.035	0.039
^{207}Bi	1063.660	0.006	0.019	—	—	1063.635	0.024	—	—	—	—	—
^{152}Eu	1085,835	0.006	0.019	—	—	—	—	—	—	1085.793	0.034	0.039
^{65}Zn	1115.555	0.006	0.020	—	—	1115.518	0.025	1115.39	0.10	—	—	—
^{60}Co	1173.236	0,007	0.021	1173.263	0.040	1173.208	0.025	1173.22	0.08	1173.210	0.006	0.021
^{22}Na	1274.531	0.006	0.023	—	—	1274.511	0.028	—	—	—	—	—
^{60}Co	1332.485	0.007	0.025	1332.524	0.046	1332.464	0.028	1332.52	0.10	1332.470	0.007	0.024
^{24}Na	1368.615	0.007	0.025	1368.558	0.044	1368.599	0.029	—	—	—	—	—
^{152}Eu	1407.974	0.009	0.026	—	—	—	—	—	—	1407.993	0.035	0.042
^{144}Ce	1489.132	0.009	0.027	—	—	1489.124	0.032	—	—	—	—	—
^{207}Bi	1770.253	0.009	0.034	—	—	1770.188	0.037	—	—	—	—	—
^{88}Y	1836.074	0.008	0.034	—	—	1836.014	0.037	—	—	—	—	—
^{144}Ce	2185.607	0.013	0.041	—	—	2185.608	0.046	—	—	—	—	—
^{56}Co	2598.435	0.011	0.047	—	—	2598.400	0.053	—	—	—	—	—
^{24}Na	2753.989	0.015	0.051	2753.99	0.12	2753.965	0.056	—	—	—	—	—
^{56}Co	3253.414	0.016	0.060	—	—	3253.341	0.065	—	—	—	—	—
^{56}Co	3451,173	0.029	0.070	—	—	3451.064	0.069	—	—	—	—	—

the γ-ray total-absorption mechanism do not report the relative intensities of the γ rays of multistandard sources obtained under these conditions, which would permit reproduction of the experimental efficiency values obtained by them.

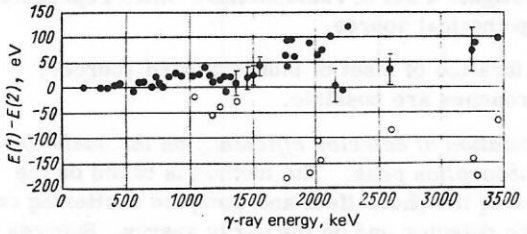

FIG. 49. Difference of γ-ray energy-standard values recommended in the present work $E(1)$ and in Ref. 36 $E(2)$ (solid circles). As the error we have given the value $[(\Phi(1))^2+(\Phi(2))+(\Phi(2))^2]^{1/2}$, where the error Φ is the greater of α_1 and α_2. Also shown are the differences of the ^{56}Co γ-ray energy values measured by us and in Ref. 38 (hollow circles).

2. *Calculation of relative γ-ray intensities by means of conversion-electron relative intensities and known multipolarities of transitions.* For multistandard sources this approach has not been used, but in some particular problems it permits obtaining information which cannot be obtained by other methods. For example, in Ref. 41 the efficiency of a Ge(Li) detector in the region 200–500 keV was determined by means of the calculated γ-ray intensities of $180m_{Hf}$. Here we must not forget the uncertainties due both to the determination of the transition multipolarity and to the use of the theoretical conversion-coefficient values.

3. *Study of spectrometer efficiency by means of activity-calibrated sources.* At the present time this method is the most direct and reliable method in the study of spectrometer efficiency, since it involves use of data on various sources. On the other hand, it is exceptionally complicated and laborious, since measurements must be made with allowance for all effects dis-

TABLE XI. Energy of ^{60}Co and ^{24}Na γ rays from various studies.

Nuclide	Present work		Ref. 33	
	E	ΔE	E	ΔE
^{60}Co	1173.236	0.021	1173.226	0.040
^{60}Co	1332.485	0.025	1332.483	0.046
^{24}Na	1368.615	0.025	1368.526	0.044
^{24}Na	2753.989	0.056	2753.920	0.120

torting the uncorrected spectrum. In addition, the problem of obtaining complete sets of activity-calibrated sources at the time of performing experiments is by no means simple to organize. The relative intensities of γ rays of a complete set of multistandard sources have been investigated in Ref. 28. We give below the essence of this method.

For investigation of the absolute efficiency of spectrometers, five different sets of standard spectrometric γ sources (SSGS) were used: one, specially prepared, had sources of activity 10^6 decays/sec; four, obtained from the All-Union Isotope Combine, contained sources of activity 10^5 decays/sec. Three sets, except for the sources of ^{203}Hg and ^{113}Sn which they included, were certified in activity with higher accuracy at the D. I. Mendeleev Institute of Metrology. The thickness of the polyethylene films between which the active layers of the sources were placed was 11 ± 3 mg/cm^2. The radioactive sources, the error in measurement of their activity ΔA, and the γ-ray yield per 100 decays are listed in Table V. We have also shown in that table the minimal efficiency errors which can be obtained for various values of ΔA. The values $\Delta A = 1.5\%$ refer to the standard set of SSGS for the 68% confidence level. The measurements were made in various semiconductor detectors. The experimental values for four spectrometers and the results of their approximation are shown in Fig. 51. Here we must note in particular the difficulties associated with the choice of the region of approximation. These difficulties are due mainly to the complicated process of γ-ray detection by Ge(Li) detectors in the region from 100 to 600 keV, where strong competition occurs between the photoeffect and multiple scattering in the

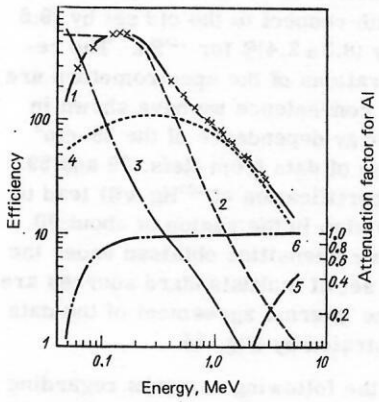

FIG. 50. Efficiency of 60 cm^3 Ge(Li) detector on the basis of the total-absorption peak: crosses—experimental points; 1—theoretical curve; 2—photoeffect; 3—Compton effect; 4—multiple Compton effect; 5—pair production; 6—attenuation factor for aluminum.

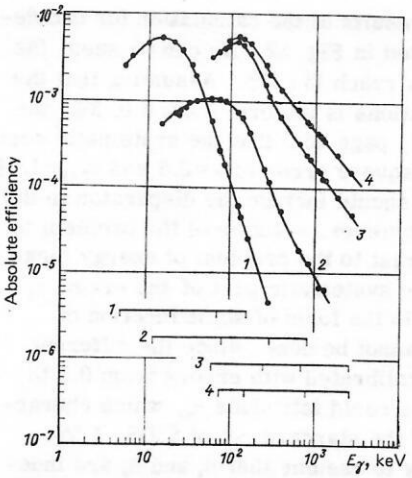

FIG. 51. Experimental efficiency values for γ spectrometers based on total-absorption peaks and their approximation by a polynomial (continuous curve). The region of the approximation is also indicated. 1—80 mm^2 ×4 mm Si(Li) detector; 2—1.3 cm^3 Ge(Li) detector; 3—11 cm^3 Ge(Li) detector; 4—37 cm^3 Ge(Li) detector.

detector sensitive volume. The difficulties are further aggravated by the fact that in this energy region there are not a sufficient number of activity-calibrated sources. The last remark refers also to the energy region 35–120 keV.

The search for possible systematic errors in the experimental technique is carried out by comparison of the relative γ-ray intensities of a number of nuclides measured with different semiconductor detectors. Three measurements were made for each source in each detector. The data were analyzed according to the following formulas:

$$\left.\begin{aligned} \nu[\%] &= [I(n) - I(m)] \times [I(n)]^{-1} \times 100; \\ \Delta\nu[\%] &= [\Delta I(n) + \Delta I(m)] \times [I(n)]^{-1} \times 100; \\ I(n) &= \sum w_i I_i / \sum w_i;\ \Delta I(n) = \left(\sum w_i\right)^{-1/2}. \end{aligned}\right\} \quad (40)$$

Here $w_i = (\Delta I_i)^{-2}$ is the weight of the i-th measurement, $N-n$ is the number of measurements in all detectors, $N-m$ is the number of measurements in a given detector, and $I(n)$ and $I(m)$ are the relative intensities obtained with all detectors and with only a given detector,

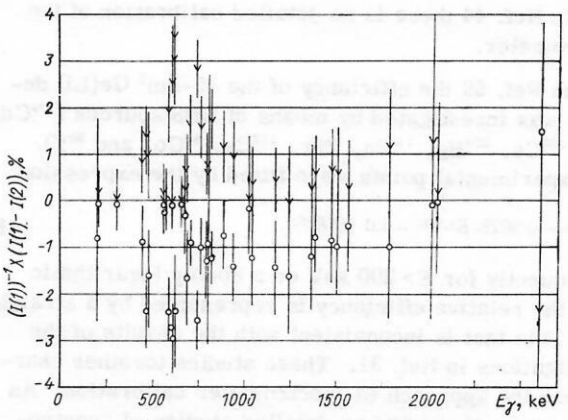

FIG. 52. Difference of relative-intensity values for each detector $I(2)$ and for all detectors $I(1)$: ●—37 cm^3 Ge(Li) detector; ∨—11 Cm^{3}Ge(Li) detector.

respectively. The results of the calculation for two detectors are illustrated in Fig. 52. As can be seen, the maximum deviations reach $(3 \pm 1)\%$. Assuming that the distribution of deviations is uniform from 0 to 3%, we can suggest (Ref. 32, page 154) that the systematic component of the mean-square error is $\varkappa = 0.6$ and $\nu_{max} = 1.8\%$. In the quantity $\varkappa$ we should include the dispersion in the absolute activity. However, solution of the problem is not simple. In contrast to the problem of energy measurement, where the systematic part of the error α_4 can be represented in the form of some function of energy, here this cannot be done, since the different sources have been calibrated with errors from 0.5 to 2.5%. Of course, we could introduce β_4, which characterizes the error of the standard set of SSGS, 1.5%. Here it is necessary to assume that β_3 and β_4 are independent, which is not obvious. Exaggeration of the relative γ-ray intensities is inconsistent with the approach (see below) that these values are considered as an intermediate step in the search for the true values.

The relative γ-ray intensities obtained under these conditions for the set of multistandard sources have been published elsewhere.[29] Comparison of our results with those in the literature has shown that in the region 200–600 keV significant discrepancies are observed. This fact has been the cause of extensive and, as far as possible, universal analysis. The discrepancy can be discussed best in the case of ^{152}Eu, since the normalization of the relative intensities is accomplished by means of the 344-keV transition, which is located in the center of the region of conflict.

First, we have analyzed the conditions of several experiments on measurement of γ-ray spectra by various authors:

a) In Ref. 42 the spectrometer efficiency was determined by the Monte Carlo method, and the correctness of the calculation was verified in a narrow energy region by means of the relative intensities of ^{133}Ba γ rays.

b) In Ref. 33 the spectrometer efficiency was investigated by means of IAEA sources. Let us consider three facts: a small planar Ge(Li) detector was used; the experimental points were not fitted by an analytic expression; there are no transitions in the region 279–661 keV.

c) In Ref. 44 there is no detailed calibration of the spectrometer.

d) In Ref. 59 the efficiency of the 45-cm^3 Ge(Li) detector was investigated by means of NBS sources (^{109}Cd, ^{57}Co, ^{139}Ce, ^{203}Hg, ^{113}Sn, ^{85}Sr, ^{137}Cs, ^{60}Co, and ^{88}Y). The experimental points were fitted by the expression

$$1/\varepsilon = 0.9023 \cdot E^{1.0625} + 6.0 \cdot 10^6 E^{-2.5}. \quad (41)$$

Consequently for $E > 200$ keV on a doubly logarithmic scale the relative efficiency is represented by a straight line. This fact is inconsistent with the results of the investigations in Ref. 31. These studies together characterize the approach to spectrometer calibration. As can be seen, there are no detailed studies of spectrometer efficiency in the region 200–600 keV.

Second, we have again analyzed the conditions of our

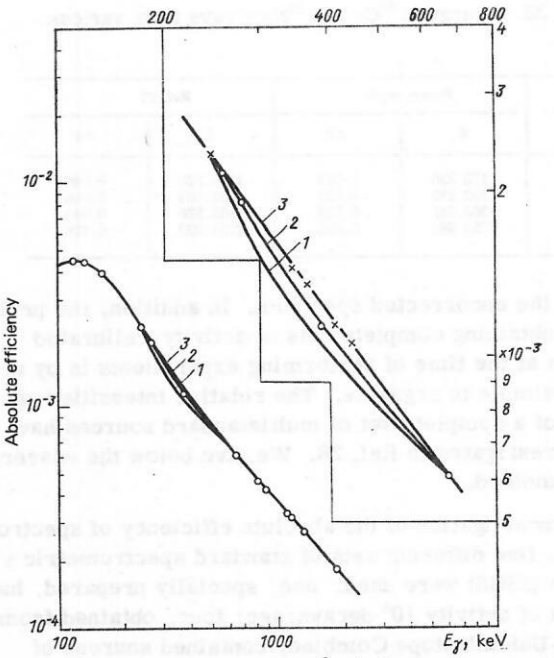

FIG. 53. Efficiency of a 38 cm^{3}Gi(Li) detector investigated by means of activity-calibrated sources of SSGS (circles); crosses—efficiency values obtained from the results of Ref. 59; the normalization was to the 122-keV transition (^{57}Co, ^{152}Eu); the lines are the fitted values obtained by the following means: 1—Ref. 29; 2—new SSGS sources; 3—Ref. 59; in the upper right corner we have shown a portion of the region of discrepancy.

experiments.[29] In principle, three assumptions are possible for explanation of the discrepancy: the decay schemes of ^{203}Hg and ^{113}Sn (see Table V) are calculated incorrectly; an error exists in the experiments; the ^{203}Hg and ^{113}Sn sources were incorrectly certified in activity. At the present time we reject the first assumption. The efficiency of the detectors was measured by means of five different sources of ^{203}Hg and ^{113}Sn and the results agree among themselves within ±1.5 and ±1.2%, respectively. The absence of systematic errors in the experiments is indicated by Fig. 52. Therefore special attention was devoted to the third assumption. For this purpose we carried out a new series of control measurements by means of three new sets of SSGS (1977). It turned out that the activities of the new set of sources differ (are reduced) with respect to the old set by $(9.6 \pm 2.7)\%$ for ^{203}Hg and by $(8.3 \pm 2.4)\%$ for ^{113}Sn. The results of repeated calibrations of the spectrometers are shown in Fig. 53. For convenience we have shown in that figure also the energy dependence of the 38-cm^3 Ge(Li) detector with use of data from Refs. 29 and 59. We note that error in certification of ^{203}Hg will lead to corrections of the data also in the region of about 80 keV. The γ-ray relative intensities obtained under the new conditions for the set of multistandard sources are given in Table XII. The internal agreement of the data from Table XII is illustrated by Fig. 44.

It is useful to make the following remarks regarding the efficiency calibration of γ spectrometers. Use of computers for processing of the uncorrected spectra has led to the result that the area of a peak can be determined with an error less than 1%. On the other hand, the average of the errors in the relative intensities of

TABLE XII. Energy and relative intensity of γ rays of radioactive nuclides used for calibration of semiconductor γ spectrometers.

E	ΔE	I	ΔI
		^{171}Lu	
19.017	0.010	33.054	0.818
27.117	0.024	1.581	0.038
51.354	*KX*	72.448	1.730
52.389	*KX*	126.594	2.882
55.690	0.011	2.550	0.070
59.3	*KX*	40.280	0.910
61.0	*KX*	10.932	0.363
66.738	0.003	5.070	0.121
72.382	0.006	3.932	0.091
75.891	0.002	12.692	0.289
85.598	0.011	2.252	0.054
91.399	0.007	0.962	0.024
109.284	0.006	1.207	0.030
627.008	0.021	1.841	0.042
630.953	0.041	0.264	0.011
667.357	0.016	23.769	0.494
689.272	0.026	5.068	0.104
712.654	0.024	2.443	0.052
739.747	0.023	100.000	1.809
767.597	0.022	1.378	0.078
780.656	0.027	9.109	0.206
839.942	0.031	6 365	0.135
853.033	0.025	5.282	0.139
		^{153}Gd	
40.901	*KX*	115.021	3.396
41.542	*KX*	206.015	6.012
47.0	*KX*	63.842	1.702
48.4	*KX*	16.420	0.491
69.672	0.003	8.275	0.153
97.432	0.003	100.000	1.808
103.181	0.002	73.596	1.357
172.848	0.015	0.128	0.030
		^{152}Eu	
39.523	*KX*	75.456	1.760
40.118	*KX*	134.048	2.821
42.308	*KX*	0.794	0.023
42.996	*KX*	1.444	0.042
45.3	*KX*	40.410	0.846
46.6	*KX*	10.044	0.233
48.6	*KX*	0.465	0.012
49.9	*KX*	0.110	0.008
121.782	0.003	100.000	2.476
244.691	0.005	25.839	0.522
295.963	0.031	1.556	0.038
344.267	0.007	96.528	1.784
367.768	0.016	3.147	0.061
411.084	0.010	7.886	0.175
443.940	0.009	10.955	0.268
488.735	0.053	1.420	0.056
564.062	0.088	1.639	0.153
678.639	0.023	1.557	0.094
688.655	0.049	2.945	0.087
719.406	0.055	1.138	0.045
778.914	0.015	44.026	1.106
867.383	0.016	14.182	0.344
964.070	0.018	49.441	1.298
1005.235	0.034	2.218	0.084
1085.835	0.019	34.609	0.965
1089.726	0.034	5.730	0.157
1112.065	0.022	46.646	1.228
1212.895	0.023	4.856	0.160
1299.108	0.024	5.649	0.167
1407.974	0.026	72.366	1.878
1457.590	0.043	1.739	0.066
1528.135	0.104	1.069	0.027
		^{182}Ta	
31.737	0.001	2.293	0.056
42.714	0.001	0.683	0.024
57.983	*KX*	26.473	0.998
59.320	*KX*	44.281	1.112
65.722	0.001	7.906	0.186
67.2	*KX*	12.060	0.386
67.750	0.001	118.835	3.068
69.1	*KX*	3.188	0.160
84.681	0.003	6.757	0.134
100.105	0.002	37.006	0.719
110.406	0.014	0.279	0.022
113.672	0.008	4.949	0.135
116.413	0.003	1.177	0.043
152.427	0.003	19.114	0.366
156.380	0.005	7.262	0.141
179.388	0.003	8.631	0.163
198.349	0.007	4.035	0.082
222.102	0.006	20.767	0.416
229.316	0.005	9.921	0.370
264.069	0.005	9.990	0.215
928.923	0.046	1.625	0.055
1001.705	0.019	5.794	0.148
1113.547	0.124	2.228	0.215
1121.290	0.020	100.000	1.905
1157.493	0.030	2.837	0.134
1189.034	0.021	47.221	0.871
1221.391	0.022	77.336	1.458
1230.988	0.023	32.555	0.619
1257.416	0.023	4.309	0.090
1273.711	0.024	1.854	0.054
1289.119	0.024	3.858	0.080
1342.656	0.034	0.721	0.020
1373.770	0.045	0.631	0.036
1387.310	0.043	0.205	0.028
		^{56}Co	
263.743	0.245	0.154	0.037
787.805	0.194	0.335	0.044
846.778	0.016	100.000	1.876
896.486	0.279	0.192	0.069
977.356	0.039	1.413	0.061
1037.843	0.019	14.079	0.272
1140.662	0.272	0.272	0.070
1159.735	0.147	0.185	0.110
1175.095	0.023	2.284	0.070
1198.952	0.228	0.033	0.019
1238.271	0.023	68.162	1.362
1335.220	0.325	0.308	0.075
1360.209	0.024	4.424	0.096
1442.515	0.310	0.176	0.042
1771.347	0.032	15.797	0.338
1810.768	0.037	0.597	0.043
1963.760	0.038	0.708	0.026
2015.196	0.040	3.049	0.081
2034.772	0.037	8.058	0.165
2113.154	0.048	0.386	0.035
2212.859	0.055	0.380	0.043
2524.466	0.280	0.146	0.045
2598.435	0.047	17.082	0.490
3009.587	0.059	1.124	0.100
3201.987	0.060	2.946	0.113
3253.414	0.060	7.276	0.177
3273.000	0.062	1.733	0.085
3451.173	0.070	0.900	0.031
3547.961	0.083	0.181	0.013
		^{144}Ce	
80.118	0.004	13.225	0.287
133.518	0.003	100.000	2.554
696.492	0.013	11.431	0.295
1489.132	0.027	2,376	0.064
2185.607	0.041	6.092	0.148
		^{75}Se	
66.050	0.003	1.809	0.068
96.734	0.003	5.690	0.249
121.117	0.003	29.037	0.934
136.000	0.003	99.052	1.895
198.603	0.005	2.367	0.087
264.652	0.005	100.000	1.846
279.535	0.006	42.631	0.876
303.908	0.010	2.256	0.055
400.646	0.008	20.768	0.780
		^{169}Yb	
49.772	*KX*	137.806	2.978
50.742	*KX*	239.165	5.629
57.5	*KX*	76.425	1.757
59.0	*KX*	20.193	0.597
63.118	0.001	113.584	2.936
93.613	0.005	6.811	0.224
109.784	0.003	45.820	1.694
118.191	0.003	4.867	0.140
130.525	0.003	30.936	0.733
177.208	0.004	62.375	1.171
197.948	0.004	100.000	1.834
240.305	0.027	0.414	0.085
261.069	0.012	4.962	0.189
307.732	0.006	29.270	0.654
		^{133}Ba	
30.625	*KX*	59.619	1.249
30.973	*KX*	109.349	2.252
34.9	*KX*	31.571	0.655
35.8	*KX*	7.493	0.168
53.160	0.004	3.573	0.088
79.629	0.005	4.162	0.157
80.993	0.003	54.594	1.181
160.613	0.008	0.975	0.075
223.307	0.063	0.712	0.033
276.397	0.005	11.372	0.220
302.850	0.006	28.847	0.600
356.005	0.007	100.000	1.868
383.831	0.008	14.322	0.392
		^{207}Bi	
72.805	*KX*	19.923	0.437
74.970	*KX*	33.892	0.798
84.5	*KX*	11.642	0.406
87.4	*KX*	3.501	0.100
569.683	0.011	100.000	1.834
897.928	0.116	0.132	0.032
1063.660	0.019	76.205	1.461
1442.228	0.281	0.099	0.010
1770.253	0.034	7.221	0.147
		^{134}Cs	
475.356	0.011	1.551	0.041
563.231	0.011	8.758	0.173
569.322	0.012	15.953	0.292
604.707	0.012	100.000	1.835
795.856	0.016	87.415	1.822
801.957	0.016	8,303	0.184
1038.608	0.013	1.029	0.020
1167.946	0.014	1.890	0.038
1365.177	0.024	3.212	0.066
		^{173}Lu	
51.354	*KX*	191.640	4.720
52.389	*KX*	331.592	7.557
59.4	*KX*	106.893	2.460
61.0	*KX*	27.904	0.889
78.651	0.006	52.115	1.190
100.719	0.007	23.331	0 531
171.402	0.004	13.834	0.379
179.363	0.004	6.362	0.177
223.200	0.038	0.756	0.031
233.603	0.005	2.604	0.065
272.111	0.005	100.000	1.886
285.369	0.006	2.802	0.080
334.316	0.012	0.538	0.031
350.750	0.008	1.603	0.033
456.769	0.015	0.725	0.026
557.485	0.019	2.634	0.105
636.129	0.013	7.286	0.185
		^{110m}Ag	
446.802	0.011	4.149	0.090
620.353	0.014	2.811	0.143
657.744	0.013	100.000	1.832
677.613	0.014	11.286	0.212
687.001	0,014	6.844	0.146
706.672	0.014	17.502	0.387
744.271	0.015	4.852	0.174
763.936	0.015	23.519	0.522
818.028	0.015	7.714	0.179
884.695	0.016	77.066	1.574
937.507	0.017	36.441	0.726
1384.279	0.026	26.668	0.513
1475.778	0.026	4.372	0.086
1505.028	0.028	14.372	0.282
1562.303	0.029	1.296	0.025
		^{160}Tb	
45.207	*KX*	20.536	0.420
45.998	*KX*	36.063	0.717
52.1	*KX*	11.333	0.232
53.5	*KX*	2.962	0.077
86.790	0.002	43.994	1.082
197.026	0.003	16.751	0.351
215.641	0.004	13.039	0.261
298.571	0.006	90.551	2.291
309.562	0.018	2.990	0.086
337.346	0.035	1.217	0.048
392.480	0.033	4.675	0.082
765.305	0.036	6.843	0.154
879.387	0.017	100.000	1.853
962.347	0.018	33.648	0.846
966.163	0.019	84.105	1.560
1002.865	0.019	3.542	0.083
1102.619	0.038	1.905	0.045
1115.156	0.027	5.103	0.099
1177.970	0.022	50.672	0.951
1199.904	0.023	8.022	0.175
1271.896	0.024	25.380	0.604
1312.174	0.026	9.702	0.190
		^{192}Ir	
136.310	0.034	0.233	0.013
201.308	0.013	0.562	0.014
205.781	0.005	3.717	0.081
283.178	0.056	0.236	0.010
295.946	0.005	33.821	0.618
308.445	0.006	35.163	0.649
316.495	0.006	100.000	1.819
374.468	0.022	0.885	0.018
416.454	0.014	0.755	0,018
468.056	0.009	56.455	1.482
484.559	0.017	3.741	0,097
489.069	0.029	0.493	0.014
588.572	0.012	5.152	0.147
604.394	0.012	9.506	0.309
612.446	0.013	6.167	0.223
884.524	0.044	0.333	0.030
1061.439	0.359	0.091	0.004
		^{226}Ra	
186.212	0.005	9.025	0.383
242.002	0.005	16.292	0.488
295.216	0.008	41.832	0.840
351.902	0.009	82.654	1.639
609.304	0.012	100.000	2.006
665.461	0.017	3.316	0.073
768.377	0.021	10.710	0.228
934.066	0.019	6.719	0.130
1120.317	0.023	32.917	0.634
1155.228	0.029	3.696	0.123
1238.151	0.024	12.961	0.272
1281.055	0.031	3.185	0.099
1377.713	0.035	8.975	0.188
1401.571	0.036	2.995	0.103
1408.027	0.029	5.344	0.119
1509.284	0.031	4.743	0.095
1729.630	0.036	6.436	0.145
1764.542	0.036	34.860	0.676
1847.459	0.039	4.613	0.096
2118.525	0.054	2.639	0.074
2204.083	0.045	11.033	0.235
2447.653	0.048	3.418	0.083

γ rays from calibrated sources can be less than 1% (see, for example, Ref. 55). However, if these results are used for spectrometer calibration, we observe a significant discrepancy in the relative-efficiency values determined by means of different sources. This is the main reason why the relative γ-ray intensities given by different authors have a significant spread. Therefore a reasonable step is to solve the inverse problem, i.e., to investigate the efficiency of a set of spectrometers by means of activity-certified sources and to measure the relative intensities of γ rays from calibrated sources under these conditions. Since the problem is solved in a single group and with the same sources, these conditions can be called fundamental. Of course, these data may have a systematic error, but as a whole they have a high internal consistency and this fact can be used subsequently in the search for such errors. In view of a number of circumstances (see above), the existing SSGS are insufficient for complete solution of the problem of spectrometer calibration, and only invoca-

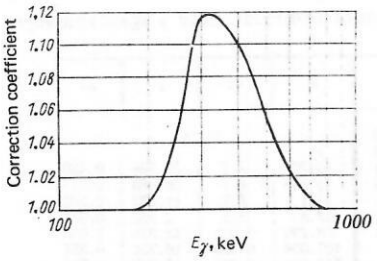

FIG. 54. Correction coefficient for relative intensities of γ rays measured on the basis of Ref. 29 for $C_1 = 6.591\,48$, $C_2 = -11.364\,51$, $C_3 = 7.028\,92$, $C_4 = -1.846\,00$, and $C_5 = 0.\,174\,64$.

tion of different physical criteria (intensity balance, internal-conversion electrons, and so forth) can assist achievement of relative-intensity errors less than 2%. In addition, the data obtained in this fundamental basis satisfy the most important requirement on the physical results: recalculation of the data for a change of the standards relative to which the comparative measurements were carried out. For example, the correction of our data can be carried out according to the following formulas:

$$\left.\begin{aligned} &k(E) = [I_1(E) - I_2(E)]\,[I_1(E)]^{-1} \\ &\text{or} \\ &k(E) = \varepsilon(I_2)/\varepsilon(I_1), \end{aligned}\right\} \qquad (42)$$

where I_1 is the basis of the data of Table XII and I_2 is the basis of the new, improved data. The values of $k(E)$ are approximated by a polynomial—this is the correction coefficient. In particular, $k(E)$ for the basis of Ref. 29 in the region 200–660 keV is shown in Fig. 54.

The results of various experiments on measurement of the relative intensities of ^{152}Eu γ rays are compared in Table XIII. We note that the intensities of the conversion electrons of certain transitions in the 200–400 keV region measured by means of the relative intensities of γ rays (the XPG method) agree with the theoretical values for the assumed multipolarities:

α_k(268 keV – ^{135}Ba) = 3.839 ± 0.099 (theory M4:3.867);

α_k(276 keV – ^{133}Ba) = 3.393 ± 0.099 (theory M4:3.392);

α_k(344 keV – ^{152}Eu) = 0.0310 ± 0.0014 (theory E2:0.0312).

This fact can be considered as a confirmation of the basis of the relative γ-ray intensities (see Table XII).

TABLE XIII. Relative intensities of ^{152}Eu γ rays.

E	[6]		[59]		[36]		[42]		[43]	
	I	ΔI	I	ΔI	I	ΔI	I	ΔI	I	ΔI
121.8	103.6	2.6	104.9	3.3	102.2	5.1	103.7	3.1	105.0	2.1
244.7	26.77	0.54	29.01	0.86	28.5	1.3	27.94	0.80	27.8	0.6
296.0	1.61	0.04	—	—	1.71	0.20	—	—	—	—
344.3	100.00	1.85	100	—	100.0	4.6	100	—	100	—
367.8	3.26	0.06	3.75	0.38	3.37	0.27	—	—	—	—
411.1	8.17	0.18	8.67	0.34	8.60	0.04	7.92	0.27	7.96	0.16
443.9	11.35	0.28	11.62	0.63	11.65	0.51	11.75	0.32	10.9	0.2
778.9	45.6	1.2	47.14	0.62	49.0	2.0	48.8	1.1	47.4	0.9
867.4	14.69	0.36	16.39	0.84	15.83	0.72	15.67	0.38	—	—
964.1	51.2	1.4	54.33	0.75	54.65	0.23	54.53	1.45	56.3	1.1
1085.8	35.9	1.0	38.53	0.77	39.68	1.74	46.25	1.10	39.6	0.8
1089.7	5.94	0.16	6.71		6.97	0.46			6.42	0.13
1112.1	48.3	1.3	50.81	0.41	50.82	2.25	51.28	1.40	50.9	1.0
1212.9	5.03	0.17	5.67	0.21	5.87	0.33	—	—	—	—
1299.1	5.85	0.17	6.37	0.39	6.28	0.36	—	—	—	—
1407.9	75.0	2.0	79.12	1.15	79.78	3.47	80.78	2.10	80	1.6

6. SPECTROMETRY OF INTERNAL-CONVERSION ELECTRONS

The basic problem of γ spectroscopy reduces to measurement of the energies and relative intensities of nuclear transitions with the best possible accuracy. Then, on the basis of these results, various versions of decay schemes are constructed (frequently with use of data on coincidences) and the excitation energies of the states are determined. However, the problem of internal-conversion electron spectroscopy reduces mainly to determination of the multipolarities of transitions and, consequently, possible quantum numbers (I^π) of the excited states. The data on conversion coefficients also permit verification of the correctness of a proposed decay scheme on the basis of the intensity balance of electromagnetic transitions.

Measurement technique for conversion coefficients of individual transitions

By definition the internal-conversion coefficient in the i shell is

$$\alpha_i = I_i/I, \qquad (43)$$

where I_i and I are the numbers of i-electrons and γ rays, respectively, emitted in the complete solid angles per unit time. It is obvious that we can construct relations of the type

$$\alpha_i/\alpha_j = I_i/I_j. \qquad (44)$$

Comparing the experimental values of α_i and α_i/α_j with theoretical calculations, the multipolarity of the transition is determined.

1. *Absolute measurements.* Assume the existence of β and γ spectrometers whose efficiency under conditions of fixed solid angle has been measured by means of activity-calibrated sources. Substituting the experimental values into Eq. (43), we obtain α_i (the AEG method[47]). On the assumption of independence of the components, the error in α_i in the ν-th measurement is

$$\Delta\alpha_{i\nu} = \alpha_{i\nu}\left[\left(\frac{\Delta S_{i\nu}}{S_{i\nu}}\right)^2 + \left(\frac{\Delta S_\nu}{S_\nu}\right)^2\right]^{1/2}, \qquad (45)$$

where $S_{i\nu}$ and S_ν are the numbers of pulses of i-electrons and γ rays; $\Delta S_{i\nu}$ and ΔS_ν are the corresponding errors. In single measurements there can be systematic errors due to adjustment of the source, allowance for half-life, and inclusion of counting losses. Therefore the measurements are carried out with different detectors, spectrometer circuits, and analyzers, in which case

$$\left.\begin{aligned} &\alpha_i = \sum_{\nu=1}^{n} \alpha_{i\nu} w_\nu \Big/ \sum_{\nu=1}^{n} w_\nu; \\ &\Delta\alpha_i = \{(\Delta\alpha_i^*)^2 + (\alpha_i\varkappa)^2 + (\alpha_i\eta)^2\}^{1/2}. \end{aligned}\right\} \qquad (46)$$

Here $\varkappa$ and η are the errors in determination of the absolute efficiency of the γ and β spectrometers; $\Delta\alpha_i^*$ is the greater of the errors in α_1 and α_2 of Eq. (30); $w_\nu = 1/(\Delta\alpha_{i\nu})^2$ (Fig. 55). The absolute efficiency of the β spectrometer was determined by means of α_k for the 661.7-keV transition of ^{137}Cs.

The systematic errors mentioned above can be avoided if a single semiconductor detector is used for detection

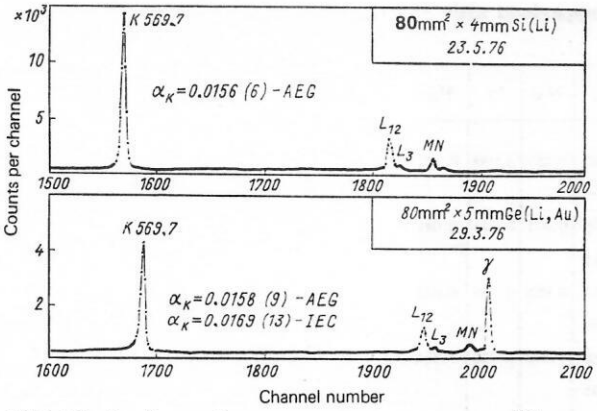

FIG. 55. Portions of spectra of the radiations of ^{207}Bi measured by Si(Li) and Ge(Li, Au) detectors under conditions of fixed solid angle, $P = 5$ cm. Values obtained in the present experiments are given.

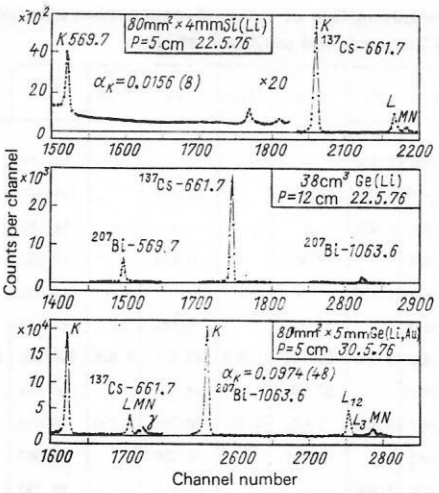

FIG. 56. Portions of spectra of the radiations of ^{207}Bi and ^{137}Cs measured by means of Si(Li), Ge(Li), and Ge(Li, Au) detectors.

of both the β and γ radiation (see Fig. 55). This method is the complete (and more accurate) analog of the internal-external conversion (IEC) method.[47]

2. *Comparative measurements.* This method is similar to that discussed above, but here it is sufficient to investigate beforehand only the relative efficiencies of the β and γ spectrometers. The standard source and the source being investigated are measured together (the NPG method[47]):

$$\alpha_{iv} = \frac{I_{iv}}{I_{\text{st } iv}} \frac{I_{\text{st } v}}{I_v} \alpha_{\text{st } v}. \tag{47}$$

The errors are calculated by means of the following formulas:

$$\Delta\alpha_{iv} = \alpha_{iv}\{(\Delta S_{iv}/S_{iv})^2 + (\Delta S_{\text{st } iv}\, S_{\text{st } iv})^2 + (\Delta S_v/S_v)^2 + (\Delta S_{\text{st } v}\, S_{\text{st } v})^2\}^{1/2};$$
$$\Delta\alpha_i = \{(\Delta\alpha_i^*)^2 + (\alpha_i\varkappa)^2 + (\alpha_i\eta)^2 + (\Delta\alpha_{\text{st } i})^2\}^{1/2}. \tag{48}$$

Here $\varkappa$ and η characterize the error in the relative efficiencies of the spectrometers (Fig. 56). The standard source used was ^{137}Cs.

3. *Relative measurements.* The energy resolution of semiconductor β spectrometers and the use of computers for processing of spectral lines permit separation of the K and L conversion lines for $Z > 10$, of the L and M lines for $Z > 35$, of the M and N lines for $Z > 60$, and of the L_2 and L_3 lines for $Z > 70$. On the assumption of independence of the errors, the error of a signal measurement of I_i/I_j is

$$\Delta(I_i/I_j) = (I_i/I_j)_v[(\Delta S_i/S_i)_v^2 + (\Delta S/S)_v^2]^{1/2}. \tag{49}$$

Here $i, j = K, L_1, L_2, M, N$, etc.; S_i and S_j are the numbers of i- and j-electrons detected; $I = S/\varepsilon$ is the intensity of i- and j-electrons; ε is the corresponding detection efficiency. The results of repeated measurements are analyzed by means of formulas similar to Eq. (46) ($\alpha_{iv} \equiv (I_i/I_j)_v$; $\varkappa = 0$). Then the quantity η characterizes the limiting error in determination of the relative intensity in the region $i - j$. We recall that the effects of addition of x rays with i- and j-electrons can lead to substantial distortions of the ratios I_i/I_j.

In Table XIV we have listed the relative intensities of conversion electrons obtained by means of Si(Li) and Ge(Li, Au) detectors. For comparison we have also shown in the same table the results of theoretical calculations for the accepted multipolarities.

4. *Measurements of the ratios I_x/I.* For β^- decay and also when there are isometric states, vacancies arise in the shells of a nuclide only as the result of the internal-conversion process. Consequently, by measuring the number of γ rays and the number of vacancies in the corresponding shell per unit time, it is easy to determine the conversion coefficients for a decay scheme with one transition (the XPG method[48]):

$$\alpha_{iv} = I_{x_i v}/(\omega_i I_v);$$
$$\Delta\alpha_{iv} = \alpha_{ij}\{(\Delta I_{x_i v}/I_{x_i v})^2 + (\Delta I_v/I_v)^2\}^{1/2}, \tag{50}$$

where I_{x_i} is the intensity of x_i x rays, ω_i is the fluorescence yield in the i shell, I is the γ-ray intensity, and ν is the number of the measurement. The results of repeated measurements are processes in accordance with the equations (46), and in this case the error in measurements of ω_i is used as η.

This approach is easily extended to more complex decay schemes where the relative intensities of i-electrons can be measured with high accuracy. This applies mainly to the case $i = k$.

The spectrum of ^{176m}Lu γ rays and the values of α_k obtained in this experiment are given in Fig. 57.

Measurement technique for internal-conversion coefficients of a group of transitions

The technique for measurement of the energy and relative intensities of monoenergetic transitions by means of semiconductor detectors has been described above. We shall make only a few remarks regarding conversion coefficients.

1. The technique developed does not assume precision measurements of the nuclear transition energies and is used only for identification of spectral lines and determination of their intensities.

2. To investigate the nonlinearity of a spectrometer

TABLE XIV. Relative intensities of internal-conversion electrons and comparison with calculations (Ref. 48) for accepted multipolarities.

Nuclide	E	σL	I_K	ΔI_K	I_{L12}	ΔI_{L12}	I_{L3}	ΔI_{L3}	I_L	ΔI_L	I_M	ΔI_M	I_N	ΔI_N
^{152}Eu	121.8	$E2$	100.000	2.146	—	—	—	—	61.718	0.770	13.887	0.257	3.039	0.162
			100.000		32.164		22.076		54.240		12.281			
^{141}Ce	145.4	$M1$	100.000	1.427	—	—	—	—	14.210	0.150	2.838	0.071	0.794	0.041
			100.000		13.402		0.185		13.587		2.861			
^{139}Ce	165.9	$M1$	100.000	1.179	—	—	—	—	14.092	0.131	2.921	0.055	0.739	0.035
			100.000		13.244		0.184		13.428		2.778			
^{167}Tm	207.8	$E3$	100.000	2.583	84.751	5.309	63.271	4.876	148.022	10.185	38.760	1.812	8.725	1.854
			100.000		97.297		48.857		146.154		36.071			
^{207}Bi	569.7	$E2$	22.082	0.246	5.692	0.257	0.798	0.098	6.490	0.355	1.387	0.075	0.486	0.053
			22.082		5.347		0.750		6.097					
^{137}Cs	661.7	$M4$	100.000	1.696	—	—	—	—	18.293	0.084	—	—	—	—
			100.000		16.175		1.639		17.814					
^{207}Bi	1063.7	$M4$	100.000	1.025	24.599	0.665	1.400	0.136	25.999	0.801	6.889	0.446	1.786	0.071
			100.000		24.021		1.804		25.825					

one can use the values of $E_{ij} = E_j - \varepsilon_i$, where E_j is the γ ray energy and ε_i is the binding energy of the electron in the i shell of the nuclide.[49]

3. It is assumed that for normal incidence of β particles the backscattering and charge-collection efficiency do not depend on the energy. Obviously, for spectrometers which permit oblique incidence of β particles it is necessary to use a method of investigating efficiency similar to that used in γ spectroscopy.

4. Energy calibration of internal-conversion electron spectra is accomplished by means of the previously used γ-ray energies. Only in rare cases (for example, a nuclide with a small number of intense transitions) does the need arise for admixture of sources with simple spectra or use of external calibration techniques.

Construction of a set of conversion-coefficient standards

As primary conversion-coefficient standards we take[47]

$$\alpha_k(661.648\,\text{keV}-{}^{137}\text{Cs}) = 0.0905 \pm 0.0010. \qquad (51)$$

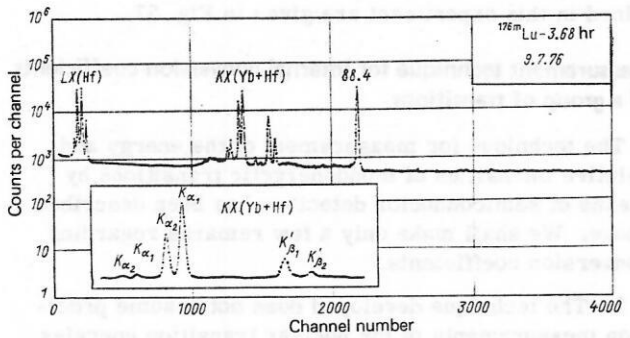

FIG. 57. Spectrum of γ rays of ^{176m}Lu measured by a 200 mm^2 ×5 mm Ge(Li) detector. The value $\alpha_k = 1.1468 \pm 0.0051$ was obtained in this experiment. $T_1 = 3$ hours, $T_2 = 2$ hours, $P = 6$ cm, no absorber.

The choice of this standard was made for the following reasons.

1. It is considered that the multipolarity of the 661.7-keV transition is pure M4; in this case it is easy to compare the theoretical and experimental values.

2. The nuclide ^{137}Cs undergoes β^- decay, and here only one transition is observed. Consequently α_k can be determined by the methods of γ spectroscopy alone (XPG).

3. The 661.7-keV transition is in the energy region where the detector entrance window does not substantially scatter or absorb β particles, and for sufficiently thick detectors (≥3 mm) the efficiency does not depend on energy.

4. The nuclide ^{137}Cs has a long half-life (30.18 years) and sources of high specific activity can be obtained in reactors. This greatly facilitates the problem of preparing high-quality β sources. In addition, the high efficiency of separation in electromagnetic mass separators permits preparation of thin sources without a carrier.

5. The SSGS set includes a ^{137}Cs source. This permits calibration of the prepared β sources in activity by comparison of γ-ray intensities.

6. The decay of ^{137}Cs has been studied on many occasions and in practically all types of β spectrometers.

7. In the approach described above, any changes of the relative intensities of the calibration sources and $\alpha_k = 661.7$ keV in the future are easily taken into account without reperforming the experiment.

The experimental values obtained for α_k are given in Table XV, and we shall consider them secondary standards. We have also given in that table the number of experiments and the results of various methods. For each method we have indicated the systematic error,

TABLE XV. Experimental values of conversion coefficients obtained by various methods.

Nuclide $T_{1/2}$	E (ΔE) E_K	I (ΔI) I_K (ΔI_K)	α_K	Φ_1 Φ_2	ζ	$\Delta\alpha_K$	Results of other methods |q|	method	α_K	Φ_1	Φ_2	ζ	$\Delta\alpha_K$
^{176m}Lu,	88.367 (3)	100.000 (1830)	1.161	0.004	0.018	0.019	5	XPG	1.161	0.004	0.004	0.018	0.019
3.68 hours	23.016	—											
^{152}Eu,	121.782 (3)	100.000 (2476)	0.636	0.007	0.023	0.016	7	AEG	0.638	0.009	0.003	0.023	0.017
13.2 years	74 947	100.000 (2146)		0.002			5	NPG	0.635	0.010	0.003	0.023	0.018
^{169}Yb,	130.525 (3)	30.936 (733)	0.499	0.012	0.023	0.017	2	AEG	0.506	0.014	0.006	0.023	0.018
30.6 days	71.135	44.525 (839)		0.010			1	NPG	0.483	0.022	—	0.023	0.025
^{141}Ce,	145.443 (3)	100.000 (1827)	0.365	0.004	0.023	0.011	5	AEG	0.366	0.007	0.004	0.023	0.011
32.51 days	103.452	100.000 (1179)		0.007			3	NPG	0.350	0.008	0.008	0.025	0.011
							5	XPG	0.374	0.007	0.007	0.032	0.012
^{149}Gd,	149.733 (6)	100.000 (1827)	0.459	0.010	0.023	0.015	2	AEG	0.458	0.014	0.000	0.023	0.018
9.5 days	101.214	100.000 (3393)		0.001			2	NPG	0.460	0.013	0.006	0.023	0.017
^{151}Gd,	153.605 (4)	100.000 (1829)	0.426	0.008	0.023	**0.013**	2	AEG	0.428	0.010	0.003	0.023	0.014
120 days	105.086	51.307 (686)		0.003			1	NPG	0.422	0.013	—	0.023	0.016
^{139}Ce,	165.854 (3)	100.000 (1827)	0.226	0.004	0.023	0.007	4	AEG	0.228	0.005	0.004	0.023	0.007
137.5 days	126.929	100.000 (1179)		0.003			3	NPG	0.222	0.007	0.005	0.023	0.009
^{173}Lu,	171.402 (4)	13.834 (379)	0.0657	0.0013	0.023	0.020	2	AEG	0.0662	0.0016	0.0012	0.023	0.0022
1.37 years	110.070	39.488 (1008)		0.0013			3	NPG	0.0634	0.0023	0.0009	0.023	0.0027
							1	IEC	0.0703	0.0042	—	0.032	0.0048
^{151}Gd,	174.697 (4)	47.342 (970)	1.731	0.014	0.023	0.043	2	AEG	1 722	0.016	0.010	0.023	0.043
120 days	126.178	100.000 (1348)		0.015			1	NPG	1.754	0.025	—	0.023	0.048
^{173}Lu,	179.363 (4)	6.362 (177)	0.214	0.004	0.023	0.006	2	AEG	0.214	0.005	0.003	0.023	0.007
1.37 years	118.031	62.952 (1551)		0.004			3	NPG	0.210	0.008	0.004	0.023	0.009
							1	IEC	0.229	0.013	—	0.032	0.015
^{172}Lu,	181.530 (4)	32.801 (1182)	0.210	0.006	0.023	0.008	2	AEG	0.211	0.006	0.001	0.023	0.008
6.7 days	120.198	100.000 (2698)		0.002			1	NPG	0.206	0.013	—	0.023	0.014
^{169}Yb,	197.948 (4)	100.000 (1834)	0.355	0.007	0.023	0.011	2	AEG	0.352	0.008	0.001	0.023	0.011
30.7 days	138.558	100.000 (1631)		0.007			1	NPG	0.369	0.016	—	0.023	0.018
^{156}Tb,	199.216 (5)	61.229 (1126)	0.155	0.006	0.023	0.008	2	AEG	0.154	0.007	0.006	0.023	0.008
5.35 days	148.977	100.000 (2506)		0.002			1	NPG	0.157	0.013	—	0.023	0.014
^{172}Lu,	203.436 (4)	7.626 (378)	0.150	0.004	0.023	0.005	2	AEG	0.149	0.004	0.000	0.023	0.005
6.7 days	142.104	17.049 (531)		0.002			1	NPG	0.154	0.010	—	0.023	0.011
^{167}Tm,	207.797 (3)	100.000 (1824)	0.479	0.010	0.023	0.015	2	AEG	0.481	0.016	0.003	0.023	0.019
9.25 days	150.311	100.000 (2583)		0.002			3	NPG	0.478	0.013	0.007	0.023	0.017
^{151}Gd,	243.293 (14)	89.836 (1836)	0.0202	0.0004	0.023	0.0006	2	AEG	0.0204	0.0005	0.0007	0.023	0.0008
120 days	194.774	2.196 (28)		0.0003			1	NPG	0.0197	0.0009	—	0.023	0.0010
^{152}Eu,	244.691 (5)	25.839 (522)	0.0846	0.0014	0.023	0.0029	3	AEG	0.0869	0.0022	0.0006	0.023	0.0028
13.2 years	197.856	3.424 (42)		0.0023			5	NPG	0.0827	0.0020	0.0008	0.023	0.0027
							1	IEC	0.0835	0.0074	—	0.032	0.0079
^{156}Tb,	262.587 (13)	9.105 (171)	0.0769	0.0024	0.023	0.0030	2	AEG	0.0771	0.0026	0.0025	0.023	0.0031
5.35 days	212.348	7.010 (130)		0.0006			1	NPG	0.0754	0.0056	—	0.023	0.0059
^{152}Tb,	271.085 (14)	14.776 (279)	0.0620	0.0018	0.023	0.0030	2	AEG	0.0614	0.0022	0.0016	0.023	0.0026
17.5 hours	220.774	29.966 (350)		0.0011			1	NPG	0.0636	0.0034	—	0.023	0.0037
^{173}Lu,	272.111 (5)	100.000 (1886)	0.0210	0.0004	0.023	0.0007	2	AEG	0.0209	0.0005	0.0001	0.032	0.0008
1.37 years	210.779	100.000 (1286)		0.0001			1	NPG	0.0214	0.0010	—	0.023	0.0011
^{148}Eu,	277.081 (5)	83.534 (1975)	0.0808	0.0014	0.023	0.0023	2	AEG	0.0800	0.0021	0.0021	0.023	0.0027
93.1 days	230.246	100.000 (2697)		0.0008			2	NPG	0.0815	0.0020	0.0011	0.023	0.0027
^{203}Pb	279.189 (6)	100.000 (1893)	0.166	0.003	0.023	0.006	2	AEG	0.163	0.006	0.003	0.023	0.007
52.1 hours	193.658	100.000 (2795)		0.002			2	NPG	0.168	0.006	0.002	0.023	0.006
							2	IEC	0.175	0.010	0.001	0.032	0.011
^{149}Gd,	298.617 (9)	59.080 (1176)	0.0723	0.0011	0.023	0.0020	2	AEG	0.0729	0.0016	0.0009	0.023	0.0024
9.5 days	250.098	9.217 (240)		0.0007			2	NPG	0.0716	0.0016	0.0001	0.023	0.0022
^{169}Yb,	307.732 (6)	29.270 (654)	0.0446	0.0014	0.023	0.0017	2	AEG	0.0450	0.0016	0.0012	0.023	0.0019
30.7 days	248.331	3.729 (72)		0.0006			2	NPG	0.0437	0.0024	0.0002	0.023	0.0026
^{151}Gd,	307.500 (9)	17.417 (344)	0.0605	0.0015	0.023	0.0020	2	AEG	0.0592	0.0020	0.0003	0.023	0.0025
120 days	258.981	1.341 (39)		0.0014			1	NPG	0.0619	0.0021	—	0.023	0.0026
^{149}Eu,	327.527 (6)	100.000 (1982)	0.0514	0.0009	0.023	0.0015	2	AEG	0.0521	0.0012	0.0002	0.023	0.0017
93.1 days	280.692	70.766 (2547)		0.0008			2	NPG	0.0504	0.0015	0.0015	0.023	0.0019
^{152}Eu,	344.267 (7)	96.528 (1784)	0.0313	0.0005	0.023	0.0009	3	AEG	0.0317	0.0007	0.0003	0.023	0.0010
13.2 years	294.028	4.729 (39)		0.0005			6	NPG	0.0310	0.0007	0.0002	0.023	0.0010
							1	IEC	0.0322	0.0020	—	0.032	0.0022
^{152}Tb,	344.267 (7)	100.000 (1923)	0.0308	0.0008	0.023	0.0011	4	AEG	0.0308	0.0008	0.0002	0.023	0.0011
17.5 hours	294.028	100.000 (755)		0.0002			1	NPG	0.0306	0.0017	—	0.023	0.0018
^{149}Gd,	346.660 (9)	49.781 (1188)	0.187	0.003	0.023	0.006	2	AEG	0.188	0.006	0.003	0.023	0.007
9.5 days	298.141	20.070 (1004)		0.001			2	NPG	0.187	0.005	0.002	0.023	0.007
^{156}Tb,	356.431 (11)	20.816 (388)	0.0277	0.0009	0.023	0.0011	2	AEG	0.0278	0.0011	0.0011	0.023	0.0013
5.35 days	306.192	6.091 (119)		0.0002			1	NPG	0.0273	0.0017	—	0.023	0.0018
^{156}Tb,	534.323 (11)	100.000 (1967)	0.0035	0.0002	0.023	0.0002	2	AEG	0.0035	0.0002	0.0002	0.023	0.0002
5.35 days	484.084	3.691 (83)		0.0000			1	NPG	0.0035	0.0003	—	0.023	0.0003
^{207}Bi,	569.683 (11)	100.000 (1834)	0.0161	0.0002	0.023	0.0005	7	AEG	0.0158	0.0003	0.0003	0.023	0.0005
30.2 years	481.678	22.082 (246)		0.0003			5	NPG	0.0162	0.0003	0.0003	0.023	0.0005
							2	IEC	0.0175	0.0010	0.0003	0.032	0.0012
^{207}Bi,	1063.660 (19)	76.205 (1461)	0.0966	0.0012	0.023	0.0025	3	AEG	0.0963	0.0022	0.0004	0.023	0.0027
30.2 years	975.655	100.000 (1025)		0.0002			10	NPG	0.0968	0.0015	0.0009	0.023	0.0031

including the error in α_k of the primary standard (661.7 keV – ^{137}Cs), which is 1.1%. In obtaining the final results, each method is used with its own weight [the error is the greater of $\Phi_{1,2} = \Delta\alpha_i^*$—see Eq. (46)] irrespective of the dependence on the number of experiments carried out. We then used as ξ the best of the systematic errors used by the method. For determination of α_k for each transition we used at least two differ-

TABLE XVI. Relative intensity of internal-conversion electrons of radioactive nuclides proposed for β spectrometer calibration.

E	ΔE	I	ΔI	I_e	ΔI_e	E_e
			^{149}Gd, 9.5 days			
149.733	0.006	100.000	1.827	100.000	3.394	K 101.214
				15.220	0.454	L 142.2
				3.169	0.306	M 147.9
				0.802	0.058	N 149.4
272.317	0.011	6.768	0.169	1.379	0.040	K 223.798
				0.202	0.014	L 264.8
298.617	0.009	59.080	1.176	9.217	0.240	K 250.098
				1.682	0.310	L 291.1
346.660	0.009	49.781	1.188	20.070	1.004	K 298.141
				3.518	0.092	L 339.1
				0.949	0.043	M 345.2
496.403	0.015	3.570	0.266	0.202	0.013	K 447.884
516.558	0.013	5.487	0.113	0.190	0.008	K 468.039
534.304	0.019	6.370	0.124	0.227	0.017	K 485.785
748.590	0.018	16.148	0.344	0.057	0.006	K 700.071
788.857	0.018	14.176	0.274	0.126	0.008	K 740.338
933.133	0.029	1.241	0.040	0.003	0.001	K 884.614
938.591	0.022	4.714	0.147	0.032	0.003	K 890.072
947.840	0.038	1.814	0.036	0.003	0.001	K 899.321
			^{151}Gd, 120 days			
106.566	0.004	1.421	0.044	1.887	0.046	K 58.047
153.605	0.004	100.000	1.829	51.307	0.686	K 105.086
				7.504	0.072	L 146.0
				1.705	0.045	M 151.8
				0.427	0.013	N 153.3
174.697	0.004	47.342	0 970	100.000	1.348	K 126.178
				19.070	0.413	L 167.1
				4.835	0.052	M 172.9
				1.199	0.039	N 174.3
239.013	0.094	1.317	0.090	0.133	0.008	K 190.494
243.293	0.014	89.836	1.836	2.196	0.028	K 194.774
260.459	0.079	0.661	0.050	0.076	0.005	K 211.940
286.098	0.014	1.619	0.039	0.142	0.009	K 237.579
307.500	0.009	17.417	0.344	1.341	0.039	K 258.981
				0.185	0.008	L 299.9
			^{152}Eu, 13.2 years			
121.782	0.003	100.000	2.476	100.000	2.146	K 74.947
				61.718	0.770	L 114.5
				13.887	0.257	M 120.4
				3.039	0.162	N 121.6
244.691	0.005	25.839	0.522	3.424	0.042	K 197.856
				0.927	0.028	L 237.4
344.267	0.007	96.528	1.784	4.729	0.039	K 294.028
				1.018	0.033	L 336.4
			^{169}Yb, 30.6 days			
93.613	0.005	6.811	0.224	52.007	1.022	K 34.223
				9.125	0.131	L 83.9
				1.745	0.228	M 91.7
109.784	0.003	45.820	1.694	40.607	0.405	L 100.2
130.525	0.003	30.936	0,733	44.547	0.642	K 71.135
				41.657	1.764	L 120.7
				9.776	0.133	M 128.6
				2.299	0.076	N 130.1
177.208	0.004	62.375	1.171	14.903	0.212	L 167.3
				3.300	0.043	M 175.3
				0.833	0.029	N 176.8
197.948	0.004	100.000	1.834	100.000	1.208	K 138.558
				16.825	0.266	L 188.1
				3 817	0.058	M 196.0
				0.915	0.025	N 197.5
261.069	0.012	4.962	0.189	0.272	0.015	K 201.679
307.732	0,006	29.270	0.654	3.729	0.072	K 248 331
			^{173}Lu, 1.37 years			
78.651	0.006	52.115	1.190	2328.396	29.544	L 68.9
				573.621	17.660	M 76.7
				143.615	11.365	N 78.3
100.719	0.007	23.331	0.531	504.533	7.711	L 90.9
				115.356	2.307	M 98.8
				26.824	1.407	N 100.4
171.402	0.004	13.834	0.379	39.488	1.008	K 110.070
				7.752	0.359	L 161.6
179.363	0.004	6.362	0.177	62.952	1.551	K 118.031
				23.421	1.721	M 177.4
				8.848	0.351	N 179.0
272.111	0.005	100.000	1.886	100.000	1.286	K 210.779
				14.949	0.355	L 262.3
285.369	0.006	2.802	0.080	3.021	0.226	K 224.037
350.750	0.008	1.603	0.033	0.935	0.079	K 289.418
456.769	0.015	0.725	0.026	1.010	0.050	K 395.437
557.485	0.019	2.634	0.105	1.545	0.132	K 496.153
636.129	0.013	7.286	0.185	4.673	0.120	K 574.797
			^{207}Bi, 30.2 years			
569.683	0.011	100.000	1.834	22.082	0.246	K 481.678
				6.490	0.355	L 554.2
				1.387	0.075	M 566.6
				0.486	0.053	N 569.1
1063.660	0,019	76.205	1.461	100.000	1.025	K 975.655
				25,999	0.801	L 1048.1
				6.889	0.446	M 1060.6
				1.786	0.071	N 1063.0
1770.253	0,034	7.221	0.147	0.295	0.008	K 1682.248
				0.044	0.006	L 1756.0
				0.011	0.004	M 1767.2

ent radioactive sources.

We make several remarks on the details of the experiments:

1. All radioactive sources were obtained by means of electromagnetic mass separation, except for ^{207}Bi, which was prepared by evaporation of a solution.

2. Special attention was devoted to correct inclusion of effects related to radioactive decay.

3. Six different sources of ^{137}Cs were used as standards. Only in one case did we observe a deterioration of the source quality due to absorption and scattering of β particles in a contaminated surface. Each source was monitored by measurement of α_k on the scale of another source. We give an example:

$$\alpha_k\,(661.7\,\text{keV}-{}^{137}\text{Cs}) = \begin{cases} 0.0900 \pm 0.0040; \\ 0.0896 \pm 0.0028; \\ 0.0879 \pm 0.0042. \end{cases} \qquad (52)$$

This result demonstrates also the reproducibility of the geometrical conditions for the three different sources.

4. The results given in Table XV were obtained by means of eight different semiconductor detectors. In the working energy regions no systematic deviations of the experimental α_k values were observed as a function of the quality of the detectors used. This fact confirms the correctness of our assumption that the charge collection is independent of the β-particle energy. We note that basic material from different firms and with different parameters was used for preparation of the detectors.

5. Relative intensities of conversion electrons have been measured for certain nuclides, which can be used for calibration of β spectrometers (Table XVI). It is proposed subsequently to extend the region of calibration sources.

Analysis of results

An analysis can be carried out by comparison with the data in the literature and with theoretical calculations (Table XVII). We note that the data on conversion coefficients existing in the literature at the present time are contradictory and it is difficult to choose criteria for selection of the most reliable values. However, a formal weighting procedure leads to large error values resulting in a spread, which excludes comparison with theoretical calculations. We shall not carry out a complete physical analysis of the results, since the principal purpose of this work is to describe measurement techniques. It is appropriate, however, to make certain remarks.

1. In Table XVII we have given the conversion coefficients which can be obtained for transitions of pure multipolarity from Table XVI. From the point of view of planning an experiment these results are useful in that it is possible to recognize the realistic errors which are achievable in an approach of this type. Also in Table XVII we have given the calculated conversion coefficients and their deviations from the experimental values, as well as data from the literature.

2. An object of special experiments has been the

TABLE XVII. Experimental values of internal-conversion coefficients and comparison with theoretical values[48] and published data.

Nuclide	$E(\Delta E)$	σL	i	α_i	$\Delta\alpha_i$, %	α_i (theor.)	Difference, %	α_i	$\Delta\alpha_i$, %	Reference
^{172}Lu	78.738 (5)	$E2$	L	5.268	6.2	5.091	+3.4	—	—	—
			M	1.319	4.9	1.253	+5.1	—	—	—
			N	0.342	6.7	—	—	—	—	—
^{176m}Lu	88.367 (7)	$E2$	K	1.161	1.8	1.210	−4.1	1.10	5.5	[52]
^{152}Eu	121.782 (3)	$E2$	K	0.636	2.5	0.684	−7.3	0.65	9.2	[52]
			L	0.393	3.7	0.375	+4.7	0.38	13.2	[50]
			M	0.0883	3.8	0.084	+5.0	—	—	—
			N	0.0193	6.3	0.0198	−2.6	—	—	—
^{169}Yb	130.525 (4)	$E2$	K	0.499	3.3	0.546	−9.0	0.53	5.7	[57]
^{141}Ce	145.443 (3)	$M1$	K	0.365	3.0	0.388	−6.1	0.379	1.1	[47]
			L	0.0519	3.5	0.0522	−0.6	—	—	—
			M	0.0104	4.4	0.0111	−6.5	—	—	—
			N	0.0027	5.8	0.0030	−10.3	—	—	—
^{149}Gd	149.733 (6)	$M1$	K	0.459	3.3	0.507	−9.9	0.475	2.7	[63]
			L	0.0699	5.6	0.072	−3.0	—	—	—
			M	0.0146	10.8	0.0155	−6.0	—	—	—
^{151}Gd	153.605 (4)	$M1$	K	0.426	3.1	0.471	−10.0	0.475	3.2	[64]
			L	0.0623	3.5	0.0669	−7.1	—	—	—
			M	0.0142	4.3	0.0144	−1.4	0.023	30.4	[64]
^{139}Ce	165.854 (5)	$M1$	K	0.226	3.1	0.225	+0.5	0.2142	0.7	[47]
			L	0.0319	3.5	0.0302	+5.5	—	—	—
			M	0.00660	3.8	0.00625	+5.5	—	—	—
			N	0.00167	5.8	0.00172	−3.0	—	—	—
^{173}Lu	171.402 (4)	$E1$	K	0.0657	3.1	0.0698	−6.1	0.065	15.4	[65]
^{151}Gd	174.697 (4)	$M2$	K	1.731	2.5	1.896	−9.1	—	—	—
			L	0.330	3.6	0.384	−15.1	0.38	18.4	[64]
^{173}Lu	179.363 (5)	$E2$	K	0.214	3.0	0.231	−7.6	0.20	15.0	[65]
^{172}Lu	181.530 (4)	$E2$	K	0.210	3.8	0.224	−6.5	0.210	6.0	[66]
^{156}Tb	199.216 (5)	$E2$	K	0.155	5.2	0.158	−2.6	—	—	—
^{172}Lu	203.436 (4)	$E2$	K	0.150	3.3	0.161	−7.1	0.160	6.3	[66]
^{167}Tm	207.797 (3)	$E3$	K	0.479	3.2	0.481	−0.4	0.510	8.8	[67]
			L	0.709	2.2	0.703	+0.9	—	—	—
			M	0.186	6.1	0 174	+6.7	—	—	—
			N	0.042	21.7	—	—	—	—	—
^{151}G	243.293 (14)	$E1$	K	0.0202	3.1	0.0222	−9.4	0.025	16.0	[64]
^{152}Eu	244.691 (6)	$E2$	K	0.0846	3.6	0.0813	+4.0	0.0846	9.0	[67]
^{156}Tb	262.587 (13)	$E2$	K	0.0769	3.9	0.0685	+11.6	0.0673	3.3	[68]
^{152}Tb	271.085 (14)	$E2$	K	0.0620	3.8	0.0622	−0.2	0.0640	12.0	[69]
^{173}Lu	272.111 (5)	$E1$	K	0.0210	3.1	0.0214	−1.9	0.0222	1.4	[65]
^{149}Eu	277.081 (5)	$M1$	K	0.0808	2.8	0.0861	−6.4	0.079	6.3	[63]
^{169}Yb	307.732 (6)	$E2$	K	0.0446	3.8	0.0485	−8.4	0.0488	3.7	[57]
^{149}Eu	327.527 (6)	$M1$	K	0.0514	2.8	0.0557	−8.0	0.050	6.0	[63]
^{152}Eu	344.267 (7)	$E2$	K	0.0313	2.9	0.0311	+0.6	0.0296	4.4	[52]
			L	0.00671	5.3	0.00684	−1.9	—	—	—
^{156}Tb	356.431 (11)	$E2$	K	0.0277	4.0	0.0282	−1.8	0.0285	7.7	[68]
^{156}Tb	534.323 (11)	$E1$	K	0.0035	4.8	0.0035	+0.1	0.0032	6.9	[68]
^{207}Bi	569.683 (12)	$E2$	K	0.0161	3.2	0.0159	+1.3	0.0160	2.5	[52]
			L	0.00474	13.9	0.00439	+7.7	—	—	—
^{137}Cs	661.648 (14)	$M4$	K	0.0905	1.1	0.0920	−1.6	—	—	—
			L	0.0166	2.1	0.0168	−1.2	—	—	—
^{207}Bi	1063.660 (19)	$M4$	K	0.0966	2.6	0.097	−0.4	0.0926	4.0	[52]
			L	0.0251	4.0	0.0251	0.0	—	—	—

121.8-keV transition of ^{152}Eu. It is considered to be pure E2, discharging the first excited state of ^{152}Sm (2^+). A favorable circumstance for performance of experiments has been the presence in the SSGS set of activity-calibrated sources of ^{57}Co (the 121.1-keV transition) and ^{137}Cs (the 661.6-keV transition). As a result, error in determination of the γ-spectrometer efficiency has been avoided. Our conversion-electron measurements in their entirety used four different sources of ^{152}Eu and five sources of ^{137}Cs. As can be seen from the data of Table XVII, α_k(121.8 keV) differs from the calculated value of 7.3 ± 2.5%.

TABLE XVIII. Comparison of experimental data on relative intensities of ^{152}Eu internal-conversion electrons with published data.

E	I	ΔI	I	ΔI [46]	I	ΔI [50]	I	ΔI [51]
K 121,8	100.000	2.146	100.000	3.821	—	—	100.000	1.988
L 121,8	61.718	0.770	78.025	6.242	61.465	7.092	56.989	1.080
K 244.7	3.424	0.042	3.376	0.127	3.593	0.236	2.045	0.102
L 244.7	0.927	0.028	0.840	0.102	—	—	0,545	0.028
K 344.3	4.729	0.039	4.586	—	4.729	—	3.409	0.171
L 344,3	1.018	0.033	1.102	0.159	—	—	0.767	0.039

One can assume that the efficiency of semiconductor detectors plays a role in the region near 80 keV. However, our experiments were carried out by means of four different Si(Li) detectors and the values obtained agree. In addition, the relative intensities obtained for the conversion electrons of ^{152}Eu agree within experimental error with the data given in Refs. 46 and 50 (except L121 in Ref. 46, Table XVIII). The data of Ref. 51 we consider to be erroneous.

Thus, two assumptions are possible: either the data on the activity and decay scheme of ^{57}Co and ^{137}Cs are incorrect, or the calculations for some reason give exaggerated values of the conversion coefficients.

3. The E2 transitions for even-even nuclei, which discharge 2^+ states to the ground state 0^+, have been

TABLE XIX. Absolute values of α-particle energies measured by means of a magnetic spectrometer.[53]

Nuclide	$T_{1/2}$	E	ΔE	Nuclide	$T_{1/2}$	E	ΔE
^{146}Gd	93 years	3182.787	0.024	^{226}Ra	$1.6\cdot10^3$ years	4784.50	0.25
^{210}Po	138 days	5304.51	0.07	^{227}Th	18.5 days	6038.21	0.15
^{211}Bi	2.1 minutes	6623.1	0.6			5977.82	0.10
^{212}Bi	61 minutes	6090.087	0.037	^{228}Th	1.9 years	5423.33	0.22
^{212}Po	$3\cdot10^{-7}$	8784.37	0.07			5340.54	0.15
		10554	2	^{232}U	72 years	5320.30	0.14
^{214}Po	$162\cdot10^{-6}$	7687.09	0.06			5263.54	0.09
^{215}Po	$1.8\cdot10^{-3}$	7386.4	0.8	^{238}Pu	88 years	5499.21	0.20
^{216}Po	$150\cdot10^{-3}$	6778.5	0.5			5456.5	0.4
^{218}Po	3.0 minutes	6002.55	0.09	^{240}Pu	$6.5\cdot10^3$	5168.30	0.15
^{219}Rn	4	6819.29	0.27			5123.82	0.23
^{220}Rn	55	6288.29	0.10	^{241}Am	433 years	5485.74	0.12
^{222}Rn	3.8 days	5489.66	0.30			5442.98	0.13
^{223}Ra	11.4 days	5747.8	0.4	^{242}Cm	163 days	6112.92	0.08
		5716.42	0.29			6069.63	0.12
		5607.6	0.6	^{244}Cm	18 years	5804.96	0.05
		5540.0	0.9			5762.835	0.03
^{224}Ra	3.6 days	5685.56	0.15	^{253}Es	20.5 days	6632.73	0.05

systematized in Ref. 52. The discrepancy for α_k(121.8 keV – ^{152}Eu) was noted there also, but the error was greater. Reference 52 also indicated a deviation of the ratios L_1/L_2 and L_1/L_3 for pure E2 transitions from the theoretical values.

4. The technique for measurement of conversion coefficients with semiconductor detectors involves in a direct way the relative γ-ray intensity basis introduced by us, and therefore any corrections of this basis should lead to corresponding corrections of the experimental conversion-coefficient values. Here, however, there may be a correction also with respect to the primary standard conversion coefficient—α_k(661.7 keV – ^{137}Cs). Consequently,

$$k_1(E)=(\alpha_k^{(2)}/\alpha_k^{(1)})/k(E), \qquad (53)$$

where $k_1(E)$ is the correction coefficient for the conversion coefficient; $k(E)$ is the correction coefficient of the relative γ-ray intensities (42); $\alpha_k^{(2)}$ and $\alpha_k^{(1)}$ are the new (2) and old (1) values of the primary-standard conversion coefficient.

7. SPECTROSCOPY OF α PARTICLES

At the present time precision α spectroscopy is carried out by means of magnetic spectrometers which have high energy resolution (see Fig. 1). Unfortunately, the absolute efficiency of these devices is low (see Fig. 2), and this places severe requirements on the activity of the sources. In addition, the procedure for obtaining information from thick-layered photographic plates is slow and difficult. Promising means of speeding up the data processing involve use of automated television cameras for track counting and use of wire chambers[71] and perhaps semiconductor coordinate detectors. In both cases the requirements on source activity remain, and in the second case there is a deterioration of energy resolution.

In certain cases the problem can be solved by use of semiconducting α spectrometers. However, although α spectroscopy was the first field of application of semiconductor detectors, a systematic technique of precision spectroscopy has not yet been developed.

Since α-particle spectrometry is carried out in a rather narrow range of pulse heights, the problem can be discussed as a special case of spectrometry of monoenergetic particles by means of semiconductor detectors (see Sec. 4). Here the principal experimental problems involve the difficulty of preparing high-quality combined α sources (simultaneous measurement of different sources involves distortion of the uncorrected spectrum; see Fig. 42) and low spectrometer energy resolution. Therefore each experiment must be prepared specially and an external or internal calibration technique chosen on the basis of a preliminary analysis.

TABLE XX. Energy and relative intensity of α particles from radioactive nuclides used for calibration of spectrometers.

Nuclide	$T_{1/2}$, years	E	ΔE	I_{tot}	I	ΔI
^{226}Ra	$1.6\cdot10^3$	4784.50	0.25	100	94.5	0.1
		4601.9	0.5		5.5	0.1
		7687.09	0.06		99	—
		6002.55	0.09		99	—
		5489.66	0.30		99	—
		5304.51	0.07		99	—
^{227}Ac	22	4954	2	1.4	47.5	1.7
		4942	3		38.8	1.7
		4871	3		6.4	0.7
^{228}Th	1.9	5423.33	0.22	100	72.7	0.4
		5340.54	0.15		26.7	0.2
^{233}U	$1.6\cdot10^5$	4824.2	1.2	100	84.4	0.2
		4782.5	1.2		13.2	0.1
^{238}Pu	88	5499.21	0.20	100	71.1	1.2
		5456.5	0.4		28.7	1.2
^{239}Pu	$2.4\cdot10^4$	5155.4	0.7	100	73.3	—
		5142.9	0.8		15.1	—
		5104.6	0.8		11.5	—
^{241}Am	433	5544.3	0.3	100	0.35	—
		5485.74	0.12		85.2	—
		5442.98	0.13		12.8	—
^{242}Cm	163 days	6112.92	0.08	100	74.0	0.5
		6069.63	0.12		26.0	0.5
^{244}Cm	18	5804.96	0.05	100	76.4	0.2
		5762.835	0.030		23.6	0.2

In contrast to γ spectroscopy, a systematic set of α-particle energy standards has already been proposed.[53] Absolute values of α-particle energies measured by means of a magnetic spectrometer are given in Table XIX. Data on the α decay of actinides have been analyzed also in Ref. 72. For calibration of spectrometers the greatest interest is presented by nuclides with comparatively long half-life and available through commercial channels (Table XX). In the USSR some sources of this series are prepared in the form of a set of standard spectrometric α sources (SSAS).[73] Here the sources are divided into three categories as a function of the intrinsic width of the α line at half-height: 1) $\Delta_{source} < 10$ keV, 2) $\Delta_{source} < 20$ keV, and 3) $\Delta_{source} < 50$ keV. In addition, from the technological point of view a distinction is made between SSAS with a firmly fixed layer of radioactive material and SSAS for precision measurements (intrinsic line width at half-height < 2 keV) prepared by vacuum evaporation of the material. Combined SSAS are also produced, for example ^{239}Pu + ^{241}Am + ^{244}Cm, ^{233}U + ^{238}Pu + ^{239}Pu, ^{226}Ra + ^{227}Ac + ^{228}Th, and so forth. We note that for SSAS with a firmly attached layer the permissible deviation of the energy and activity from the nominal values is ±100 keV and ±20%, respectively. Consequently the quality of the calibration sources substantially determines the design of an experiment for measurement of α-particle energies by means of semiconductor detectors.

The range of α particles (see Fig. 33) falls entirely within the thickness of the sensitive layer of Si(Au) de-

TABLE XXI. Energy of α particles from ^{226}Ra and its daughter products (see Fig. 58) obtained by an internal-calibration technique.

Variant	E	ΔE	E	ΔE	E	ΔE	E	ΔE	E	ΔE	E	ΔE
1	4599.656	0.699	4782.356	0.542	5304.510	0.388	5489.708	0.340	6002.550	0.411	7685.715	0.931
Deviation	+2.244		+2.144		0		−0.048		0		+1.375	
2	4599.249	0.596	4782.054	0.459	5304.510	0.388	5489.815	0.353	6002.953	0.385	7687.090	0.410
Deviation	+2.651		+2.446		0		−0.155		−0.403		0	
3	4602.367	0.633	4784.500	0.470	5305.036	0.386	5489.660	0.389	6000.913	0.584	7678.861	1.350
Deviation	−0.467		0		−0.526		0		+1.637		+8.229	
4	4602.121	0.616	4784.500	0.470	5305.737	0.378	5490.609	0.344	6002.550	0.411	7682.757	0.714
Deviation	−0.221		0		−1.227		−0.949		0		+4.333	
5	4601.849	0.605	4784.500	0.471	5306.516	0.401	5491.665	0.367	6004.371	0.395	7687.090	0.409
Deviation	+0.051		0		−2.006		−2.005		−1.821		0	
6	4600.448	0.585	4783.172	0.447	5305.396	0.380	5490.617	0.347	6003.527	0.386	7686.915	0.434
Deviation	+1.452		+1.328		−0.885		−0.957		+0.977		+0.175	
7	4600.823	0.609	4783.508	0.473	5305.626	0.398	5490.810	0.362	6003.615	0.390	7686.658	0.427
Deviation	+1.077		+0.992		−1.116		−1.150		−1.065		+0.432	
8	4600.247	0.598	4782.961	0.459	5305.153	0.385	5490.365	0.351	6003.245	0.391	7686.534	0.488
Deviation	+1.653		+1.539		−0.643		−0.705		−0.695		+0.556	
Data of Table XIX	4601.9	0.5	4784.50	0.25	5304.51	0.07	5489.66	0.30	6002.55	0.09	7687.09	0.06

Note. Energies used for calibration are underlined. We have also given the deviations from the data of Table XIX.

tectors, and therefore there are no difficulties in measurement of the relative intensities of α groups. However, the problem of measuring absolute intensities of α particles is appreciably more complicated. There is no doubt that it is possible to solve the problem by a careful consideration of all geometrical factors. In particular, the activity of ^{241}Am was determined by this method with an error $\leq 0.2\%$.[74] However, a simpler method is the comparison of standard activities with the activity being studied.

An example of a single measurement of a ^{226}Ra SSAS (with a firmly attached layer) by the internal-calibration method is shown in Fig. 58. If we assume that ^{226}Ra and its daughter products are uniformly distributed over the thickness of the source itself and that there is no nonlinearity due to energy loss in the thickness or to the quality of the apparatus, we can determine the energies of α particles by means of various sets of standard peaks (Table XXI). From the data presented, however, we can conclude that the conditions of an ideal experiment have been violated and therefore the systematic deviations of the energy are as much as ±2.7 keV. In analysis of repeated measurements on the basis of the equations (30) we used the following parameters:

a) Since the energy calibration is accomplished by means of α-particle energies measured by an absolute method, we set $\alpha_3 = 0$.

b) If the calibration is accomplished by means of only two standards, which according to the data of Table XXI is justified in a narrow energy region, then

$$\alpha_4 = [(\Delta E_1)^2 + (\Delta E_2)^2]^{1/2}, \tag{54}$$

where ΔE_1 and ΔE_2 are the errors in the calibration energies.

With use of various pairs it is necessary to use as α_4 the pair with the least error.

c) Inclusion of the systematic error α_5 in single measurements is a complicated question. For repeated measurements we assume that $\alpha_5 = 0$ and the contribution of α_5 is transferred to the value of the error α_2 due to the spread. On the other hand, in single measurements we assume

$$\alpha_5 = \frac{1}{n\sqrt{3}} \sum_{i=1}^{n} |E_{i\,\mathrm{calc}} - E_{i\,\mathrm{tab}}|, \tag{55}$$

where E is the energy of a standard peak located inside the calibration region but not used in calculations of the coefficients B_1 and B_2.

The comments above also refer in their entirety to the external-calibration method. In this case such factors as the source quality, counting rate, source-detector distance, chamber vacuum, and so forth have exceptional significance and the systematic error associated with these factors may be as high as 100 keV. For example, an experiment on measurement of the energy of the α particles of a ^{238}Pu SSAS (with a firmly attached layer, Fig. 59) by means of the technique of external calibration on the basis of ^{226}Ra gave 5499.913 ± 0.794 and 5540.818 ± 0.495 keV. Comparing these results with the data from Table XX, we determine a difference of 43.413 and 41.608 keV, respectively. The exaggeration of the energy relative to ^{226}Ra can be explained by the

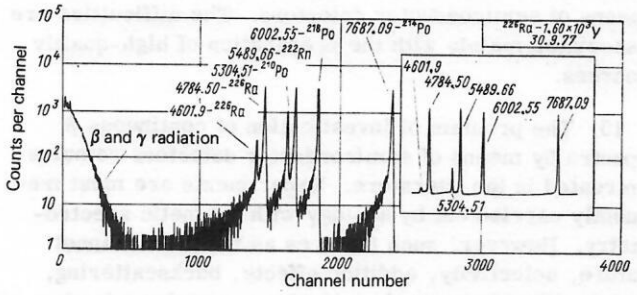

FIG. 58. Spectrum of α particles from ^{226}Ra measured by a 30 mm^2 × 0.3 mm Si(Au) detector. The insert is shown on a linear scale. $T_1 = 1$ year, $T_2 = 2$ hours, $P = 4$ cm.

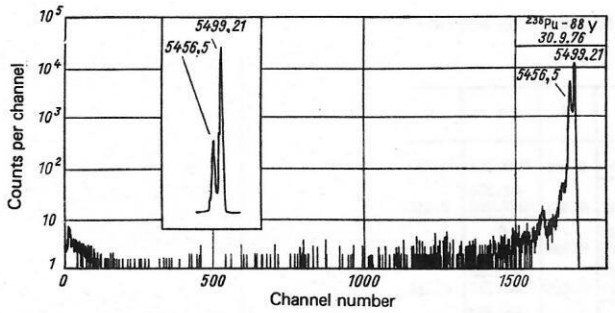

FIG. 59. Spectrum of α particles from ^{238}Pu measured by a 30 mm^2 ×0.3 mm Si(Au) detector. The insert is to a linear scale. $T_1 = 1$ year, $T_2 = 2$ hours, $P = 4$ cm.

influence of the thickness of the shielding film of the ^{226}Ra source, which is a source with emanation.[74]

CONCLUSION

At the present time semiconductor detectors are the principal instruments in experimental nuclear spectroscopy. Spectrometry techniques are finding ever increasing application in intermediate and high energy physics,[75] and also in solution of problems of an applied nature (activation and elemental analysis). However, it should be stated that the development of techniques of spectrometry of radiations stands apart somewhat from the development of the technology of preparing semiconductor detectors. As is well known, these processes are related to each other.

We draw certain conclusions from the analysis carried out in the present work.

1. Detectors based on Si and Ge have essentially reached the energy resolution possible for the crystal configuration chosen. Although there have been some achievements in the technology of preparing detectors of GaAs and CdTe, the requirements of experimental nuclear spectroscopy are still satisfied only by Si and Ge detectors. From the point of view of future promise, special interest is presented by coordinate-sensitive detectors in combination with classical magnetic spectrometers.

2. The planning and performance of experiments to study the spectra of radiations of radioactive nuclides is meaningless without performance of a complete analysis of effects which distort the uncorrected spectrum (see Tables II and III).

3. A number of physics experiments involve precision measurements of γ-ray energies. At the present time discussions are going on regarding the choice of secondary standards which relate the γ-ray energy values with the fundamental constants. Here the error of such a standard has particular significance, since it enters as a systematic component into the total error of the γ-ray energies.

4. The technique of γ-ray energy measurements by means of semiconductor detectors is based on comparison with energy standards. On the assumption of Eq. (35) with use of the ^{182}Ta and ^{192}Ir γ-ray energies (see Table IV) and the energies of transitions obtained by addition of cascade transitions for nuclides with well studied decay schemes (see Table VI), a complete set of standards has been constructed (see Table VII). If the new value of E_γ (411.8 keV) is adopted, the correction procedure becomes simple [Eq. (39)]. Here the model for calculation of the errors [Eq. (30)], which provides conversion to the new standard basis, is of central importance.

5. Measurement of γ-ray energies in the region below 100 keV involves significant difficulties in the choice of energy standards, as the result of distortion of the uncorrected spectrum by the characteristic radiation of the standard nuclides and also by the KX radiation in the semiconductor detectors. In order to reduce these distortions it is necessary to carry out a careful analysis of the experimental conditions.

6. The technique of measuring relative intensities of γ rays by means of semiconductor detectors is based on use of data on the relative intensities of the γ rays of standard radionuclides (see Table XII). These results were obtained by means of activity-calibrated sources (in the USSR, from SSGS). Since in the regions 35–120 and 200–600 keV there are comparatively few transitions whose energies can be calibrated with high accuracy, it is necessary to invoke various physical criteria which permit the correctness of the basis to be verified (see Table XII). If there is a deviation, the correction procedure can be carried out in accordance with Eq. (42).

7. We have described here the technique for measurement of conversion coefficients by means of semiconductor detectors. As primary standard for conversion coefficients we have used α_k(661.7 keV – ^{137}Cs) from Eq. (51). On this assumption we have constructed a set of secondary standards for conversion coefficients (see Table XV). This approach necessarily provides a procedure for correction of the data [Eq. (53)].

8. The transition 121.8 keV – ^{152}Eu has been the object of special experiments. It is considered to be pure E2 and to discharge the first excited state of ^{152}Sm (2^+). The experimental value of α_k obtained differs from the calculated value[48] by 7.3 ± 2.5%. We propose to carry out a series of experiments to check the agreement of the experimental and theoretical conversion coefficients for transitions of pure multipolarity.

9. At the present time there is no systematic technique for precision spectrometry of α particles by means of semiconductor detectors. The difficulties are associated mainly with the preparation of high-quality sources.

10. The problem of investigation of continuous β spectra by means of semiconductor detectors remains untreated in the literature. Experiments are most frequently carried out by analogy with magnetic spectrometry. However, such features as the multichannel nature, selectivity, addition effects, backscattering, and the like hinder such an analogy, and there is obviously a need for development of a special technique for semiconductor detectors.

11. We have devoted our principal attention to describing methods of spectrometry of radiations of radioactive nuclides by means of semiconductor detectors. The questions of application of this technique and the physical consequences present independent interest.

In conclusion we wish to thank Professor K. Ya. Gromov for his constant interest in this work.

[1]A. N. Tikhonov, Dokl. Akad. Nauk SSSR **151**, 501 (1963).
[2]Ts. Vylov *et al.*, Preprint R6-9071, JINR, Dubna, 1975.
[3]Prikladnaya spektroskopiya s poluprovodnikovymi detektorami (Applied spectrometry with Semiconductor Detectors), Moscow, Atomizdat, 1974.
[4]V. S. Aleksandrov *et al.*, Preprint 13-7306, JINR, Dubna, 1973.
[5]Ts. Vylov *et al.*, Preprint R6-9072, JINR, Dubna, 1975.
[6]Ts. Vylov *et al.*, Preprint R6-11085, JINR, Dubna, 1977.
[7]Ts. Vylov *et al.*, Preprint 13-10056, JINR, Dubna, 1976.
[8]Ts. Vylov *et al.*, Preprint R6-8378, JINR, Dubna, 1974.
[9]P. Paris and J. Treherne, Rev. Sci. Appl. 4, 291 (1969).
[10]E. B. Shera, M. P. Bedesem, and K. Y. Casper, Rev. Scientific Instruments **38**, 1110 (1967).
[11]R. L. Watson *et al.*, Rev. Sci. Instrum. **38**, 905 (1967).
[12]V. S.Aleksandrov *et al.*, Preprint 11-7319. JINR, Dubna, 1973.
[13]N. G. Klyukin and S. I. Ormandzhiev, Preprint 13-8629, JINR, Dubna, 1975.
[14]C. M. Lederer, in: Radioactivity in Nuclear Spectroscopy, Ed. by J. H. Hamilton and J. C. Manthuruthile, Vol. 2, Gordon and Breach, N. Y.–London–Paris, 1972, p. 73.
[15]V. Gadzhokov, Prib. Tekh. Eksp., No. 5, 82 (1970 [Instrum. Exper. Tech., No. 5, 1338 (1970)].
[16]V. Gadzhokov, Preprint 10-5255, JINR, Dubna, 1970.
[17]L. A. Vylova *et al.*, Preprint R10-7061, JINR, Dubna, 1973.
[18]L. Aleksandrov and V. Gadzhokov, Preprint R5-5294, JINR, Dubna, 1970.
[19]R. G. Helmer, R. J. Gerhke, and R. G. Greenwood, Nucl. Instrum. Methods **123**, 51 (1975).
[20]Ts. Vylov *et al.*, Dokl. Bolg. Akad. Nauk (Bulletin of the Bulgarian Academy of Sciences) **21**, 219 (1968).
[21]G. Knop and W. Paul, in: Alpha, Beta, and Gamma-Ray Spectroscopy, Hafner, Riverside, New Jersey, 1965, Ed. by K. Seigbahn.
[22]A. Strömich, H. Ostertag, and B. Gonsior, Izv. Akad. Nauk SSSR Ser. Fiz. **36**, 2239 (1972) [Bull. USSR Acad. Sci., Phys. Ser., p. 1963..
[23]M. Waldschmidt and S. Wittig, Nucl. Instrum. Methods **64**, 189 (1968).
[24]E. K. Stepanov, S. A. Stoyanova, and N. V. Tyutikov, Prib. Tekh. Eksp., No. 1, 44 (1974) [Instrum. Exper. Tech. **17**, 39 (1974)].
[25]B. M. Golovin and L. A. Permyakova, Preprint 13-7238, JINR, Dubna, 1973.
[26]E. Rotondi and K. W. Geiger, Nucl. Instrum. Methods **40**, 192 (1966).
[27]N. G. Volkov, V. G. Chubchenko, and O. Kh. Belov, in: Prikladnaya yadernaya spektroskopiya (Applied Nuclear spectroscopy), No. 4, Moscow, Atomizdat, 1974, p. 177.
[28]Ts. Vylov *et al.*, Preprint R6-9073, JINR, Dubna, 1975.
[29]Ts. Vylov *et al.*, Preprint R6-10414, JINR, Dubna, 1977.
[30]Ts. Vylov *et al.*, Preprint R6-10415, JINR, Dubna, 1977.
[31]B. N. Taylor, W. Parker, and D. Langenberg, Fundamental Constants and Quantum Electrodynamics, Academic Press, 1969.
[32]B. S. Dzhelepov, Metody razrabotki slozhnykh skhem raspada (Methods of Analysis of Complicated Decay Schemes), Leningrad, Nauka, 1974.
[33]G. Murray, R. L. Graham, and J. S. Geiger, Nucl. Phys. **63**, 353 (1965).
[34]A. L. Carter *et al.*, Phys. Rev. Lett. **37**, 1380 (1976).
[35]C. L. Borchert, Annual Report, 1975, KFA-iKP 10/76, p. 43.
[36]R. L. Heath, Gamma-Ray Spectrum Catalogue, ANCR-1000-2, 1974.
[37]W. Beer and J. Kern, Nucl. Instrum. Methods **117**, 183 (1974).
[38]J. Kern, Proc. Panel Meeting on Charged-Particle-Induced Radiative Capture, IAEA, Vienna, 1972.
[39]Yu. K. Akimov *et al.*, Poluprovodnikovye detektory yadernykh chastits i ikh primenenie (Semiconductor Nuclear Particle Detectors and Their Application), Atomizdat, Moscow, 1967.
[40]F. Hajnal and C. Klusek, Nucl. Instrum. Methods **122**, 559 (1974).
[41]L. J. Jardine, Nucl. Instrum. Methods **96**, 259 (1971).
[42]G. Aubin *et al.*, Nucl. Instrum. Methods **76**, 93 (1969).
[43]R. S. Mowatt, Can. J. Phys. **48**, 2606 (1970).
[44]L. L. Riedinger, N. R. Johnson, and J. H. Hamilton, Phys. Rev. C **2**, 2358 (1970).
[45]V. S. Aleksandrov *et al.*, Preprint R6-7308, JINR, Dubna, 1973.
[46]G. Malmsten, Ö. Nilsson, and I. Andersson, Ark. Fys. **33**, 361 (1966).
[47]J. H. Hamilton, in: The Electromagnetic Interaction in Nuclear Spectroscopy, North-Holland Publishing Company, Amsterdam, 1975, p. 441.
[48]R. S. Hager and E. C. Seltzer, Nucl. Data **4**, 1 (1968).
[49]K. Siegbahn *et al.*, in: Elektronnaya spektroskopiya (Electron Spectroscopy), Mir, Moscow, 1971.
[50]E. P. Grigor'ev *et al.*, in: Programma i tezisy dokladov XXVI soveshchaniya po yadernoĭ spektroskopii i strukture atomnogo yadra (Program and Abstracts of the Twenty-Sixth Conference on Nuclear Spectroscopy and Nuclear Structure), Nauka, Leningrad, 1976, p. 104.
[51]V. M. Kartashov *et al.*, in: Programma i tezisy dokladov XXVI soveshchaniya po yadernoĭ spektroskopii i strukture atomnogo yadra (Program and Abstracts of the Twenty-Sixth Conference on Nuclear Spectroscopy and Nuclear Structure), Nauka, Leningrad, 1976, p. 105.
[52]J. C. Manthuruthil and J. H. Hamilton, in: Radioactivity in Nuclear Spectroscopy, Ed. by J. H. Hamilton, Vol. 2, Gordon and Breach, N. Y.–London–Paris, 1972, p. 753.
[53]A. Rytz, Atomic Data and Nucl. Data Sheets **12**, 479 (1973).
[54]A. H. Wapstra and N. B. Gove, Nucl. Data Tables **A9**, Nos. 4–5, 265 (1971).
[55]J. Legrand *et al.*, Table de Radionucleides, Commissariat a L'Energie Atomique, France, 1975.
[56]J. J. Reidy, The Electromagnetic Interaction in Nuclear Spectroscopy, Ed. by W. D. Hamilton, North-Holland Publishing Company, Amsterdam, 1975, p. 839.
[57]V. A. Balalaev, V. S. Dzhelepov, and V. E. Ter-Nersesyants, in: Izobarnye yadra s massovym chislom A-169 (Isobaric Nuclei with Mass Number A =169), Nauka, Leningrad, 1976.
[58]H. Inoue, Y. Yoshizawa, and T. Morii, Nucl. Instrum. Methods **108**, 385 (1973).
[59]Lin Chien-Chang, J. Inorg, Nucl. Chem. **38**, 1409 (1976).
[60]R. J. Gehrke and R. A. Lokken, Nucl. Instrum. Methods **97**, 219 (1971).
[61]M. J. Martin and P. H. Blichert-Toft, Nucl. Data Tables **A8**, Nos. 1–2, (1970).
[62]J. F. Emery, S. A. Reynolds, and E. I. Wyatt, Nucl. Sci. Eng. **48**, 319 (1972).
[63]V. S. Aleksandrov *et al.*, in: Programma i tezisy dokladov XXVII soveshchaniya po yadernoĭ spektroskopii i strukture atomnogo yadra (Program and Abstracts of the Twenty-Seventh Conference on Nuclear Spectroscopy and Nuclear Structure), Nauka, Leningrad, 1977, p. 72.
[64]A. Höglund and S. Malmskog, Nucl. Phys. **A138**, 470 (1969).
[65]B. S. Dzhelepov and N. Lyutorovich, Izv. Akad. Nauk SSSR Ser. Fiz. **40**, 1115 (1976) [Bull. USSR Acad. Sci., Phys. Ser.].
[66]S. R. Avramov *et al.*, Preprint R6-8781, JINR, Dubna, 1975.
[67]J. H. Hamilton, *et al.*, Nucl. Data **1**, No. 6, 531 (1966).
[68]M. Fujioka, Nucl. Phys. A153, 337 (1970).

[69]D. R. Zolnowski, E. G. Funk, and J. W. Mihelich, Nucl. Phys. A177, 513 (1971).
[70]V. P. Afanas'ev *et al.*, Preprint R6-4972, JINR, Dubna, 1970.
[71]V. A. Biryukov *et al.*, Prib. Tekh. Eksp., No. 2, 71 (1975) [Instrum. Exper. Tech. 18, No. 2, 408 (1975)].
[72]S. A. Baranov, A. G. Zelenkov, and V. M. Kulakov, At. Energ. 41, 342 (1976) [Sov. Atomic Energy].
[73]A. F. Beletskiĭ *et al.*, in: Prikladnaya yadernaya spektroskopiya (Applied Nuclear Spectroscopy), No. 1, Atomizdat, Moscow, 1970.
[74]A. M. Geĭdel'man *et al.*, in: Prikladnaya yadernaya spektroskopiya (Applied Nuclear Spectroscopy), Ed. by V. G. Nedovesov, No. 4, Atomizdat, Moscow, 1974, p. 108.
[75]Yu. K. Akimov, Fiz. Elem. Chastits At. Yadra 8, 193 (1977 [Sov. J. Part. Nucl. No. 8, 80 (1977)].

Translated by Clark S. Robinson